# Kinetic and mechanistic studies of the reactivity of Zn–$OH_n$ ($n = 1$ or 2) species in small molecule analogs of zinc-containing metalloenzymes

Lisa M. Berreau

*Department of Chemistry and Biochemistry, Utah State University, Logan, UT, USA*

## Abstract

Reactive Zn–$OH_n$ (n = 1 or 2) species are proposed in the catalytic cycles of several zinc-containing enzymes. In order to gauge the chemical factors that influence the formation and reactivity of Zn–$OH_n$ species, synthetic model complexes have been prepared and systematically examined for biologically relevant stoichiometric and catalytic reactivity. Systems that promote the hydration of $CO_2$, the activation and oxidation of alcohols, and amide and phosphate ester cleavage reactions are discussed.




## 1 Introduction

Metalloenzymes containing a Zn–$OH_n$ ($n = 1$ or 2) moiety catalyze a variety of chemical reactions.[1] These include $CO_2$ hydration, alcohol oxidation using a redox



ADVANCES IN PHYSICAL ORGANIC CHEMISTRY
VOLUME 41 ISSN 0065-3160 DOI: 10.1016/S0065-3160(06)41002-9

active $NAD^+$/NADH cofactor, and the hydrolysis of amide and phosphate ester groups. One approach toward elucidating detailed chemical information regarding the role of Zn–$OH_n$ species in enzyme-catalyzed reactions involves the preparation and studies of the reactivity of small molecule analog complexes.[2] Over the past few decades, this synthetic analog approach has led to the development of a multitude of reactive model systems for zinc enzymes.[3–7] The primary purpose of this contribution is to provide a detailed description of reactive synthetic systems involving a Zn–$OH_n$ moiety. In some cases, the stoichiometric and/or catalytic reactivity of these model systems will be compared/contrasted with reaction pathways proposed for zinc enzymes. Overall, this contribution is not meant to be exhaustive in terms of presenting all reported synthetic model systems for zinc enzymes. Instead, it is focused on a detailed presentation of kinetic and mechanistic studies of reactive complexes and builds on previous reviews that also focused primarily on reactivity.[8–14] Excellent reviews are also available that place a stronger emphasis on the structural aspects of model systems for zinc centers in metalloenzymes.[3–5]

## PROPERTIES OF DIVALENT ZINC AND ZN–$OH_n$ SPECIES

Divalent zinc has a $3d^{10}$ electron configuration and is redox inactive and diamagnetic. As a consequence of its filled shell electronic structure, ligand field stabilization effects do not influence the coordination properties of Zn(II). Instead, the coordination number of a Zn(II) center and the geometric arrangement of its ligands in a coordination complex are primarily determined by the steric and electronic properties of the ligands. An overall coordination number of four and a distorted tetrahedral geometry are most common for Zn(II) in biological systems, albeit Zn(II) centers having a coordination number of 5 are also prevalent.[5] In terms of hard–soft acid–base properties, Zn(II) is an intermediate metal ion which forms complexes with both hard (oxygen, nitrogen) and soft (sulfur) donor ligands.[1,15] Zn(II) undergoes rapid ligand exchange for monodentate ligands such as water ($k_{ex}$ ($H_2O$) $= 2 \times 10^7\,s^{-1}$), which enables this metal ion to facilitate catalytic reactions. This rate of water exchange is slower than that of alkali metal ions ($k_{ex}$ ($H_2O$) $\sim 10^8$–$10^9\,s^{-1}$), but faster than most other divalent $3d$ metal ions (Fe(II): $4 \times 10^6\,s^{-1}$, Co(II): $3 \times 10^6\,s^{-1}$, Ni(II), $4 \times 10^4\,s^{-1}$, Cu(II) $1 \times 10^9\,s^{-1}$).[1] In terms of ligand reactivity, it is important to note that Zn(II)–OH species exhibit nucleophilic behavior.

Zinc aqua (Zn–$OH_2$) species are prevalent in biological systems. When coordinated to a Zn(II) center, a water molecule can have a p$K_a$ value that varies from ~6 to 11, with $[Zn(OH_2)_6]^{2+}$ having a p$K_a = 9.0$.[5] The position of a specific Zn–$OH_2$ unit in this range depends on the primary and secondary ligand coordination environment of the zinc center. A more Lewis acid Zn(II) center, and hence a lower Zn–$OH_2$ p$K_a$ value, is produced when the total number of primary ligands is low (e.g. 4) and these ligands are neutral donors. For example, the Zn–$OH_2$ moiety in $[(THB)Zn(OH_2)]^{2+}$ (Fig. 1a) exhibits a p$K_a$ value of 6.2.[16] This indicates that a tetrahedral $(N_{His})_3Zn(II)$–$OH_2$ moiety, as is found in active site of carbonic anhydrase (CA), could have a p$K_a$ at or below physiological pH for the zinc-bound aqua

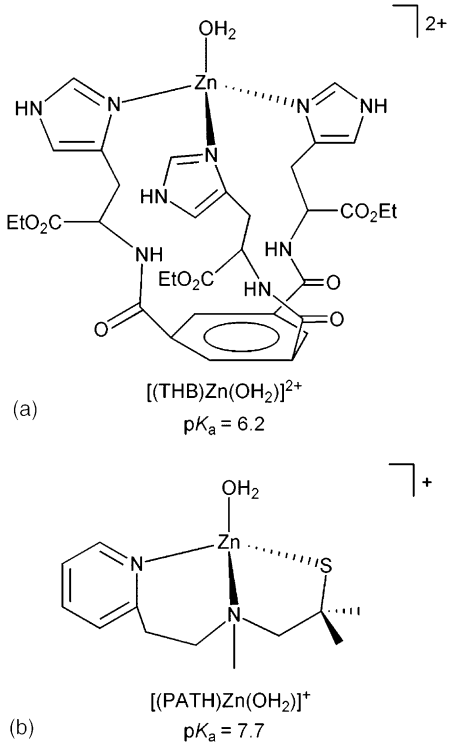


**Fig. 1** Examples of four-coordinate Zn(II)–$OH_2$ complexes for which p$K_a$ values have been determined. Comprehensive listings of LZn–$OH_2$ p$K_a$ values for synthetic complexes have been recently compiled.[5]

ligand. Substitution of a neutral donor with an anionic ligand in the primary coordination sphere of the Zn(II) reduces the Lewis acidity of the zinc center and thus raises the p$K_a$ of a Zn(II)–$OH_2$ moiety. For example, a tetrahedral $[(N_2S)Zn(OH_2)]^+$ species ($[(PATH)Zn(OH_2)]^+$, Fig. 1b) akin to the active site zinc center in peptide deformylase exhibits a p$K_a$ value of 7.7.[17]

In terms of secondary effects, recent studies of zinc complexes supported by tripodal, tetradentate ligands indicate that the presence of intramolecular hydrogen-bonding interactions involving the oxygen atom of a zinc-bound water molecule lowers the p$K_a$ of that water molecule.[18–20] As shown in Fig. 2, zinc complexes having a single internal hydrogen-bond donor exhibit a Zn–$OH_2$ p$K_a$ value that is ~0.7–0.9 p$K_a$ units above analogs having two internal hydrogen-bond donor groups.

## ROLES FOR ZN(II) IN CATALYSIS

As zinc-containing enzymes do not exhibit spectroscopic features, such as *d–d* electronic transitions or an electron spin resonance (EPR) signal, which can be used to

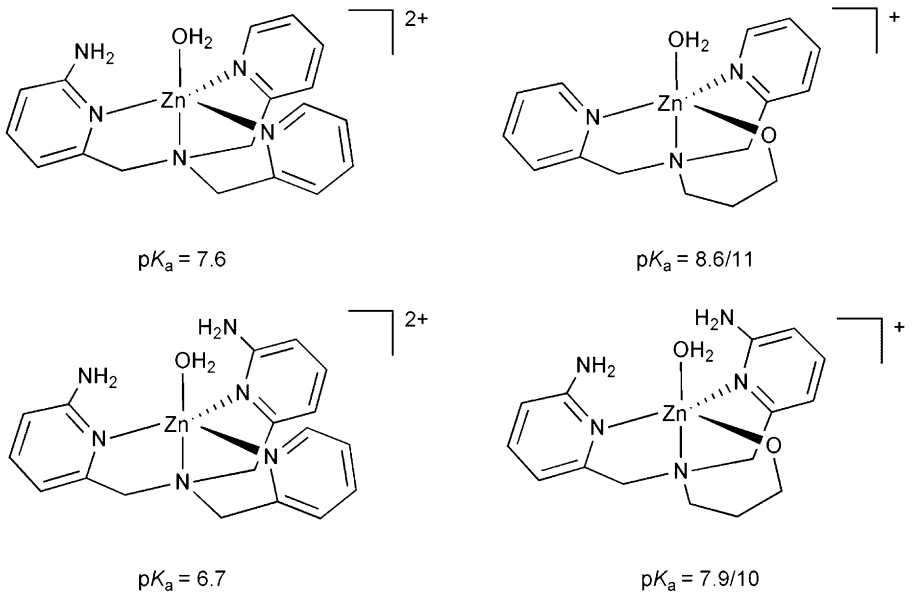


**Fig. 2** Cationic portions of $N_4$- and $N_3O$-ligated Zn–$OH_2$ complexes having variable numbers of internal hydrogen-bond donors. The two p$K_a$ values shown for the $N_3O$-ligated complexes correspond to ionization of the Zn–$OH_2$ and Zn–OR groups, albeit the individual values have not been assigned.

detect substrate-, intermediate-, product- or inhibitor-bound forms of the enzyme, structure–function relationships and proposed catalytic mechanisms for zinc-containing enzymes have been developed and evaluated primarily on the basis of the combined results of X-ray crystallographic, kinetic (using native and altered substrates), site-directed mutagenesis, and metal-ion substitution studies.[21,22] From these studies, it is apparent that catalytic zinc sites in metalloenzymes typically contain at least one water-occupied coordination position, in addition to three or four Zn(II)-coordinated amino acid ligands.[23] The zinc-bound water molecule can undergo one of three types of reactions within an enzyme active site. The Zn–$OH_2$ can (1) undergo ionization to produce a zinc hydroxide species, (2) be polarized via interaction with a catalytic base to produce a reactive nucleophile, or (3) be displaced by a substrate.[24,25] Other roles for an active site catalytic Zn(II) ion in a metalloenzyme active site can include polarization of a substrate via coordination, and/or stabilization of negative charge build-up in a transition state.

## GENERAL NOTE

For the model systems described herein, when not specifically indicated, the reader should assume that the solvent is water.

## 2 $CO_2$ hydration

Carbonic anhydrases (CAs) catalyze the reversible hydration of $CO_2$ to form bicarbonate (Fig. 3, bottom). Four classes of CAs (α, β, γ, δ) have been identified.[26] In α-CAs, a mononuclear active site zinc center having distorted tetrahedral ligation from three histidine nitrogen donors and one water/hydroxide ligand, $(N_{His})_3Zn–OH_n$ ($n = 1$ or 2), is proposed to provide the nucleophile for $CO_2$ hydration.[27,28] Additionally, within the active site there is a threonine residue (Thr-199) that forms a hydrogen-bonding interaction with the Zn–$OH_n$ moiety (Fig. 3). This threonine residue in turn forms a hydrogen bond with a glutamate residue. The secondary interaction between the Zn–$OH_n$ moiety and Thr-199 is suggested to influence the p$K_a$ of the Zn–$OH_2$ moiety, and orient the Zn–OH for nucleophilic attack on $CO_2$.[28,29] Notably, in a structurally characterized mutant of human CA-II (Thr-200 → His), a bound bicarbonate anion forms a hydrogen-bonding interaction involving Thr-199.[30,31] Overall, these results, combined with X-ray crystallographic studies of Co(II)-substituted human CA-II,[32] indicate that secondary hydrogen-bonding interactions are important toward influencing the chemistry of zinc-bound anions, including bicarbonate, in CAs.

A p$K_a$ value of ~7 has been assigned to the active site zinc-bound water molecule in human CA-II.[28,33] Above pH = 7, the hydration of $CO_2$ is the dominant reaction, whereas below pH = 7, dehydration of $CO_2$ occurs. A proposed mechanism for $CO_2$ hydration catalyzed by a α-type CA is shown in Scheme 1. Following deprotonation of the zinc-bound water molecule, the Zn–OH acts as a nucleophile toward $CO_2$ to

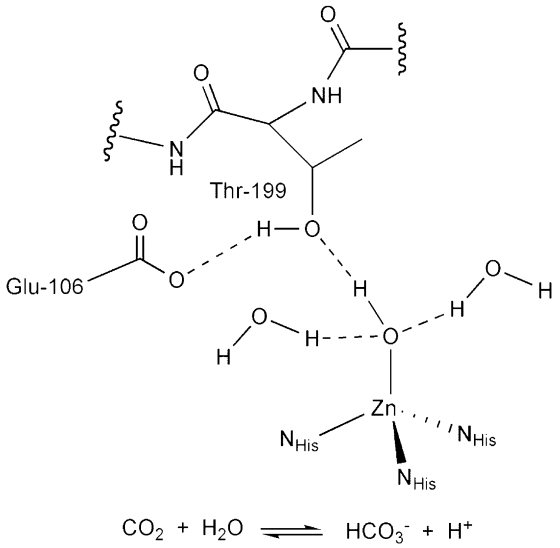


**Fig. 3** (top) Active site features of a typical mammalian α-CA and (bottom) reaction catalyzed by CAs.

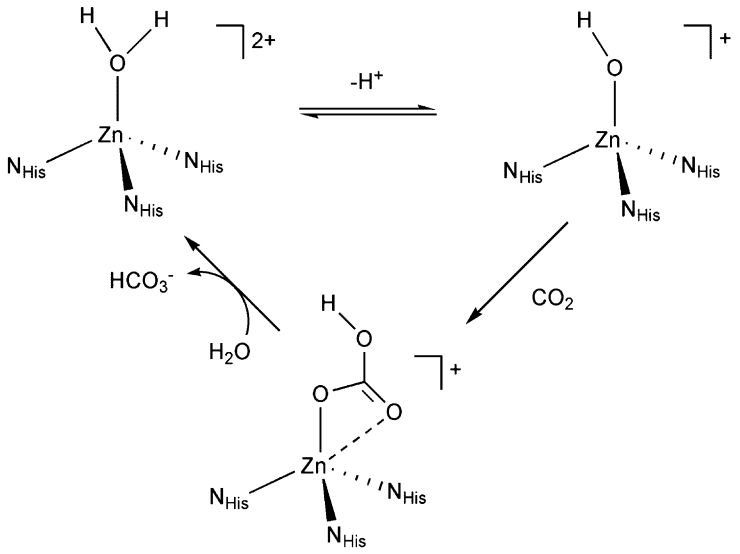


**Scheme 1** Proposed catalytic mechanism of a α-type CA.

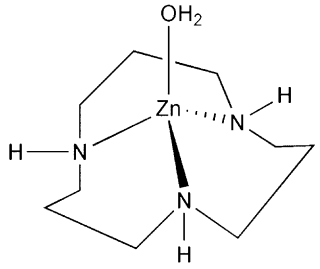


**Fig. 4** [([12]aneN$_3$)Zn(OH$_2$)]$^{2+}$.

yield a zinc-bound bicarbonate anion. Displacement of the bicarbonate anion by water results in regeneration of the zinc–aqua species.[26–28,34,35]

Relatively few catalytically active model complexes for CAs have been reported. Kimura and coworkers reported a catalytically active model complex, [([12]aneN$_3$)Zn(OH$_2$)](ClO$_4$)$_2$ (Fig. 4), for α-type CAs that has been extensively examined via kinetic and mechanistic investigations.[36] This complex exhibits a p$K_a = 7.30 \pm 0.02$ (25 °C, $I = 0.1$ (NaClO$_4$)) for the zinc-bound water molecule, a value that is very similar to that found for the Zn–OH$_2$ unit in CA. Upon deprotonation, a trinuclear [([12]aneN$_3$Zn)$_3$(μ-OH)$_3$](ClO$_4$)$_3 \cdot$ HClO$_4$ species is formed, which was isolated and

crystallographically characterized. In aqueous solution, pH titration experiments indicated that $[([12]aneN_3Zn)_3(\mu\text{-}OH)_3](ClO_4)_3 \cdot HClO_4$ breaks down into two $[([12]aneN_3)Zn(OH)]^+$ cations, one $[([12]aneN_3)Zn–OH(H_2O)]^+$ cation, and four perchlorate anions.[37] Examination of the observed catalytic rate of $CO_2$ hydration ($(k^h_{cat})_{obs}$) versus pH (6.1–9.0) catalyzed by $[([12]aneN_3)Zn(OH)]^+$ yielded a sigmoidal-shaped curve characteristic of a kinetic process controlled by an acid–base equilibrium with a kinetic $pK_a = 7.4$. This value is similar to that found for $[([12]aneN_3)Zn(OH_2)](ClO_4)_2$ via potentiometric titration, thus indicating that the Zn–OH form of the complex is the reactive species involved in the catalytic $CO_2$ hydration reaction. From this data, a mechanism for the model system was proposed (Scheme 2).

Examination of the rate of bicarbonate dehydration reactivity of $[([12]aneN_3)Zn(OH_2)](ClO_4)_2$ as a function of zinc complex concentration and pH revealed that this reaction is only slightly catalyzed by the aqua ($Zn–OH_2$) form of the complex. A proposed mechanism for bicarbonate dehydration is shown in Scheme 3. Once again, the kinetically determined $pK_a$ value matched well with that determined for $[([12]aneN_3)Zn(OH_2)](ClO_4)_2$, indicating the validity of the proposed mechanism.

Overall, $[([12]aneN_3)Zn(OH_2)](ClO_4)_2$ exhibits pH-dependent catalytic behavior for the hydration of $CO_2$ and dehydration of $HCO_3^-$. The rate-determining step of the $CO_2$ hydration reaction is the uptake of $CO_2$ by the zinc hydroxide complex. The rate-determining step in bicarbonate dehydration is substitution of the labile zinc-bound water molecule by the bicarbonate anion. The overall catalytic mechanism for both reactions is shown in Scheme 4. In considering this mechanism, it is

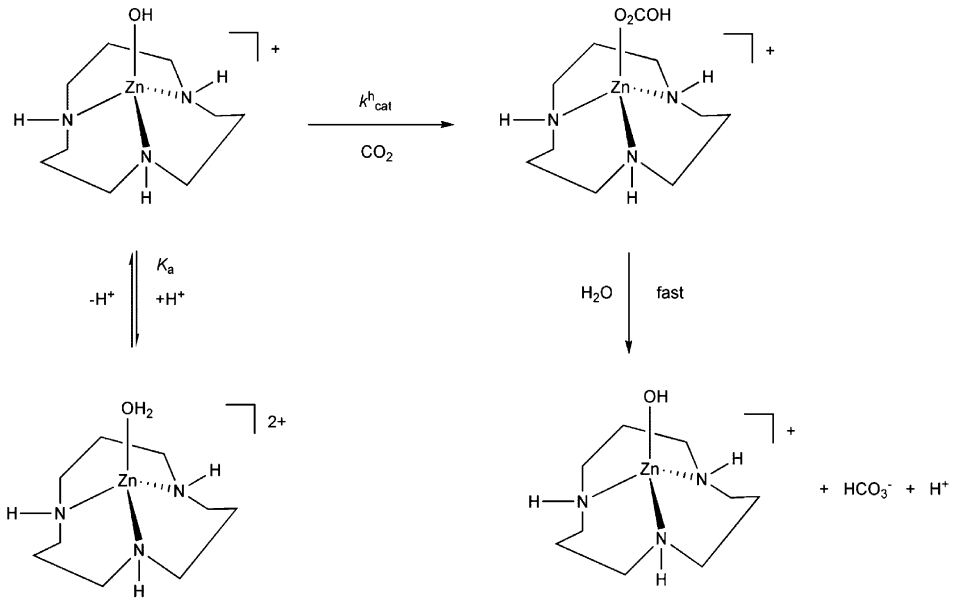


**Scheme 2** Suggested mechanism for $CO_2$ hydration catalyzed by $[([12]aneN_3)Zn(OH)]^+$.

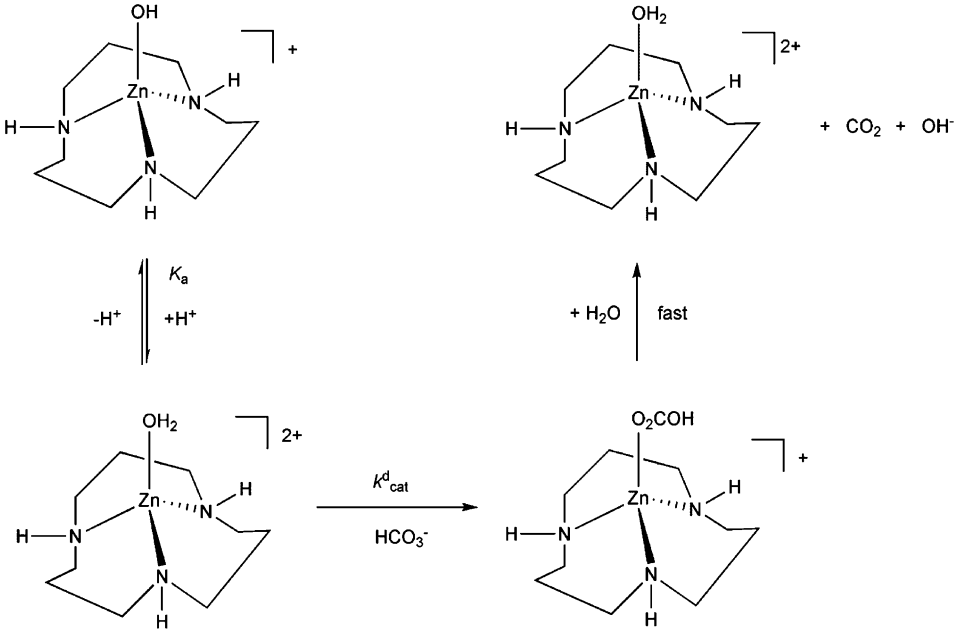


**Scheme 3** Proposed mechanism for $HCO_3^-$ dehydration catalyzed by $[([12]aneN_3)Zn(OH_2)]^{2+}$.

important to note the proton transfer processes. For example, ionization of $[([12]aneN_3)Zn(OH_2)](ClO_4)_2$ to produce the reactive zinc hydroxide species requires loss of a proton. A proton transfer process is also involved in the bicarbonate release reactivity of $[([12]aneN_3)Zn(OCO_2H)]^+$. This being the case, studies of the effect of changes in buffer type for the uncatalyzed and catalyzed hydration of $CO_2$ were performed. For buffers having a variety of different functional residues, no significant affect was found on the rate of either the uncatalyzed or catalyzed processes. This indicates that proton transfer is rapid and not involved in the rate-determining step of $CO_2$ hydration.

Similar thermodynamic and kinetic studies were performed using $[([12]aneN_4)Zn(OH_2)]^{2+}$ ([12]aneN$_4$ = 1,4,7,10-tetraazacyclododecane, cyclen, Fig. 5).[38] This complex has a thermodynamic $pK_a = 7.9 \pm 0.2$ for the zinc-bound water molecule. The hydroxide derivative of this complex, $[([12]aneN_4)Zn(OH)]^+$ ($k^h_{cat} = 3300 \pm 100\,s^{-1}$), is over five times more reactive than $[([12]aneN_3)Zn(OH)]^+$ ($k^h_{cat} = 654 \pm 57\,s^{-1}$) for the hydration of $CO_2$. The aqua derivative $[([12]aneN_4)Zn(OH_2)](ClO_4)_2$ ($k^d_{cat} = 51 \pm 8\,M^{-1}\,s^{-1}$) is 11 times more reactive than $[([12]aneN_3)Zn(OH_2)](ClO_4)_2$ ($k^d_{cat} = 4.7 \pm 0.6\,M^{-1}\,s^{-1}$ at 25 °C) for the dehydration of bicarbonate. While still well below the reported $k^h_{cat}$ values for $CO_2$ hydration ($\sim 10^7$–$10^8\,M^{-1}\,s^{-1}$, assigned to the proton transfer step) and dehydration of bicarbonate ($k^d_{cat} \sim 10^7\,M^{-1}\,s^{-1}$, assigned to proton transfer and simultaneous release of $CO_2$) for α-type CAs, these complexes exhibit the highest reactivity reported to date in a model system.[33,39]

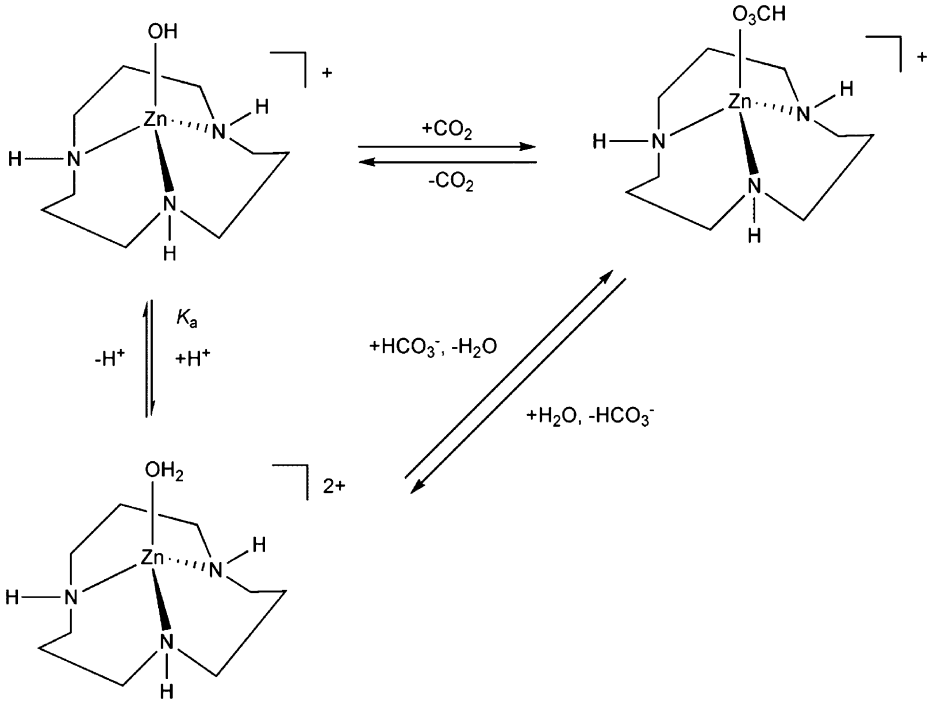


**Scheme 4** Proposed mechanism for catalytic reactivity.

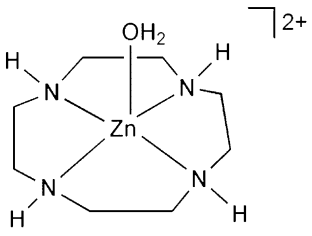


$[([12]aneN_4)Zn(OH_2)]^{2+}$

$pK_a = 7.9$

**Fig. 5** $[([12]aneN_4)Zn(OH_2)]^{2+}$.

Other catalytically active species for $CO_2$ hydration include $[(CR)Zn–OH]^+$ ($CR = Me_2pyo[14]trieneN_4$, $k_{cat}^h = 225 \pm 23\ M^{-1}\ s^{-1}$, Fig. 6a), which exhibits a $pK_a$ value of 8.69 at 25 °C.[40] Zinc complexes supported by tris(imidazole)phosphine-type (Fig. 6b–d) or tris(imidazole)phosphineoxide-type ligands also exhibit catalytic $CO_2$ hydration reactivity.[41–44] All of these complexes exhibit maximum rate constants for $CO_2$ hydration below $2500\ M^{-1}\ s^{-1}$ in the pH = 6–7 range. Above or below this pH

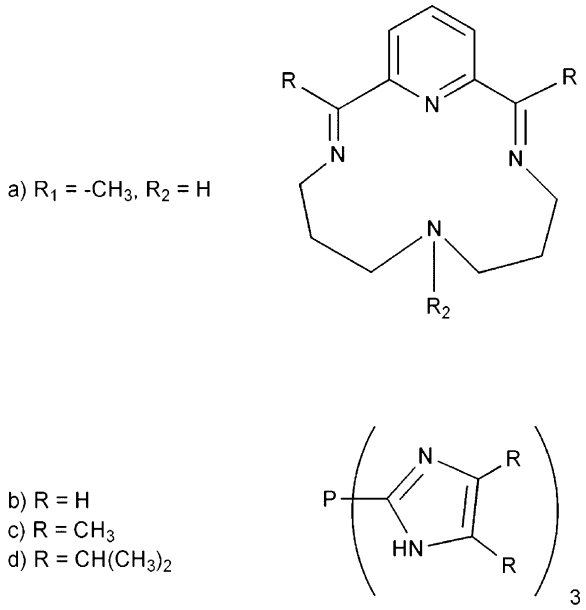


**Fig. 6** Supporting chelate ligands for which catalytic $CO_2$ hydration reactivity has been reported for zinc derivatives.

range, the reactions are complicated by ligand protonation (low pH) or loss of Zn(II) from the chelate ligand (high pH).

The high catalytic activity of $[([12]aneN_4)Zn(OH_n)](ClO_4)_n$ ($n = 1$ or 2) derivatives in $CO_2$ hydration and dehydration, relative to other reported model systems, has been attributed, in part, to high stability constants for zinc binding to the supporting chelate ligand. Enhanced stability imposed by the chelate structure should make the coordinated water molecule more labile for displacement by $HCO_3^-$, and the zinc-bound hydroxide more nucleophilic toward $CO_2$.

A factor that can influence $CO_2$ hydration/dehydration reactivity is the overall coordination number of the zinc center and the coordination mode of a bicarbonate ligand (Fig. 7). It is reasonable to suggest that a unidentate coordinated $HCO_3^-$ will be easier to displace, which could influence the rate of the overall hydration reaction. Data discussed below in terms of single turnover experiments supports the notion that bidentate bicarbonate coordination inhibits catalytic $CO_2$ hydration. Similarly, bidentate coordination of $HCO_3^-$ could be expected to slow the dehydration reaction. Notably, X-ray crystallographic studies of bicarbonate-bound forms of a mutant CA-II, and a Co(II)-substituted form of the enzyme, have revealed both monodentate and bidentate coordination modes for the bicarbonate anion.[28,32,45]

A limitation of the above-mentioned catalytically active model systems for α-type CAs is a lack of structural characterization for the reactive species. In particular, it is of interest to independently examine, if possible, the structural and reactivity features of discrete mononuclear, tetrahedral Zn–OH, Zn–$OH_2$, and Zn–$O_2COH$

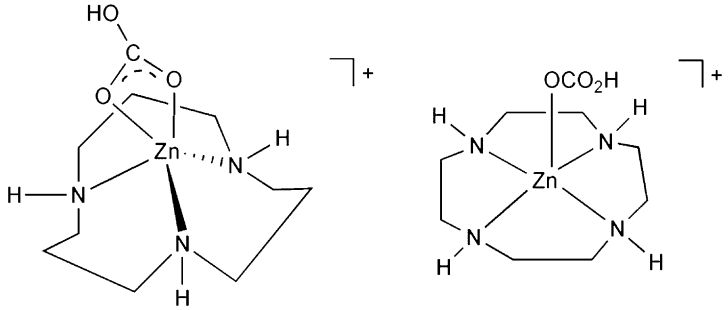


**Fig. 7** Possible structures of zinc bicarbonate species supported by the [12]ane$N_3$ and [12]ane$N_4$ ligands.

complexes. In this regard, the preparation and structural characterization of mononuclear Zn–OH complexes supported by tris(imidazolyl)phosphine ($Pim^{Pri,But}$)[46] and tris(pyrazolyl)borate ($Tp^{R,R'}$)[47–49] ligands, as well as a Zn–$OH_2$ complex supported by the $Tp^{But,Me}$ ligand,[50] have been reported (Fig. 8).[3–5] The hydroxide complexes exhibit a Zn–O(H) bond distance (~1.85 Å) that is considerably shorter than the Zn–$OH_2$ (1.94 Å) distance in the zinc aqua complex {[$Tp^{But,Me}$]Zn–$OH_2$}{HO–B($C_6F_5$)$_3$}. Of particular note in the synthetic Zn–$OH_2$ complex is the presence of a hydrogen-bonding interaction between the zinc-bound water molecule and the anion in the solid state. This interaction mimics that involving Thr-199 in the active site of human CA (Fig. 3).

The isolation and characterization of [$Tp^{But,Me}$]Zn–OH and {[$Tp^{But,Me}$]Zn–$OH_2$}{HO–B($C_6F_5$)$_3$} enabled the first direct comparison of the $CO_2$ reactivity of tetrahedral Zn–OH and Zn–$OH_2$ species. Notably, while the hydroxide complex reacts with $CO_2$ reversibly to produce a spectroscopically identifiable [$Tp^{But,Me}$]Zn–$O_2$COH species,[51] the Zn–$OH_2$ complex is unreactive toward $CO_2$.[52] This comparison provides conclusive evidence to support the notion that a Zn–OH moiety is the reactive species both in α-type CA enzymes and in the catalytically active model systems described above.

The zinc carbonate complex [$Tp^{But,Me}$]Zn–$O_2$COH could not be isolated due to a condensation reaction with [$Tp^{But,Me}$]Zn–OH, which results in the formation of a bridging carbonate complex, {[$Tp^{But,Me}$]Zn}$_2$(μ-$\eta^1$:$\eta^1$-$CO_3$) (Fig. 9). However, this carbonate complex is reactive toward water to regenerate [$Tp^{But,Me}$]Zn–OH and $CO_2$. In this regard, in the presence of $H_2^{17}O$, [$Tp^{But,Me}$]Zn–OH catalyzes oxygen atom transfer between $CO_2$ and the $^{17}$O-labeled water, indicating CA-type reactivity. While {[$Tp^{But,Me}$]Zn}$_2$(μ-$\eta^1$:$\eta^1$-$CO_3$) is reactive toward water, the zinc carbonate complex of $Tp^{iPr2}$, {[$Tp^{iPr2}$]Zn}$_2$(μ-$\eta^1$:$\eta^2$-$CO_3$) (Fig. 9, bottom), is unreactive. This difference is attributed to the differing coordination modes of the carbonate ligands in these complexes. Specifically, the bidentate coordination found for the carbonate ligand in {[$Tp^{iPr2}$]Zn}$_2$(μ-$\eta^1$:$\eta^2$-$CO_3$) is proposed to inhibit displacement of the carbonate ligand by water.

In regard to the reactivity of metal hydroxide complexes with $CO_2$, a variety of binuclear metal hydroxide complexes, supported by hydrotris(pyrazolyl)borate

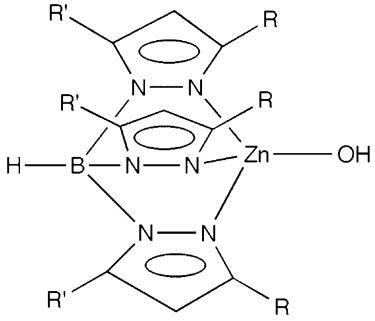


$[Tp^{But,Me}]Zn\text{-}OH$
$[Tp^{Cum,Me}]Zn\text{-}OH$

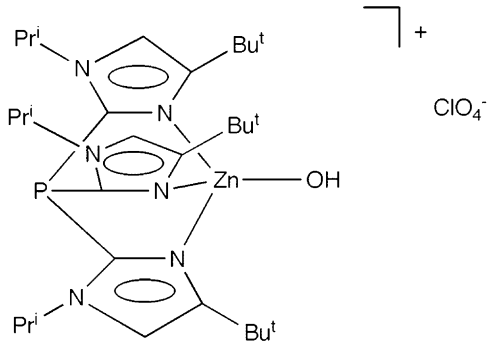


$[Pim^{But,Pri}]Zn\text{-}OH$

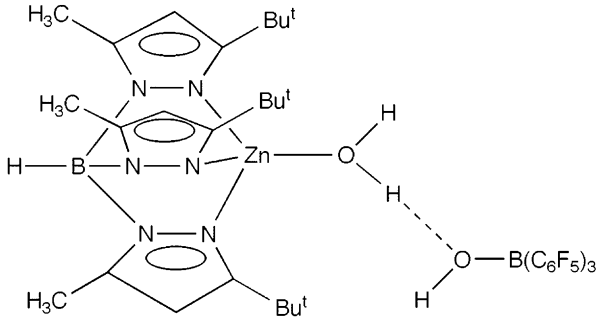


$\{[Tp^{But,Me}]Zn\text{-}OH_2\}\{HOB(C_6F_5)_3\}$

**Fig. 8** Structurally characterized mononuclear tetrahedral zinc hydroxide and aqua complexes.

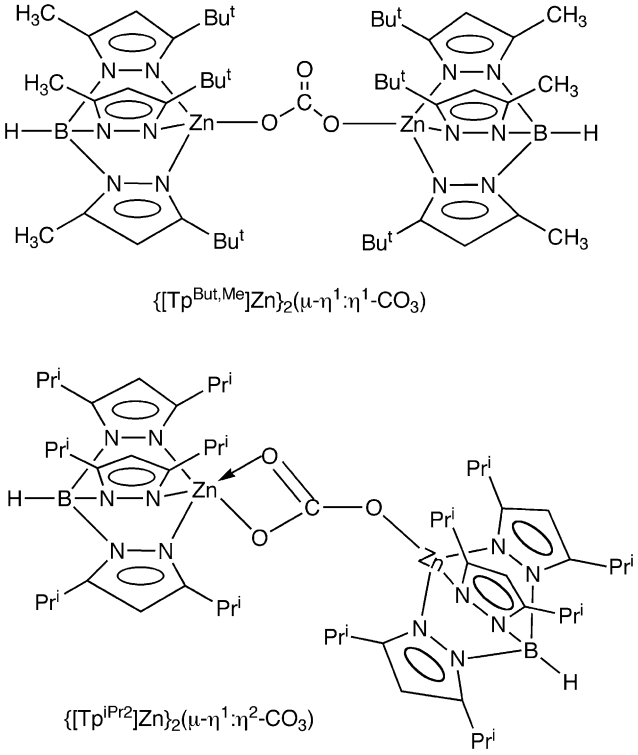


**Fig. 9** Drawings of bridging bicarbonate complexes.

ligands, have been demonstrated to undergo a stoichiometric reaction with $CO_2$ to yield bridging carbonate complexes.[53]

An interesting, relatively unexplored area to date in terms of synthetic systems concerns the impact of secondary interactions (e.g. hydrogen bonding or hydrophobic effects) on catalytic $CO_2$ hydration and dehydration reactivity. As noted above, secondary hydrogen bonding likely influences the orientation and reactivity of the zinc-bound hydroxide nucleophile, as well as the coordination properties of the zinc-bound bicarbonate anion, in α-type CAs. To begin to investigate how hydrogen bonding can influence the chemistry of a Zn–OH species relevant to CAs, the $CO_2$ reactivity of a mononuclear zinc hydroxide complex supported by a tripodal tetradentate chelate ligand containing three internal hydrogen-bond donors, [(tnpa)Zn–OH]$ClO_4$ (tnpa = tris((neopentylamino)methyl)amine, Fig. 10), has been investigated.[54] In methanol solution, this complex reacts with $CO_2$ to produce a mononuclear zinc bicarbonate species, [(tnpa)Zn–$O_2$COH]$ClO_4$, that has been characterized by $^1$H and $^{13}$C NMR, and electrospray ionization mass spectrometry. While the X-ray crystal structure of [(tnpa)Zn–OH]$ClO_4$ has been reported, and moderate intramolecular hydrogen-bonding interactions involving the zinc-bound hydroxide anion were identified,[55] the solid-state structure of the bicarbonate

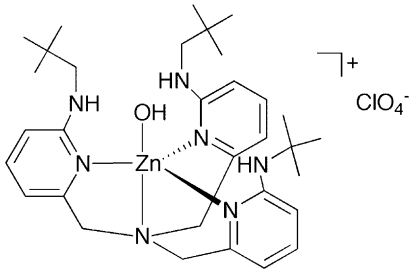


**Fig. 10** [(tnpa)Zn–OH]$ClO_4$.

complex has not been reported. Notably, hydrogen-bonding interactions may also play a role in the $CO_2$ binding properties of a recently reported mononuclear zinc hydroxide complex supported by the tris(hydroxy-2-benzimidazolylmethyl)amine ligand.[56]

## 3 Alcohol oxidation

Zinc-containing alcohol dehydrogenase enzymes catalyze the oxidation of alcohols, or the reduction of aldehydes or ketones, using $NAD^+$/NADH as a required co-factor. The active site zinc center in horse liver alcohol dehydrogenase is tetrahedral and is ligated by one histidine imidazole nitrogen, two cysteine thiolates, and a water molecule.[57] A proposed catalytic cycle (Scheme 5) involves displacement of the zinc-bound water molecule by a primary or secondary alcohol substrate, followed by deprotonation of the alcohol to produce a zinc alkoxide species, which is suggested to be the active species for hydride transfer to $NAD^+$.[58] This hydride transfer reaction results in the formation of a zinc-bound aldehyde or ketone and NADH. Following displacement of the carbonyl compound by water, NADH is released. In this mechanism, the mononuclear distorted tetrahedral Zn(II) center is proposed to lower the $pK_a$ of the alcohol substrate via coordination, and to stabilize the zinc-bound alkoxide species. Importantly, a nearby serine residue (Ser-48) is suggested to assist in stabilization of the zinc alkoxide via formation of a strong hydrogen-bonding interaction involving the zinc-bound oxygen atom.[58,59] From a chemical perspective, the presence of this hydrogen-bonding interaction is not surprising, as the alkoxide-bound oxygen can be expected to be a site of high electron density. This is due to the presence of filled *d*-orbitals for the Zn(II) center which prevents π-donation of electron density from the alkoxide oxygen, thus yielding a strongly polarized Zn–OR bond.[60]

Alternative mechanisms for liver alcohol dehydrogenase have also been proposed. For example, on the basis of a recent atomic resolution (1 Å) X-ray structure of horse liver alcohol dehydrogenase in complex with NADH, a proposal was put forth wherein the zinc center has a coordination number of five, with a zinc-bound water molecule being involved in protonation/deprotonation of the zinc-coordinated

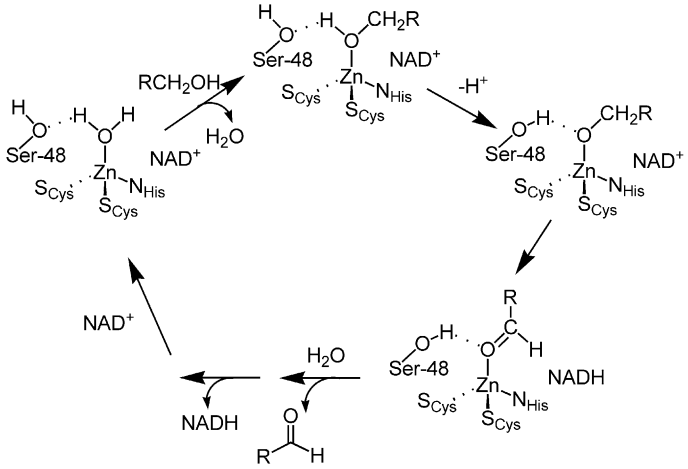


**Scheme 5** Proposed catalytic cycle of horse liver alcohol dehydrogenase.

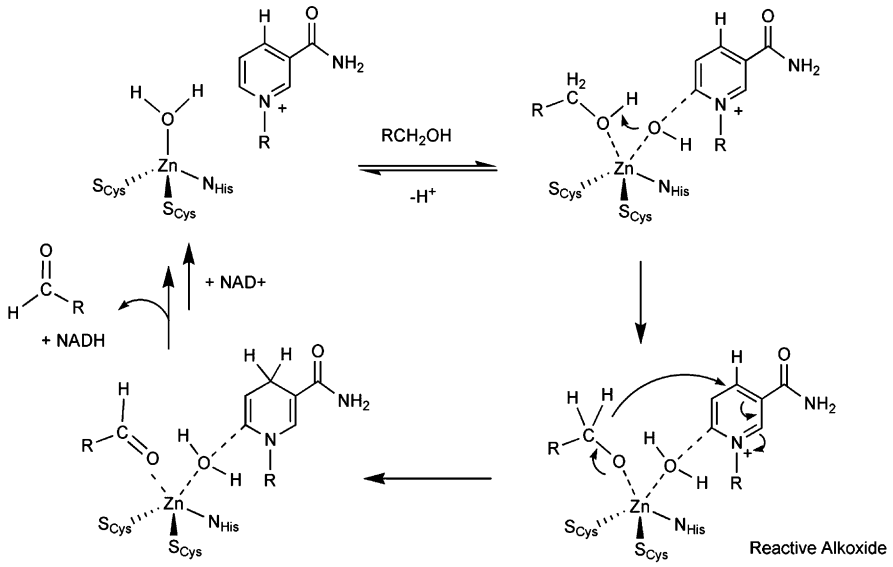


**Scheme 6** Proposed mechanism for liver alcohol dehydrogenase involving a five-coordinate zinc center.

alcohol substrate (Scheme 6). Similar to the mechanism outlined in Scheme 5, a zinc alkoxide species, albeit having a coordination number of five for the metal center, is proposed as the reactive species for hydride transfer.[61] Notably, EPR spectroscopic characterization of Co(II)-substituted liver alcohol dehydrogenase, as well as time-resolved X-ray absorption spectroscopic studies of a bacterial alcohol

dehydrogenase from *Thermoanaerobacter brockii*, are consistent with the presence of a five-coordinate metal center in the presence of alcohol.[62,63]

Catalytically active model systems relevant to liver alcohol dehydrogenase are rare. In one reported system, hydride transfer between isopropanol and *p*-nitrobenzaldehyde is catalyzed by a zinc complex supported by the [12]ane$N_3$ ligand.[64] Specifically, heating of an isopropyl alcohol solution of *p*-nitrobenzaldehyde, containing a catalytic amount of $[([12]aneN_3)Zn(OH)]^+$ for 24 h at reflux results in the formation of $\geqslant 78$ turnovers of *p*-nitrobenzylalcohol. The source of the hydride equivalent was shown to be the methine hydrogen of $(CH_3)_2CHOH$ via labeling with deuterium ($(CH_3)_2CDOH$), which yielded monodeuterated *p*-nitrobenzylalcohol labeled at the benzylic position. This reaction is proposed to proceed via initial formation of a zinc alkoxide species, $[([12]aneN_3)Zn(OCH(CH_3)_3)]^+$ (Scheme 7). Coordination of the aldehyde to the four-coordinate zinc alkoxide species then permits hydride transfer and product formation. For this reaction to proceed, formation of the zinc alkoxide must be thermodynamically favored, and the Zn–OR bond kinetically labile.

Because *p*-nitrobenzaldehyde is a rather poor model for $NAD^+$, the catalytic hydride transfer reactivity of $[([12]aneN_3)Zn(OH)]^+$ in isopropanol solution was

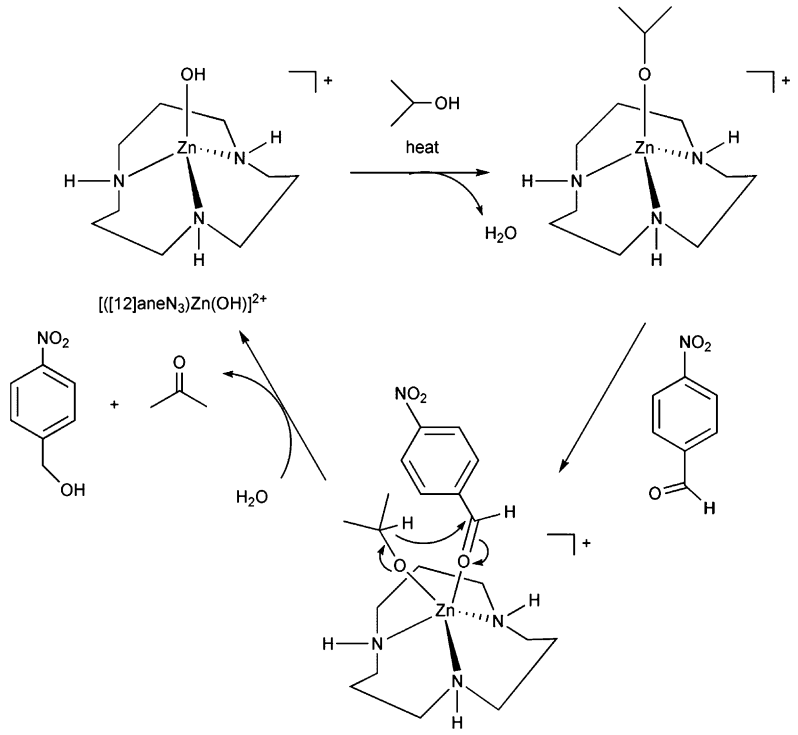


**Scheme 7** Proposed mechanism for hydride transfer catalyzed by a macrocyclic zinc complex.

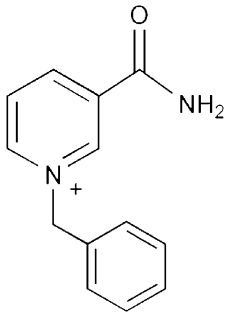


**Fig. 11** *N*-benzylnicotinamide cation.

also examined using the $NAD^+$ mimic *N*-benzylnicotinamide chloride (Fig. 11). Though produced in low yield (17% after 24 h at reflux), formation of the 1,4-hydride transfer product is favored over the 1,6-product (~7.5:1).[64] The low overall yield of the reaction is presumably due to electrostatic repulsion between $[([12]aneN_3)Zn(OH)]^+$ and the *N*-benzylnicotinamide cation.

To examine structure/reactivity relationships for species relevant to those proposed in the catalytic cycle of liver alcohol dehydrogenase, several laboratories targeted mononuclear nitrogen/sulfur-ligated zinc alcohol and alkoxide complexes for synthesis, characterization, and reactivity studies. Preparation of these complexes required the development of new chelate ligands. For example, Parkin and Vahrenkamp employed thioimidazole derivatives to prepare new $S_3$- and $N_2S$-donor chelate ligands that enabled the isolation of rare pseudo-tetrahedral zinc alcohol complexes (Fig. 12).[65,66] These complexes exhibit Zn–O(alcohol) bond distances (1.970(3) and 1.993(3) Å) that are similar to that found in a pentafluorobenzylalcohol-bound structure of liver alcohol dehydrogenase (2.0 Å).[67] Also, both complexes exhibit a hydrogen-bonding interaction between the zinc-coordinated alcohol and another molecule of alcohol in the crystalline lattice. These secondary interactions are characterized by O···O heteroatom distances of ~2.58 Å, which is similar to the distance involving a zinc-bound alcohol and Ser-48 (2.6 Å) in an X-ray structure of liver alcohol dehydrogenase.[67]

Deprotonation of the zinc alcohol complexes shown in Fig. 12 to produce zinc alkoxide species has not been reported. Instead, mononuclear, tetrahedral zinc alkoxide complexes, supported by hydrotris(pyrazolyl)borate ligands, ($[Tp^{But,Me}$ or $Tp^{Ph,Me}$, Scheme 8), have been generated via treatment of zinc hydride precursor complexes with aliphatic alcohols.[68–70] A zinc ethoxide complex, $[Tp^{But,Me}]Zn–OEt$, was also prepared via decarboxylation of the ethyl carbonate complex, $[Tp^{But,Me}]Zn–OC(O)OEt$.[49] X-ray crystallographic studies of $[Tp^{Ph,Me}]Zn–OCH_3$ and $[Tp^{But,Me}]Zn–OEt$ revealed Zn–O bond lengths of 1.874(2) and 1.826(2) Å, respectively.[68,71] These bond distances are $\leqslant$0.1 Å shorter than found for the alcohol complexes shown in Fig. 12.

The alkoxide complexes are very water sensitive, forming equilibrium mixtures with the corresponding zinc hydroxide complex (Scheme 8) that lie far toward

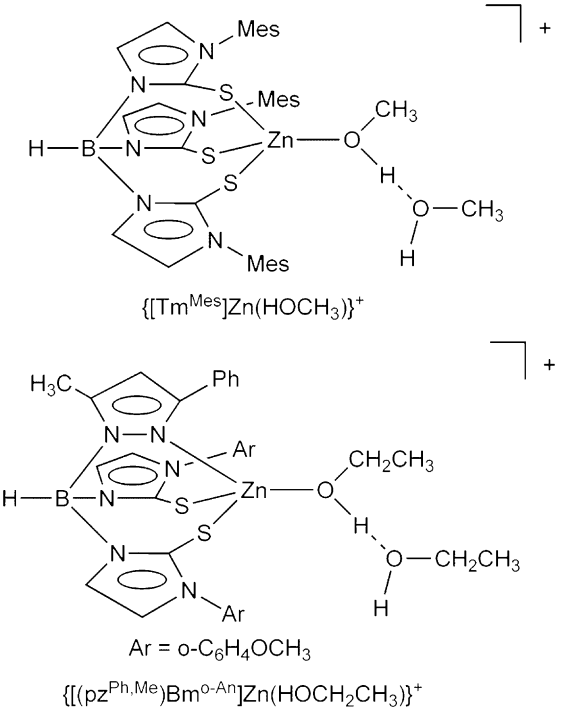


**Fig. 12** Mononuclear tetrahedral zinc alcohol complexes.

the hydroxide derivative.[68,69] This indicates that in a hydrophobic secondary microenvironment, zinc alkoxide species are unstable with respect to hydrolysis. Examination of the equilibrium parameters for the methanolysis of $[Tp^{But,Me}]Zn–OH$ as a function of temperature yielded $\Delta H_{Me} = 1.2(1)\,kcal\,mol^{-1}$ and $\Delta S_{Me} = -9(1)\,eu$.[69]

Mononuclear zinc aryloxide complexes supported by hydrotris(pyrazolyl)borate ligands have enhanced stability with respect to hydrolysis (Scheme 8) as compared to the alkoxide derivatives, and can in some cases be prepared directly from the reaction of the corresponding zinc hydroxide or methoxide complex with the appropriate phenol.[69,72,73] Overall, the hydrolytic stability of each zinc aryloxide complex depends on the electronic properties of the parent phenol, with zinc aryloxide complex formation being favored for phenols having an electron-withdrawing substituent in the para position. This is evident by comparison of the equilibrium constants for the reaction of $[Tp^{But,Me}]Zn–OH$ with 4-nitrophenol ($K = 3.5(8) \times 10^3$) and *p*-methoxyphenol ($K = 4.2(9)$) at 300 K. Construction of a Hammett plot for equilibria involving a variety of substituted phenols yielded a log $K$ versus $\sigma$ plot with good linear correlation and a $\rho$ value of 2.8.[69] DFT calculations indicate that the trend in the Hammett plot is due to the electron-withdrawing substituent enhancing the Zn–OAr bond dissociation energy to a greater extent than the H–OAr bond dissociation energy of the parent phenol. This can be rationalized by the fact

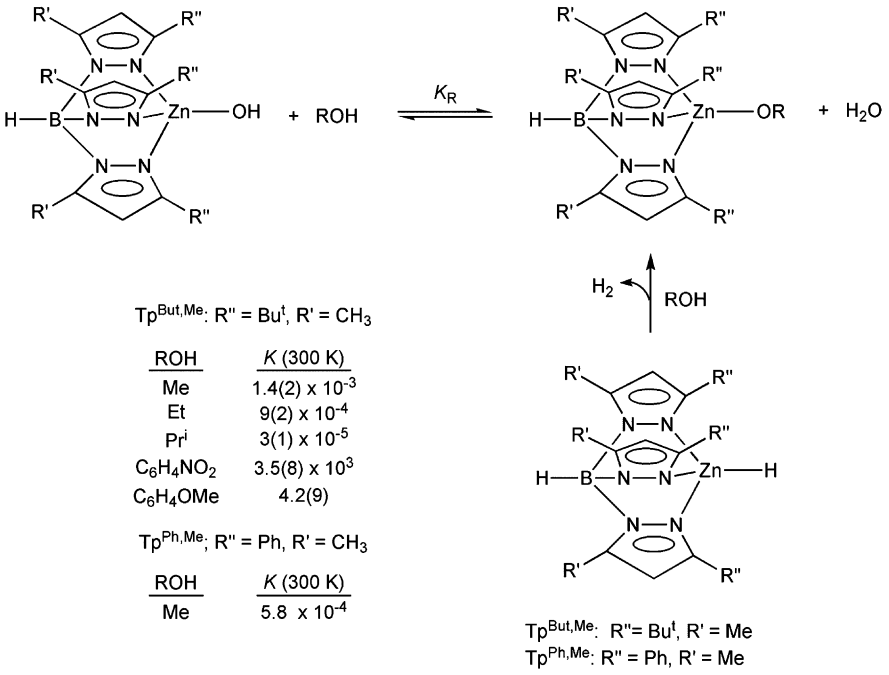


**Scheme 8** Equilibrium formation of tetrahedral zinc-alkoxide and aryloxide complexes. The alkoxide complexes can be independently prepared via treatment of a zinc hydride precursor complex with the appropriate alcohol. Experimental methods for the determination of $K_R$ (300 K) are given in reference 69.

that the more polar Zn–OAr bond would be influenced to a greater extent by an electron-withdrawing substituent than would the H–OAr bond. In the zinc complex the electron withdrawing substituent will help stabilize the enhanced anionic character at the aryloxide oxygen atom.

Similar to the hydrotris(pyrazolyl)borate zinc aryloxide complexes described above, mononuclear zinc complexes having an arylmethoxide ($-OCH_2C_6H_4-p-NO_2$, $-OCH_2C_6F_5$, $-OCH_2C_6F_5$) or alkylated methoxide ($-OCH_2CF_3$ (Scheme 9), $-OCH_2CCl_3$) group with electronegative substituents can be isolated directly from the reaction of a zinc hydroxide complex with the parent alcohol.[70,72]

In a model reaction for liver alcohol dehydrogenase, the zinc ethoxide complex $[Tp^{But,Me}]$Zn–OEt reacts stoichiometrically with *p*-nitrobenzaldehyde in benzene to produce $[Tp^{But,Me}]Zn–OCH_2C_6H_4NO_2$ and acetaldehyde (Scheme 10).[68] For a series of similar reactions involving the zinc isopropoxide complex $[Tp^{Ph,Me}]Zn–OCH(CH_3)_2$ and various aromatic aldehydes in toluene (Scheme 10), the zinc-containing products of the reaction, $[Tp^{Ph,Me}]Zn–OCH_2Ar$, were isolated in 60–70% yield, while the acetone produced was identified using $^1H$ NMR.[70]

Reaction of the hydrotris(pyrazolyl)borate zinc alkoxide complex $[Tp^{Cum,Me}]$Zn–OiPr with the $NAD^+$ mimic *N*-benzylnicotinamide chloride in isopropanol yielded a

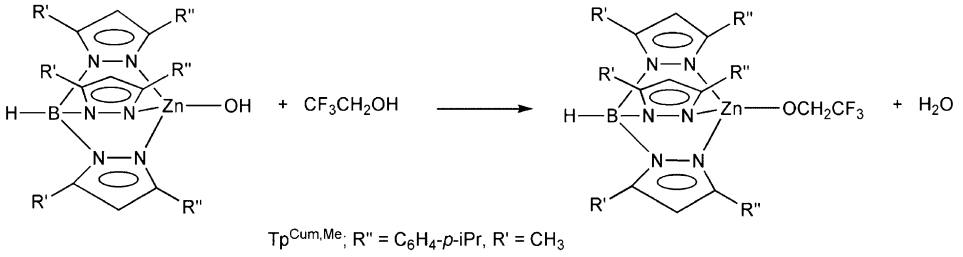


**Scheme 9** Reaction of a zinc hydroxide complex with trifluoroethanol.

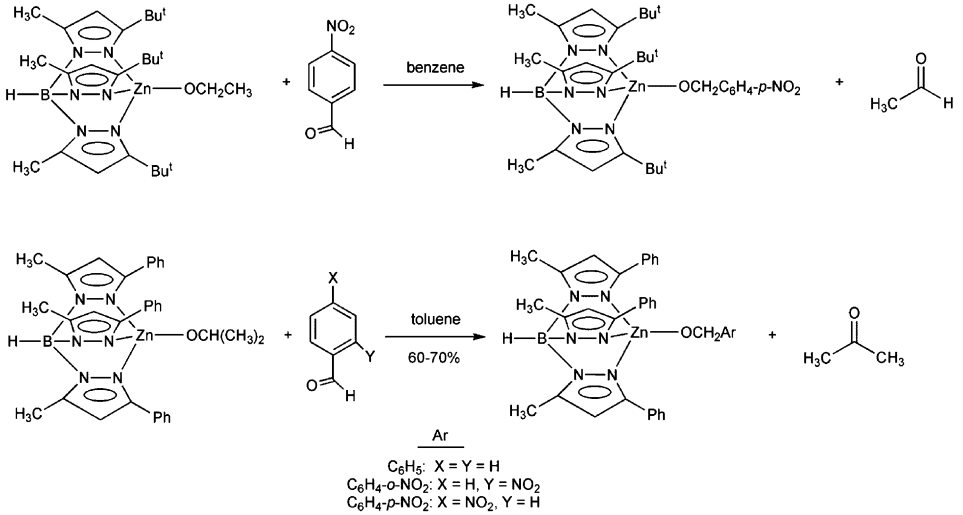


**Scheme 10** Hydride transfer reactivity of zinc alkoxide complexes.

variety of products in low yields.[74] These include acetone (10–20%), as well as the zinc chloride complex [Tp$^{Cum,Me}$]Zn–Cl, reduced *N*-benzylnicotinamide (14%), and the radical coupling product $(BNA)_2$ (1%).

Overall, studies of hydrotris(pyrazolyl)borate-ligated zinc complexes have provided valuable insight into the chemical factors governing the formation, structural properties, and hydrolytic reactivity of tetrahedral zinc alkoxide complexes. However, the low hydride transfer reactivity of these alkoxide complexes indicates that additional factors, including perhaps secondary hydrogen-bonding interactions involving the protein, likely influence catalytic activity in alcohol dehydrogenases. To gauge the influence of hydrogen bonding on the chemistry of zinc alkoxide and hydroxide species, a new ligand (ebnpa, *N*-2-(ethylthio)ethyl-*N,N*-bis(6-neopentylamino-2-pyridylmethyl)amine, Scheme 11) was developed which combined a nitrogen/sulfur donor environment with internal hydrogen-bond donors.[75] Treatment of

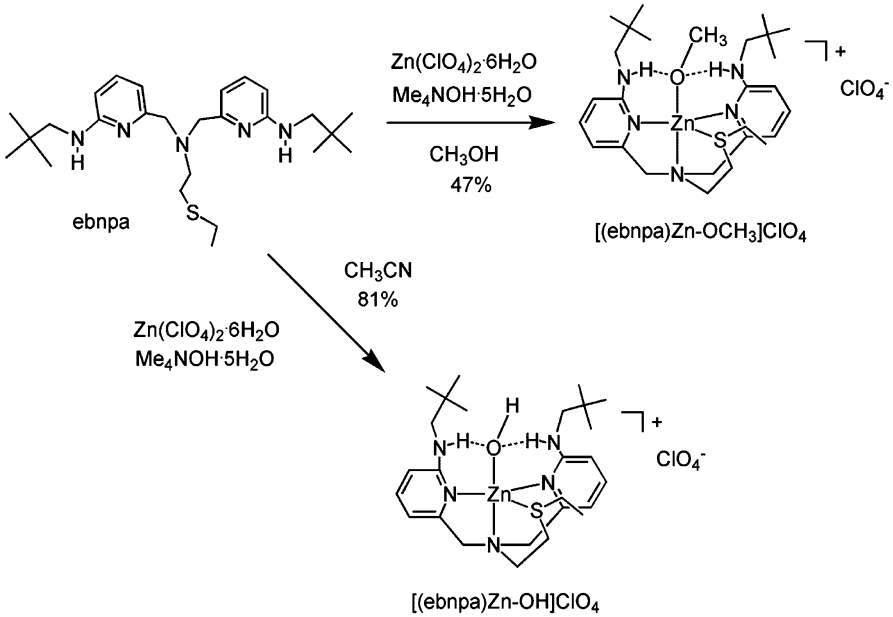


**Scheme 11** Preparative routes for [(ebnpa)Zn–$OCH_3$]$ClO_4$ and [(ebnpa)Zn–OH]$ClO_4$.

the ebnpa ligand with equimolar amounts of $Zn(ClO_4)_2 \cdot 6H_2O$ and $Me_4NOH \cdot 6H_2O$ in methanol yielded [(ebnpa)Zn–$OCH_3$]$ClO_4$, a mononuclear $N_3S$-ligated zinc methoxide complex (Scheme 11). Importantly, this reaction demonstrates that use of a chelate ligand containing two internal hydrogen-bond donors enables the isolation of a zinc methoxide complex directly from methanol solution. In this regard, two mononuclear zinc methoxide complexes, $[Tp^{Ph,Me}]Zn–OCH_3$ and $[(L1)Zn(OCH_3)] \cdot [(L1)Zn(OH)] \cdot (BPh_4)_2$ (L1 = *cis*,*cis*-1,3,5-tris[(*E*,*E*)-3-(2-furyl) acrylideneamino]cyclohexane) have been found to co-crystallize with the corresponding zinc hydroxide complexes from methanol solution.[71,76] In the case of the ebnpa-ligated system, the zinc hydroxide complex [(ebnpa)Zn–OH]$ClO_4$ can be cleanly produced using acetonitrile as the solvent (Scheme 11).

The ebnpa-ligated zinc methoxide and hydroxide complexes exhibit nearly identical metal coordination environments, with both having a distorted trigonal bipyramidal geometry for the Zn(II) center and very similar zinc–ligand bond distances. The only notable difference involves the Zn–S distance ([(ebnpa)Zn–$OCH_3$]$ClO_4$: 2.490(3) Å; [(ebnpa)Zn–OH]$ClO_4$: 2.533(1) Å). For both complexes, the zinc-bound anion is involved in two moderate hydrogen-bonding interactions, each characterized by an N···O(anion) distance of 2.73–2.77 Å.

Treatment of [(ebnpa)Zn–OH]$ClO_4$ with methanol in acetonitrile results in the formation of an equilibrium mixture involving [(ebnpa)Zn–$OCH_3$]$ClO_4$ and water (Scheme 12). The equilibrium constant for this reaction at 304(1) K is 0.30(8). Variable temperature studies of this equilibrium yielded $\Delta H_{Me} = -0.9(1)$ kcal $mol^{-1}$

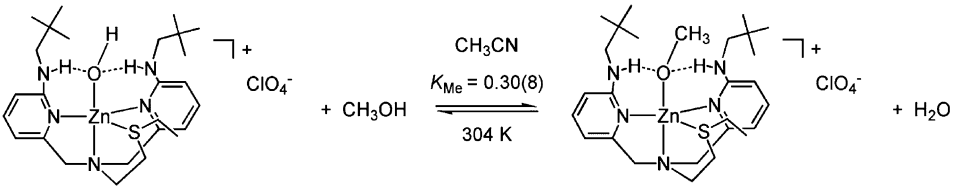


**Scheme 12** Methanolysis equilibrium of ebnpa-ligated zinc hydroxide complex in acetonitrile solution.

and $\Delta S_{Me} = -5(1)$ eu. These values are notably different from those obtained for the equilibrium mixture involving $[Tp^{But,Me}]Zn–OH$ and $[Tp^{But,Me}]Zn–OCH_3$ ($K_{Me}$ (300 K) $1.4(2) \times 10^{-3}$; $\Delta H_{Me} = 1.2(1)$ kcal mol$^{-1}$ and $\Delta S_{Me} = -9(1)$eu; Scheme 8). These combined results indicate that the nature of the supporting chelate ligand dramatically influences the stability of zinc alkoxide species with respect to hydrolysis. While it is tempting to attribute the enhanced hydrolytic stability of $[(ebnpa)Zn–OCH_3]ClO_4$ to the presence of internal hydrogen-bond donors, additional structural features of this complex may also be important. For example, the alkoxide methyl carbon and the thioether ethyl substituent both limit water access to the alkoxide oxygen in $[(ebnpa)Zn–OCH_3]ClO_4$. Thus, steric factors may also influence the water reactivity of this complex.

## 4 Amide hydrolysis

REACTIONS INVOLVING MONONUCLEAR ZINC COMPLEXES

Zinc enzymes catalyze the hydrolysis of amide bonds using a variety of active site structural motifs.[77] An extensively studied enzyme of this class is carboxypeptidase A, which contains a mononuclear zinc center (Fig. 13) within the enzyme active site and catalyzes the hydrolysis of a *C*-terminal amino acid.[78,79] The mechanism of amide cleavage in carboxypeptidase A has been studied extensively.[77,78] In one proposed mechanistic pathway for this enzyme (Scheme 13), termed the ''zinc hydroxide mechanism'', the zinc center activates a water molecule for deprotonation and also assists in polarization of the substrate carbonyl moiety, thus making it more susceptible to nucleophilic attack. The zinc center also provides transition state stabilization through charge neutralization.

A structurally similar active site to that of carboxypeptidase A is found for the endopeptidase thermolysin.[77] While several crystallographic and biochemical studies favor a zinc hydroxide mechanism for thermolysin (involving Glu-143 as a general base),[80] in an alternative proposed mechanism for this enzyme, the zinc center is proposed to activate the substrate for nucleophilic attack by a non-coordinated water molecule (Scheme 14).[81,82]

In both of these mechanisms additional active site residues are indicated to play key roles in the amide cleavage process. For example, in the zinc hydroxide

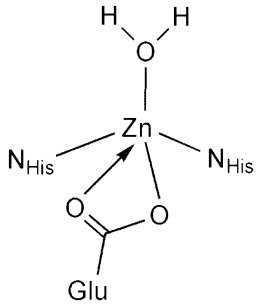


**Fig. 13** Structural features of the active site zinc center in carboxypeptidase A.

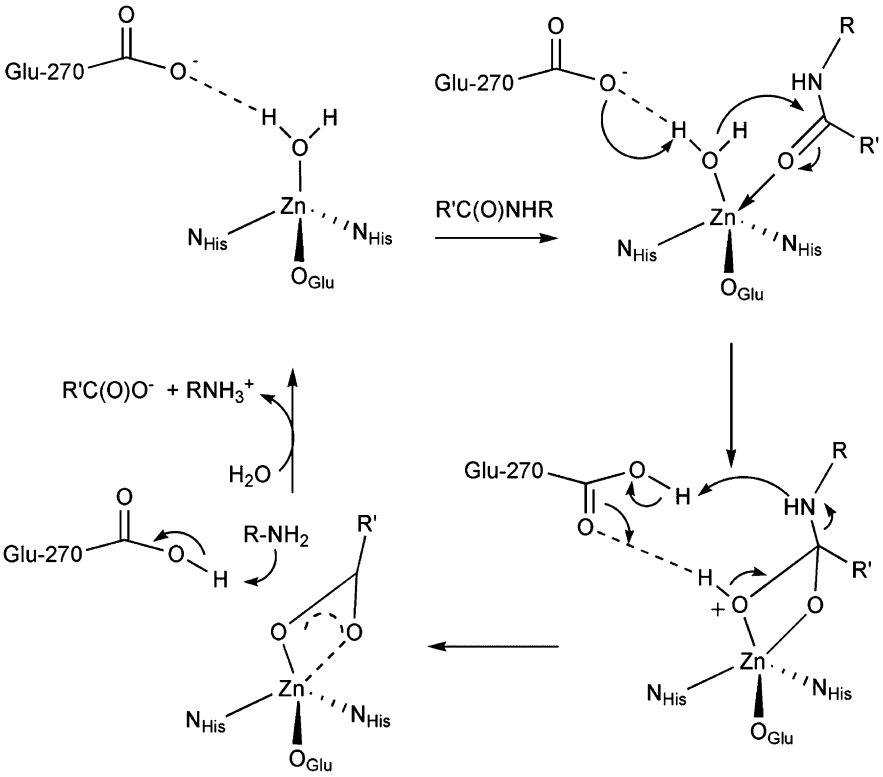


**Scheme 13** Proposed mechanism for amide hydrolysis in carboxypeptidase A involving a zinc-bound hydroxide as the nucleophile.

mechanism proposed for carboxypeptidase A, positively charged residues (Arg-127 and Arg-145) provide electrostatic stabilization of the substrate. In addition, as shown in Scheme 13, Glu-270 acts as a general base to first deprotonate the zinc-bound water molecule and then protonate the amino moiety of the leaving group. In

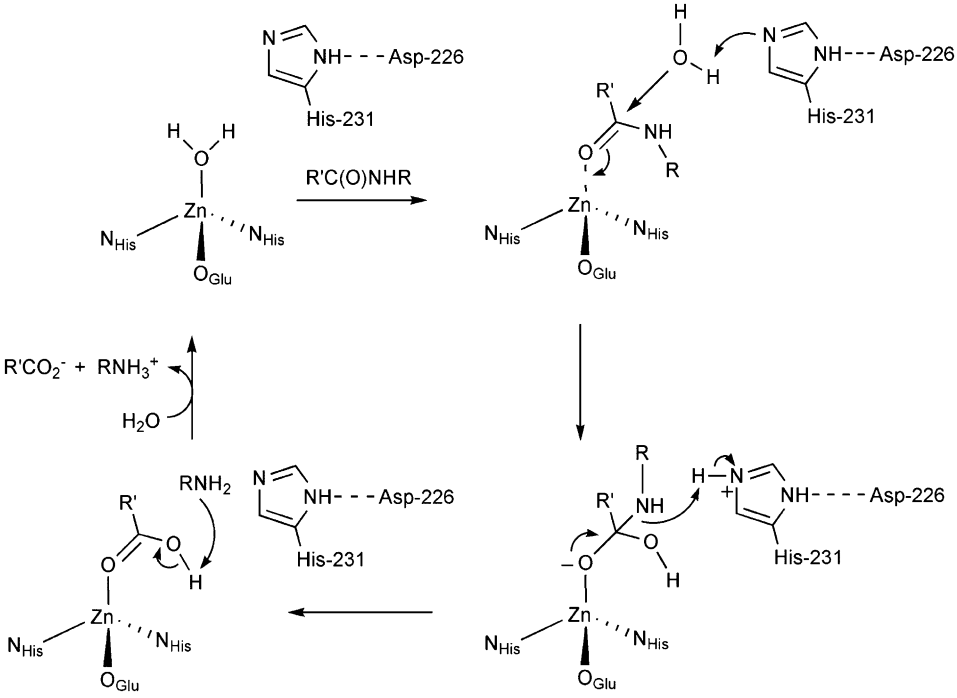


**Scheme 14** Mechanism proposed for peptide hydrolysis catalyzed by thermolysin.

the mechanism proposed for thermolysin, an active site histidine residue (His-231 in thermolysin) acts as a general base to deprotonate an active site water molecule and then protonate the amine group.

There are several additional examples of zinc enzymes that contain an active site mononuclear zinc center and catalyze the hydrolysis of peptides bonds. These include carboxypeptidase B[83] and neutral protease[84] both of which contain a $[(N_{His})_2(O_{Glu/Asp})Zn–OH_2]$ coordination motif within the enzyme active site. Zinc peptidases that contain a $[(N_{His})_3Zn–OH_2]$ active site metal center include matrix metalloproteinases[85,86] and other members of the metzincins superfamily.[77,85]

Early model studies for amide-hydrolyzing metalloenzymes centered on studies of stoichiometric amide hydrolysis reactions involving exchange inert Co(III) complexes in aqueous solution.[87] These studies provided evidence that amide hydrolysis can proceed via activation of the amide carbonyl by the Co(III) center and attack by an external $OH^-$, or via an intramolecular pathway wherein a Co(III)–$OH_n$ moiety ($n = 1$ or 2) attacks a chelated, but non-coordinated amide carbonyl (Fig. 14). Co(III) complexes having either amide substrate or water/hydroxide coordination exhibit significant rate enhancement for amide hydrolysis.[88,89] However, a comparative investigation of the stoichiometric formylmorpholine hydrolysis reactivity of a Co(III) complex of the 1,4,7,11-tetraazacclododecane (cyclen) ligand (Fig. 14, center column)

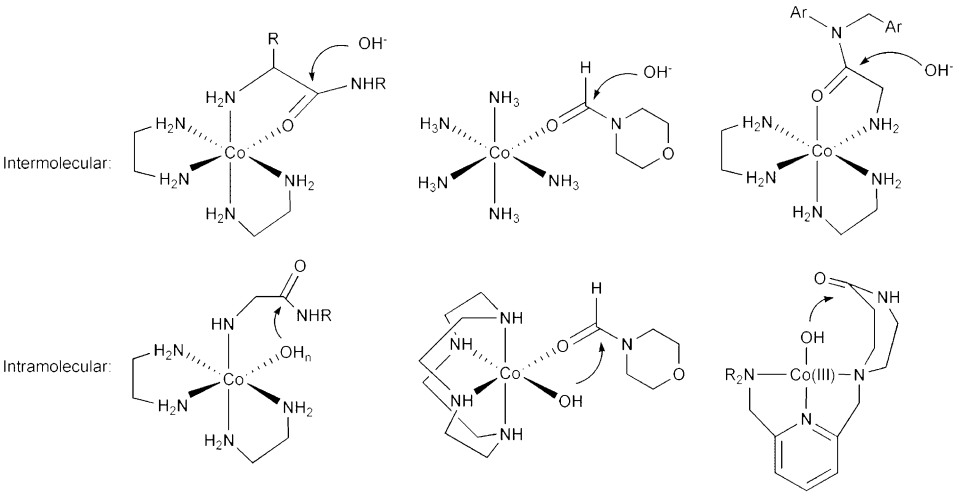


**Fig. 14** Cobalt(III) complexes that exhibit inter- or intramolecular amide cleavage reactivity.

versus that of $[(NH_3)_5Co(OH_2)]^{3+}$ revealed that the greatest rate acceleration occurs when both amide substrate and hydroxide nucleophile are coordinated to the metal center simultaneously in a *cis* orientation.[90]

Sayre proposed five possible mechanisms for metal-mediated amide hydrolysis (Fig. 15).[91,92] In these proposed pathways, the metal center can be involved in electrophilic carbonyl activation (A), metal hydroxide nucleophile activation (B), and a combined mechanism involving both of these processes (C). Amide hydrolysis may also involve a metal-bound hydroxide or water molecule acting as a general base or general acid (Fig. 15d and e).

A limited number of mechanistic studies of stoichiometric amide hydrolysis reactions promoted by Zn(II) complexes have been reported. Groves and Chambers reported studies of the zinc-mediated hydrolysis of an internal amide substrate wherein amide carbonyl coordination to the zinc center is not possible (Scheme 15).[93] Examination of the rate of this reaction as a function of pH (6.5–10.5) yielded a kinetic $pK_a = 9.16$. First-order rate constants at 70 °C ($\mu = 0.5$ ($NaClO_4$)) for the Zn–$OH_2$ and Zn–OH-mediated amide hydrolysis reactions differed by a factor of ~100 when the data was fit to Equation (1) for the proposed mechanism shown in Scheme 16. The activation parameters determined for this reaction ($\Delta H^{\ddagger} = 22(1)\,\text{kcal mol}^{-1}$ and $\Delta S^{\ddagger} = -18(3)\,\text{eu}$) are consistent with an intramolecular hydrolysis process wherein a zinc-bound hydroxide acts as an intramolecular nucleophile to attack the amide carbonyl in the rate-determining step.

A mononuclear zinc hydroxide complex supported by a hydrophobic hydrotris(pyrazolyl)borate ligand mediates the stoichiometric hydrolysis of an activated amide.[94] As shown in Scheme 17, treatment of [($Tp^{Cum,Me}$)Zn–OH] with

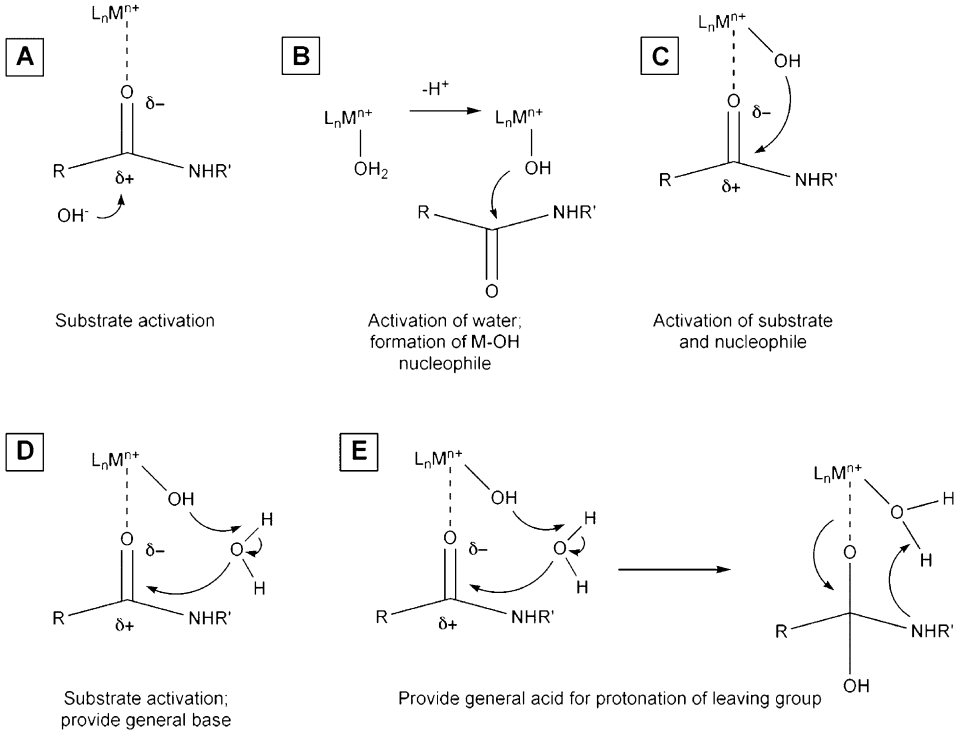


**Fig. 15** Role of metal center in proposed mechanistic pathways for amide cleavage.

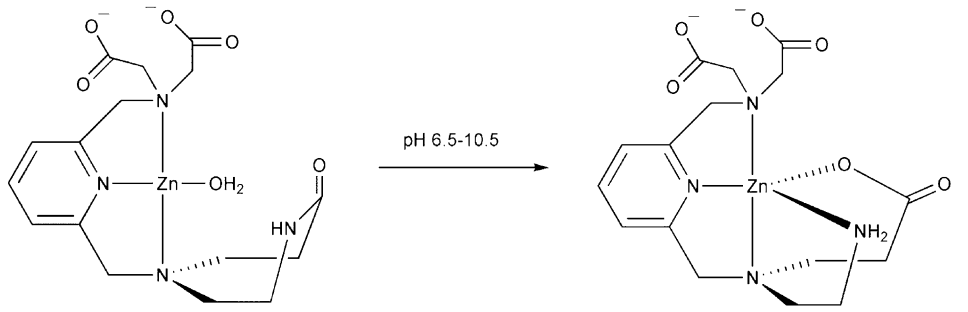


**Scheme 15** Role of metal center in proposed mechanistic pathways for amide cleavage. Adapted from reference 92.

trifluoroacetamide results in the formation of a new zinc carboxylate complex.[95] The geometrical changes that occur at the zinc center during this and related hydrolysis reactions (e.g. phosphate and carboxy ester hydrolysis) have been elucidated using a Bürgi–Dunitz structural correlation method.[96] Specifically, analysis of a series of

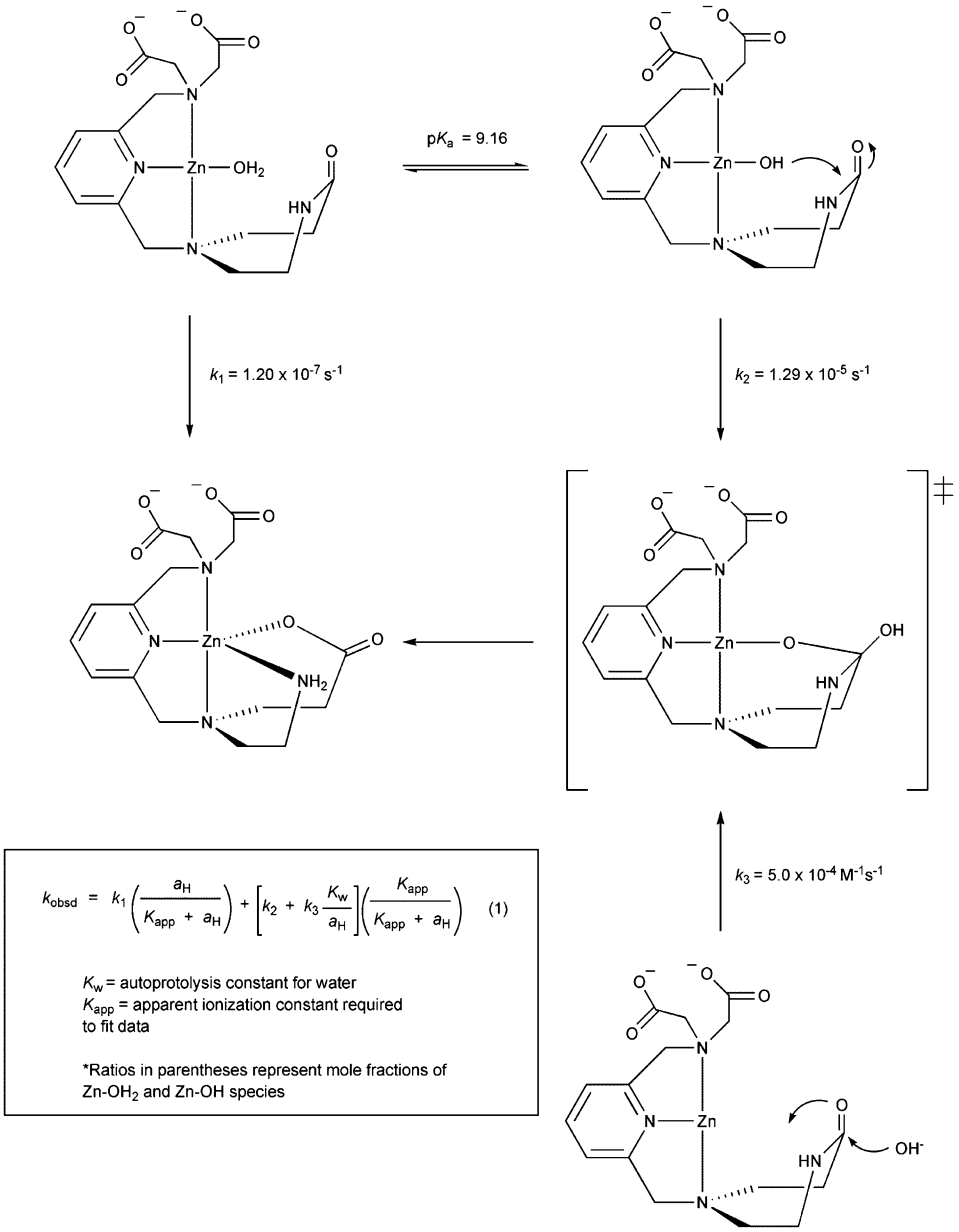


**Scheme 16** Proposed mechanism and rate law for the zinc-mediated amide hydrolysis reaction.

four- and five-coordinate structures of $Tp^{R,R'}$-ligated zinc complexes suggests that the first step in substrate hydrolysis involves approach of the substrate oxygen atom to the mononuclear Zn–OH center along a three-fold axis of an incipient trigonal bipyramidal zinc structure (Scheme 18). Berry pseudorotation, which proceeds via

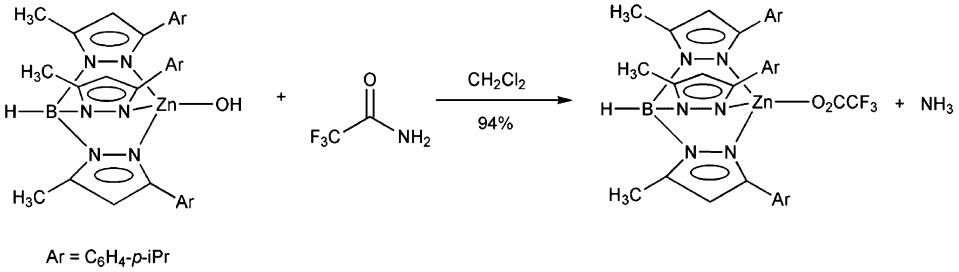


**Scheme 17** Activated amide hydrolysis reactivity of [($Tp^{Cum,Me}$)Zn–OH].

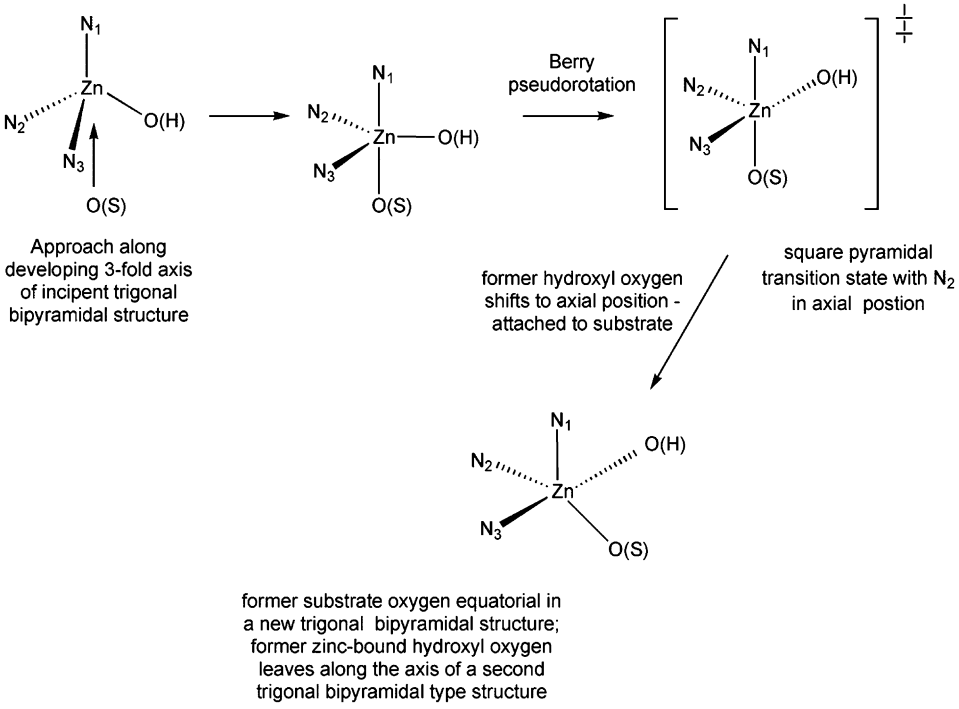


**Scheme 18** Proposed geometrical changes that occur at the zinc center during a Zn–OH-promoted substrate hydrolysis reaction. This proposed pathway is based on a Bürgi–Dunitz-type structural correlation for $Tp^{R,R'}$-ligated zinc complexes.

a square pyramidal transition state, results in the substrate oxygen occupying an equatorial position and the former hydroxyl oxygen atom, which is now attached to the substrate, being placed in an axial position. If operative for the zinc centers in enzymes such as CA and carboxypeptidase A, this type of transformation indicates that product release should occur from an axial position of a five-coordinate trigonal bipyramidal-type structure.

## CARBOXY ESTER HYDROLYSIS REACTIVITY OF MONONUCLEAR ZINC COMPLEXES

Carboxy esters are more easily hydrolyzed than amides and several studies of carboxy ester hydrolysis mediated by discrete mononuclear zinc complexes have been reported. These reactions are relevant to the esterase activity exhibited by some zinc hydrolases (e.g. CA[97] catalyzes the hydrolysis of 4-nitrophenyl acetate) and in some cases are also used as model reactions for amide hydrolysis.[17,36,96,98–101] For example, the mononuclear zinc hydroxide complex [([12]aneN$_3$)Zn(OH)]ClO$_4$ catalyzes the hydrolysis of methyl acetate in neutral water at 25(1)°C with a turnover time of approximately 60 min at [$CH_3C(O)OCH_3$] = 1 M and pH = 8. Development of a rate-pH profile for this reaction yielded a sigmoidal plot with a kinetic p$K_a$ of 7.3. This value is identical to the p$K_a$ value for [([12]aneN$_3$)Zn($OH_2$)](ClO$_4$)$_2$ (Fig. 4) determined by potentiometric titration (7.30 ± 0.02) thus indicating that the zinc hydroxide form of the complex attacks the ester carbonyl in the rate-determining step of the reaction.[36]

Similar results were found for the hydrolysis of 4-nitrophenyl acetate catalyzed by [([12]aneN$_3$)Zn(OH)]ClO$_4$. The second-order rate constant for this reaction is $(3.6 \pm 0.3) \times 10^{-2}\,M^{-1}\,s^{-1}$ at 25 °C, pH = 8.2, and $I$ = 0.10 ($NaClO_4$).[36,98] From the temperature dependence of the rate constant, an Arrhenius plot was constructed, which revealed an activation energy of $49 \pm 2\,kJ\,mol^{-1}$ for this carboxy ester hydrolysis reaction.[98] Using the zinc cyclen complex [([12]aneN$_4$)Zn(OH)]ClO$_4$, the second-order rate constant is $(1.0 \pm 0.1) \times 10^{-1}\,M^{-1}\,s^{-1}$ at 25 °C and the activation energy for the reaction is $45 \pm 2\,kJ\,mol^{-1}$.[99] The similarity of the activation energies for the [([12]aneN$_3$)Zn(OH)]ClO$_4$ and [([12]aneN$_4$)Zn(OH)]ClO$_4$ catalyzed reactions to that of the aqueous $OH^-$-catalyzed reaction ($43 \pm 2\,kJ\,mol^{-1}$) suggests that all of these 4-nitrophenyl acetate hydrolysis reactions proceed via rate-determining attack of hydroxide (either free or zinc bound) on the ester carbonyl carbon atom (Fig. 16).[99]

Notably, addition of a methyl group to the cyclen ring (Fig. 17) results in a considerably slower reaction ($k'' = 4.7(1) \times 10^{-2}\,M^{-1}\,s^{-1}$ at 25 °C).[102] This has been attributed to steric hindrance imposed by the methyl group, which is suggested to lower the nucleophilicity of the Zn–OH moiety toward the ester substrate.

The mononuclear zinc hydroxide complex [($Tp^{Cum,Me}$)Zn–OH] promotes the stoichiometric hydrolysis of activated esters such as 4-nitrophenylacetate, triflouroacetate, and trifluorolactone (Scheme 19). Following the hydrolysis of 4-nitrophenyl acetate, the liberated product 4-nitrophenol rapidly reacts with [($Tp^{Cum,Me}$)Zn–OH] to yield [($Tp^{Cum,Me}$)Zn–O–$C_6H_4$–*p*-$NO_2$].[95,96] By monitoring the formation of [($Tp^{Cum,Me}$)Zn–O–$C_6H_4$–*p*-$NO_2$] using UV–visible spectroscopy, the second-order rate constant for the 4-nitrophenylacetate hydrolysis reaction at 25 °C was found to be $3.5 \times C\ 10^{-3}\,M^{-1}\,s^{-1}$. This rate is considerably slower than that found for the hydrolysis of 4-nitrophenylacetate by [([12]aneN$_3$)Zn(OH)]ClO$_4$ and [([12]aneN$_4$)Zn(OH)]ClO$_4$ ($(3.6 \pm 0.3) \times 10^{-2}\,M^{-1}\,s^{-1}$ and $(1.0 \pm 0.1) \times 10^{-1}\,M^{-1}\,s^{-1}$, respectively) in aqueous solution,[36,99] or by aqueous base ($9.5\,M^{-1}\,s^{-1}$ at 25 °C).[103] The slower rate of the [($Tp^{Cum,Me}$)Zn–OH]-promoted reaction is attributed to the chloroform solvent employed in the kinetic studies, which is less polar than water. Variable temperature kinetic studies of the [($Tp^{Cum,Me}$)Zn–OH]-promoted reaction, and

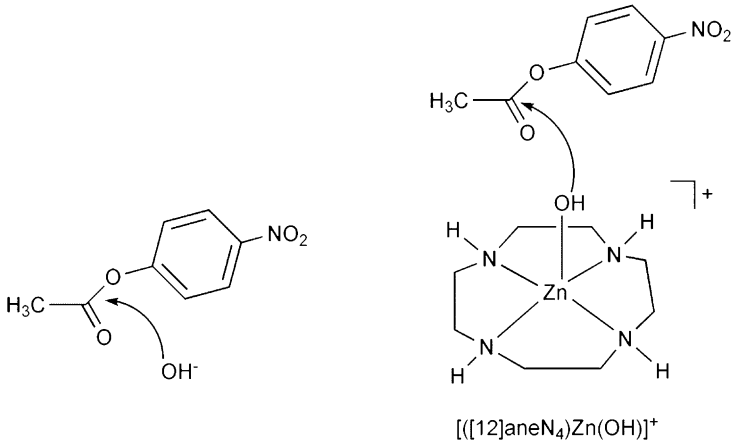


**Fig. 16** Proposed pathways of 4-nitrophenyl acetate hydrolysis catalyzed by aqueous hydroxide ion and $[([12]aneN_4)Zn(OH)]^+$.

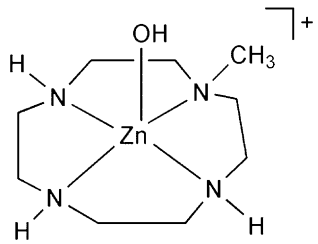


**Fig. 17** $[(CH_3cyclen)Zn–OH]^+$.

construction of an Arrhenius plot, yielded an activation energy of 64.3 kJ mol$^{-1}$. The activation enthalpy ($\Delta H^{\ddagger} = 61.8$ kJ mol$^{-1}$) and entropy ($\Delta S^{\ddagger} = -85.6$ J mol K$^{-1}$) for this reaction were determined from a plot of $\ln(k''/T)$ versus $1/T$. Notably, these values are similar to those found for the hydrolysis of 4-nitrophenylacetate catalyzed by the $N_2S$(thiolate)-ligated zinc hydroxide complex [(PATH)Zn–OH] (Scheme 20; $E_a = 54.8$ kJ mol$^{-1}$; $\Delta H^{\ddagger} = 52.4$ kJ mol$^{-1}$; $\Delta S^{\ddagger} = -90.0$ J mol K$^{-1}$).[17] The activation parameters for the [(PATH)Zn–OH]-catalyzed reaction have been interpreted as corresponding to rate-determining attack of the zinc hydroxide moiety on the 4-nitrophenylacetate carbonyl carbon, as has been discussed for $[([12]aneN_4)Zn(OH)]^+$ (Fig. 16).

Presented in Table 1 is a summary of the second-order rate constants for the hydrolysis of 4-nitrophenyl acetate promoted by various zinc complexes in aqueous solution. A conclusion that may be drawn from this data is that change in the nature of the supporting chelate ligand dramatically influences the second-order rate constant for the carboxy ester hydrolysis reaction. Notably, the slowest rate is found for the four-coordinate zinc hydroxide species $[([12]aneN_3)Zn(OH)]^+$ which has three

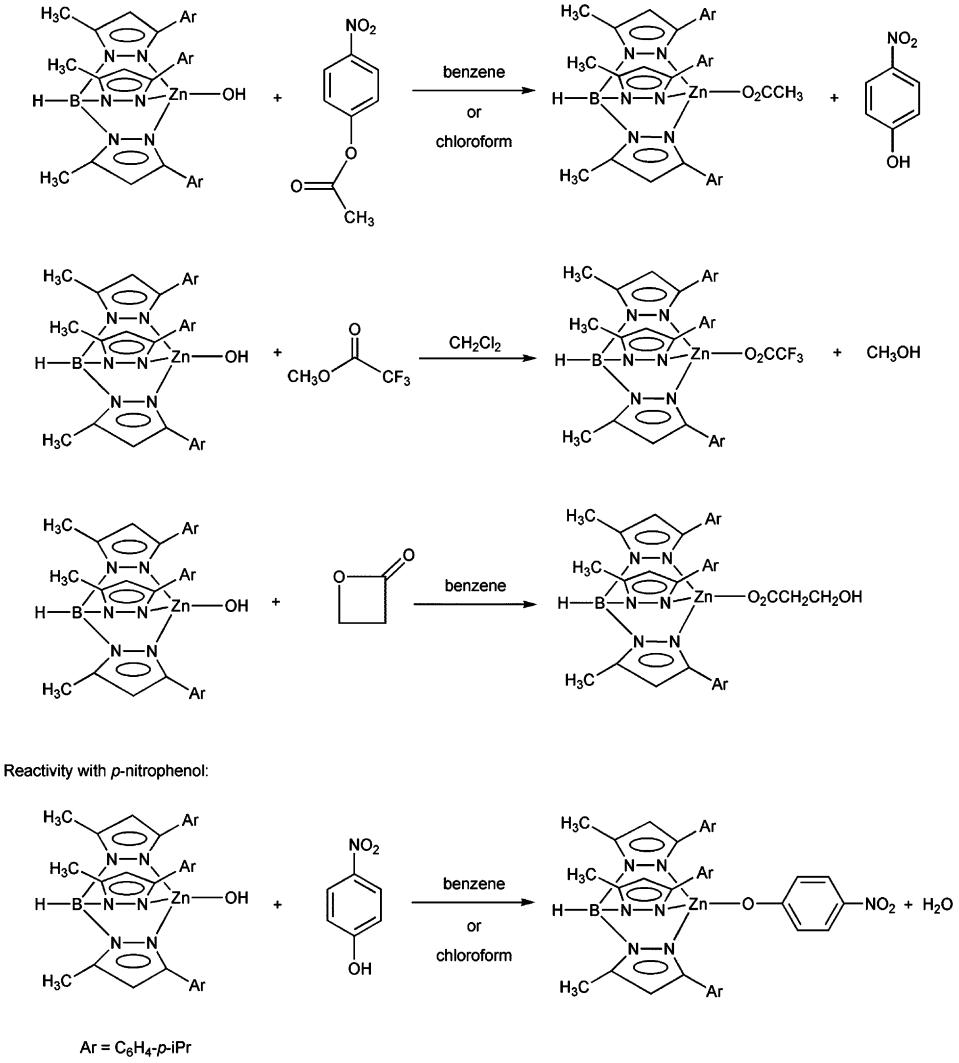


**Scheme 19** Ester hydrolysis reactivity of [($Tp^{Cum,Me}$)Zn–OH].

neutral nitrogen donors, in addition to the hydroxide anion, as ligands to the zinc center. This complex also exhibits the lowest p$K_a$ for the zinc-bound water molecule. For complexes having one additional neutral nitrogen donor (e.g. [([12]ane$N_4$)Zn(OH)]$^+$ and [($CH_3$cyclen)Zn–OH]$^+$), the zinc center has enhanced electron density, which in turn raises the Zn–$OH_2$ p$K_a$ value, and enhances the nucleophilicity of the Zn–OH moiety and the rate of carboxyester hydrolysis. As noted above, the rate of carboxyester hydrolysis mediated by [($CH_3$cyclen)Zn–OH]$^+$ (Fig. 17) is influenced by steric hindrance from the methyl substituent. In [(PATH)Zn–OH], the

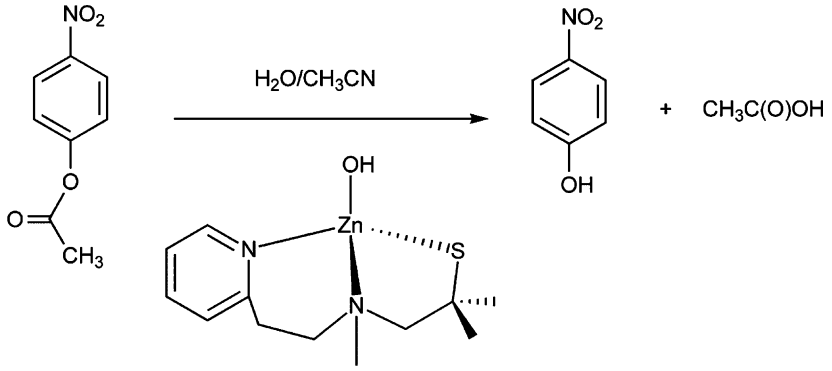


**Scheme 20** 4-Nitrophenyl acetate hydrolysis catalyzed by [(PATH)Zn–OH].

**Table 1** Comparison of p$K_a$ values of zinc complexes and second-order rate constants $k''$ ($M^{-1}\,s^{-1}$) for the hydrolysis of 4-nitrophenyl acetate at 25 °C with that of human CA-II. Adapted from reference 17.

| | p$K_a$ | $k''$ ($M^{-1}\,s^{-1}$) | Reference |
|---|---|---|---|
| $OH^-$ | 15.7 | 9.5 | 103 |
| $[([12]aneN_3)Zn(OH)]^+$ | 7.3 | $0.036 \pm 0.003$[a] | 98 |
| $[([12]aneN_4)Zn(OH)]^+$ | 7.9 | $0.1 \pm 0.01$[a] | 99 |
| $[(CH_3cyclen)Zn–OH]^+$ | 7.68 | $0.047 \pm 0.001$[a] | 102 |
| [(PATH)Zn–OH] | 8.05(5) | $0.089 \pm 0.003$[b] | 17 |
| $[([15]aneN_3O_2)Zn–OH]^+$ | 8.8 | $0.6 \pm 0.06$[c] | 104,105 |
| $[(L2)Zn–OH]^+$ | 8.74 | 0.934[d] | 107 |
| Human carbonic Anhydrase II | 6.8(1) | $2500 \pm 200$[e] | 108 |

[a] 20 mM CHES (pH = 9.3), $I = 0.10$ ($NaNO_3$), 10% (v/v) $CH_3CN$.
[b] $H_2O/CH_3CN$ (90:10 v/v), $I = 0.10$ M ($NaClO_4$).
[c] $I = 0.15$ M NaCl.
[d] $H_2O/CH_3CN$ (90:10 v/v), $I = 0.10$ M ($KNO_3$).
[e] $k_{cat}/K_M$.

four-coordinate zinc center has two neutral nitrogen donors, an alkyl thiolate, and the hydroxide anion as ligands. This complex has a p$K_a$ value of 8.05(5) for the zinc-bound water molecule. The presence of the anionic thiolate donor enhances the electron density at the zinc center, which in turn enhances the rate of the 4-nitrophenyl acetate hydrolysis reaction relative to that found for $[([12]aneN_3)Zn(OH)]^+$. Interestingly, the p$K_a$ values and second-order rate constants for $[([12]aneN_4)Zn(OH)]^+$ and [(PATH)Zn–OH] are similar, indicating that the Lewis acidity of the zinc centers in these two complexes are similar. In other words, the four neutral nitrogen donor ligands in $[([12]aneN_4)Zn(OH)]^+$ provide a similar amount of electron density to the zinc center as do two neutral nitrogen donors and an alkyl thiolate in [(PATH)Zn–OH].

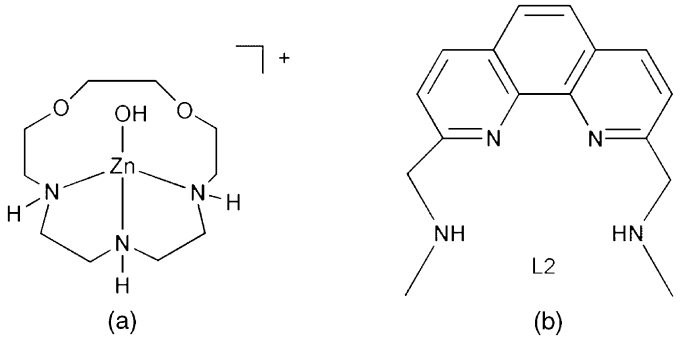


**Fig. 18** (a) $[([15]aneN_3O_2)Zn(OH)]^+$ and (b) L2 ligand.

In $[([15]aneN_3O_2)Zn(OH)]^+$ (Fig. 18a), the mononuclear zinc center is ligated by three neutral nitrogen donors.[104,105] However, the $pK_a$ for the zinc-bound water molecule (8.8) in the corresponding aqua complex is considerably higher than that found for $[([12]aneN_3)Zn(OH_2)]^{2+}$ (7.3).[98] This was suggested to be due to hydrogen bonding between the hydrogen atoms of the zinc-bound water molecule and the oxygen atoms of the macrocycle.[104,106] Despite the reduced acidity of the $[([15]aneN_3O_2)Zn(OH)]^+$ cation, it exhibits enhanced nucleophilicity toward 4-nitrophenyl acetate, with $k'' = 0.6 \pm 0.06\ M^{-1}\ s^{-1}$. This enhanced reactivity may be due to a more exposed Zn–OH moiety, as the ethylenic chains in $[([15]aneN_3O_2)Zn(OH)]^+$ may produce a subtly different coordination environment than the propylenic chains found in $[([12]aneN_3)Zn(OH)]^+$.

A zinc(II) hydroxo complex supported by a secondary amine-appended phenanthroline ligand (L2, Fig. 18b) has been reported to catalyze the hydrolysis of 4-nitrophenyl acetate with a second-order rate constant of $0.934\ M^{-1}\ s^{-1}$.[107] A mechanism involving attack of a terminal zinc hydroxide moiety on the 4-nitrophenyl acetate substrate has been proposed.

The catalytic activity of the zinc complexes given in Table 1 for 4-nitrophenylacetate hydrolysis is well below that found for free $OH^-$ or for the zinc center for human CA-II.[108] In the case of $OH^-$, this is consistent with the proposed mechanism for 4-nitrophenyl acetate hydrolysis shown in Fig. 16 wherein the rate-determining step is attack on the substrate carbonyl. In this reaction, the best nucleophile will be free $OH^-$. In metalloenzymes such as CA, the presence of the zinc center insures that a hydroxide nucleophile can be generated at relatively low concentrations of free $OH^-$.

Outside the scope of coverage of this contribution are Zn(II)-promoted carboxyester hydrolysis reactions involving multinuclear zinc complexes or systems wherein the first step involves transesterification.[98,100–102,105,109–114]

## β-LACTAM HYDROLYSIS

Metallo-β-lactamases catalyze the hydrolytic ring opening of a β-lactam ring in antibiotics containing this structural unit (e.g. penicillins, cephalosporins, carbapenems),

thus making the antibiotic inactive (Fig. 19).[115–118] These enzymes are gaining increasing attention in the clinical sector due to their ability to hydrolyze all β-lactam derivatives, and because there are currently no clinically useful inhibitors for metallo-β-lactamases.[119]

All metallo-β-lactamases require Zn(II) for catalytic activity.[117,118,120] The active site ligands for the zinc centers include histidine, aspartate, and cysteine amino acid ligands, and a bridging hydroxide/water moiety (Fig. 20).[121–123] For the majority of metallo-β-lactamases, maximal activity is obtained when both Zn(II) binding sites are fully occupied. However, the physiologically active form may contain only a single zinc ion in the tetrahedral $(N_{His})_3Zn_1$ binding site.[124] When two zinc centers are present, the Zn···Zn distance is approximately 3.5 Å and both metal centers are involved in coordination of a water/hydroxo moiety. The role of the second zinc center in several metallo-β-lactamases ($Zn_2$, Fig. 20) is still under investigation.

Distinct mechanisms may be operative for the bimetallic versus the monometallic forms of these enzymes.[125–128] Generally, mechanistic pathways have been proposed wherein the β-lactam carbonyl is polarized via interaction with a zinc center. Following nucleophilic attack by a zinc-bound hydroxide and formation of a tetrahedral intermediate, cleavage of the C–N bond occurs. Protonation of the β-lactam nitrogen atom then occurs, along with dissociation of the carboxylate moiety from the zinc center resulting in the release of the ring-opened product.

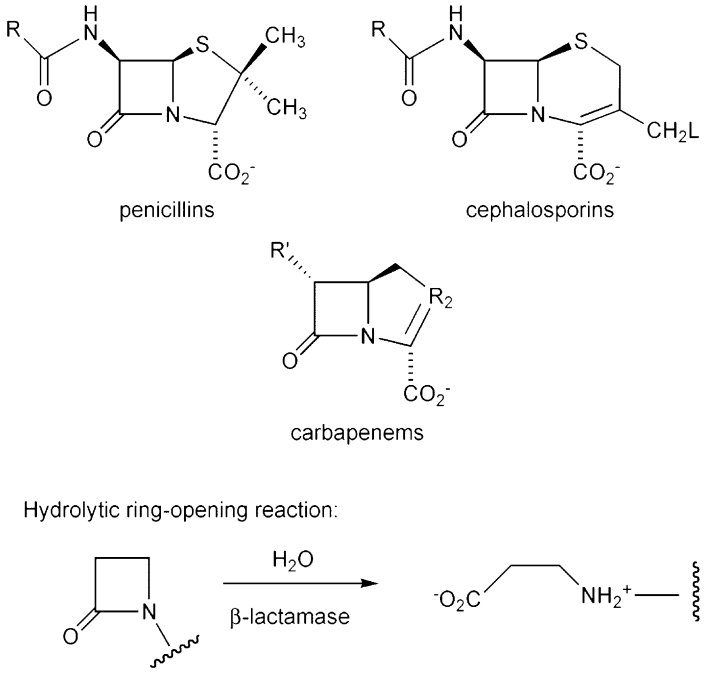


**Fig. 19** (top) Types of β-lactam antibiotics and (bottom) hydrolytic ring opening catalyzed by β-lactamase enzymes.

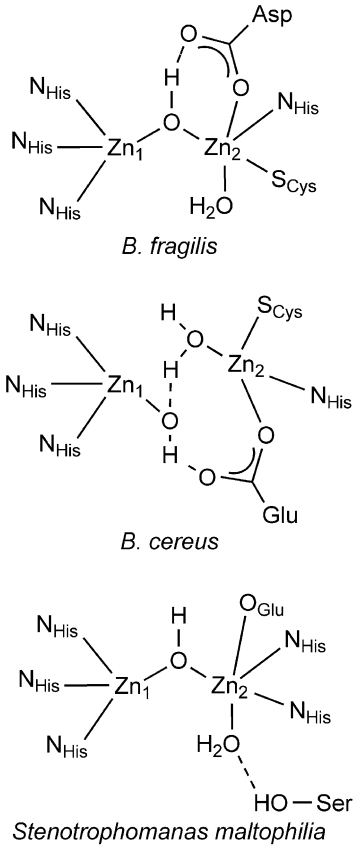


**Fig. 20** Structural features of the active site zinc centers in metallo-β-lactamases.

Model studies for metallo-β-lactamases have been performed using mononuclear zinc hydroxide complexes.[99,129,130] The breadth of β-lactam hydrolysis reactivity of hydrotris(pyrazolyl)borate-ligated mononuclear zinc hydroxide complexes has been explored.[129] Treatment of the mononuclear zinc hydroxide complex [($Tp^{Ph,Me}$)Zn–OH] with simple β-lactams (β-propiolactam, 4-phenyl-β-propiolactam, Scheme 21) does not result in ring opening, but instead results in the formation of β-lactamide complexes and water. Treatment of [($Tp^{Ph,Me}$)Zn–OH] with *N*-alkyl or -aryl β-lactam derivatives instead results in no reaction (Scheme 21). Use of natural derivatives of penicillin and cephalosporin (Scheme 22) did not yield β-lactam hydrolysis, but instead coordination of the carboxylate moiety of the antibiotic derivatives to the mononuclear Zn(II) center and release of water.

Notably, only for β-lactams containing a *N*-nitrophenyl or *N*-acyl group (Scheme 23) was ring-opening lactam hydrolysis identified, albeit under rather forcing conditions (boiling toluene solution).[129] In the case of a β-lactam containing a *N*-fluoroacetyl substituent, reaction is found at the exocyclic acetyl functionality. The reactions of

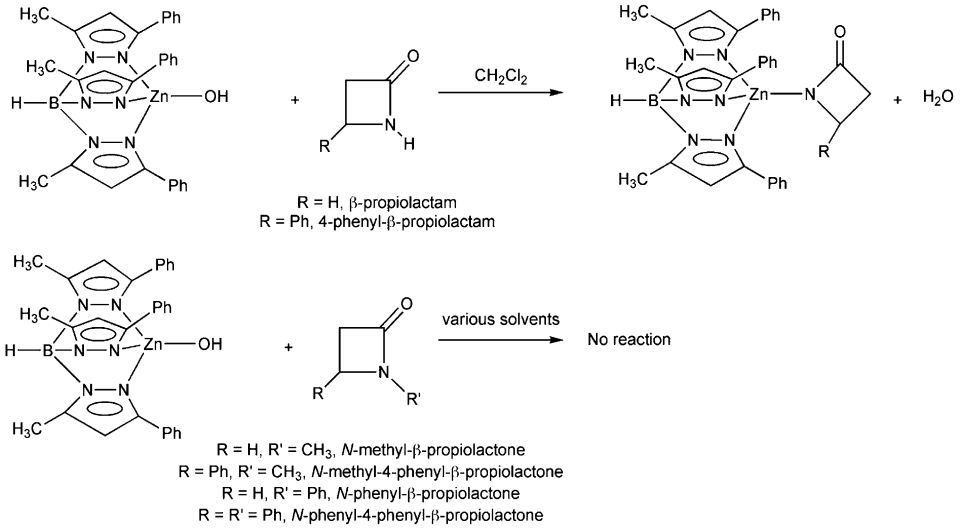


**Scheme 21** Reactivity of [(Tp$^{Ph,Me}$)Zn–OH] with unactivated β-lactams.

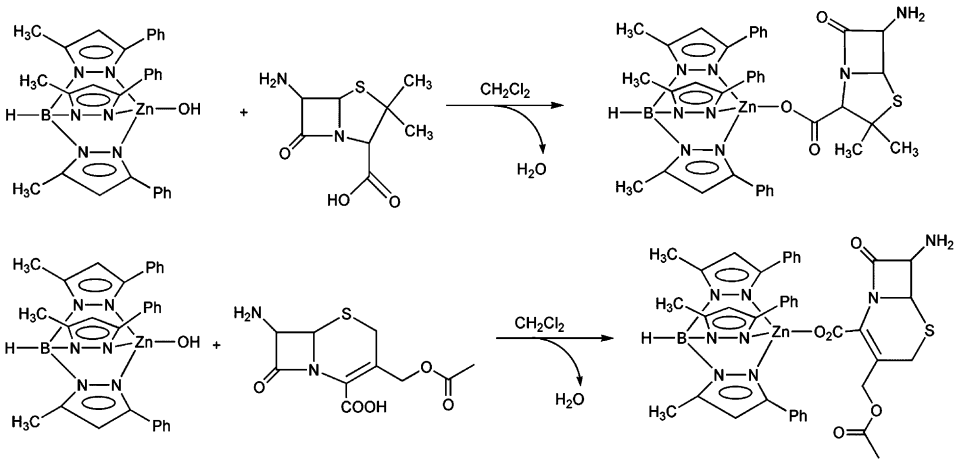


**Scheme 22** Reactivity of [(Tp$^{Ph,Me}$)Zn–OH] with derivatives of penicillin and cephalosporin.

[(Tp$^{Ph,Me}$)Zn–OH] and [(Tp$^{Cum,Me}$)Zn–OH] with the *N*-2,4-dinitrophenyl-appended β-lactam substrate were monitored by $^1$H NMR under pseudo first-order conditions in $CDCl_3$. The second-order rate constants for these reactions were determined to be $0.57\,M^{-1}\,s^{-1}$ (Tp$^{Ph,Me}$) and $0.13\,M^{-1}\,s^{-1}$ (Tp$^{Cum,Me}$) at 40 °C. The slower rate for the reaction involving [(Tp$^{Cum,Me}$)Zn–OH] is consistent with the enhanced steric hindrance and hydrophobicity of the Tp$^{Cum,Me}$ ligand relative to Tp$^{Ph,Me}$.

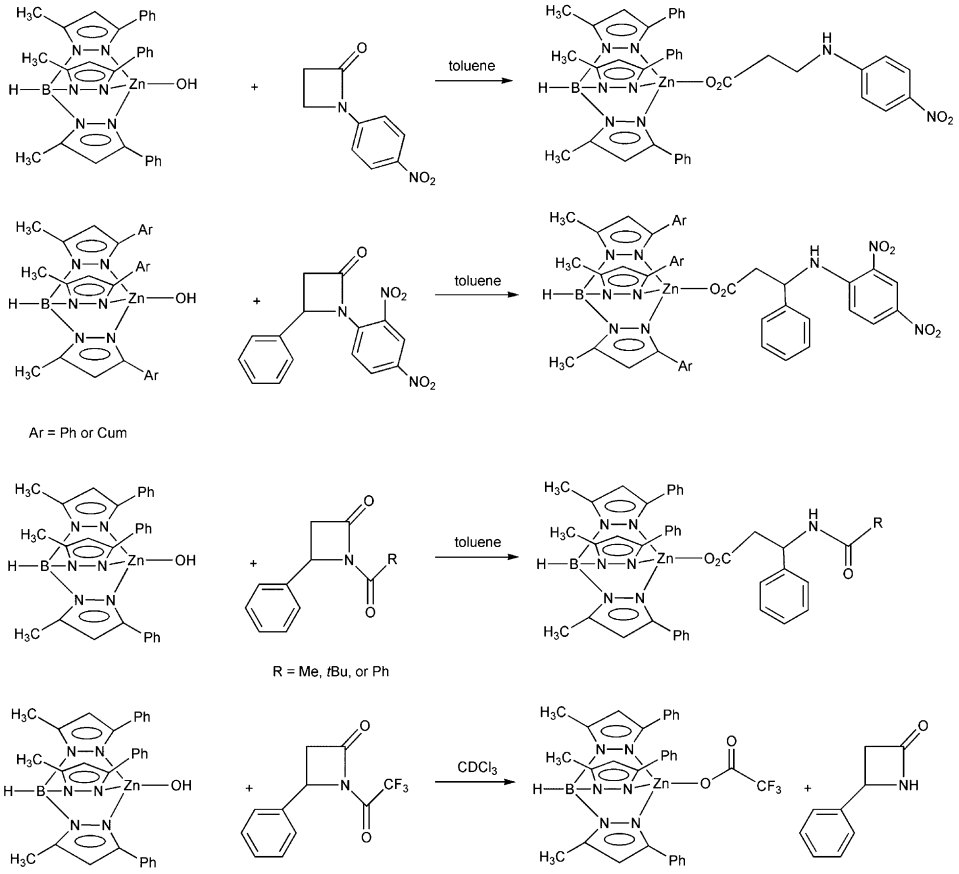


**Scheme 23** Reactivity of [($Tp^{Ar,Me}$)Zn–OH] (Ar = Ph or Cum) with activated β-lactams.

Treatment of $[([12]aneN_4)Zn(OH)]^+$ with penicillin G (benzylpenicillin) at 25 °C ($pD = 9$) results in the formation of both the hydrolysis product, (5*R*)-benzylpenicilloate (Scheme 24) and an epimer of this product (5*S*-benzylpenicilloate).[99] Notably, no spectroscopic evidence was found during the course of this reaction for interaction between $[([12]aneN_4)Zn(OH)]^+$ and the β-lactam nitrogen of penicillin G. Measurement of the rate of reaction as a function of pH (6.6–9.6) yielded a sigmoidal curve and an inflection at pH = 7.9. This value is identical to the thermodynamic $pK_a$ measured for $[([12]aneN_4)Zn(OH_2)]^{2+}$ via potentiometric titration, thus indicating that the zinc hydroxide species $[([12]aneN_4)Zn(OH)]^+$ is the reactive species for penicillin G hydrolysis. The second-order rate constant for this hydrolysis reaction is $(4.1 \pm 0.1) \times 10^{-2}\,M^{-1}\,s^{-1}$ at 25 °C and $I = 0.10$ ($NaNO_3$).[99] Variable temperature kinetic measurements in the range of 15−35 °C and construction of an Arrhenius plot yielded an activation energy for lactam hydrolysis of

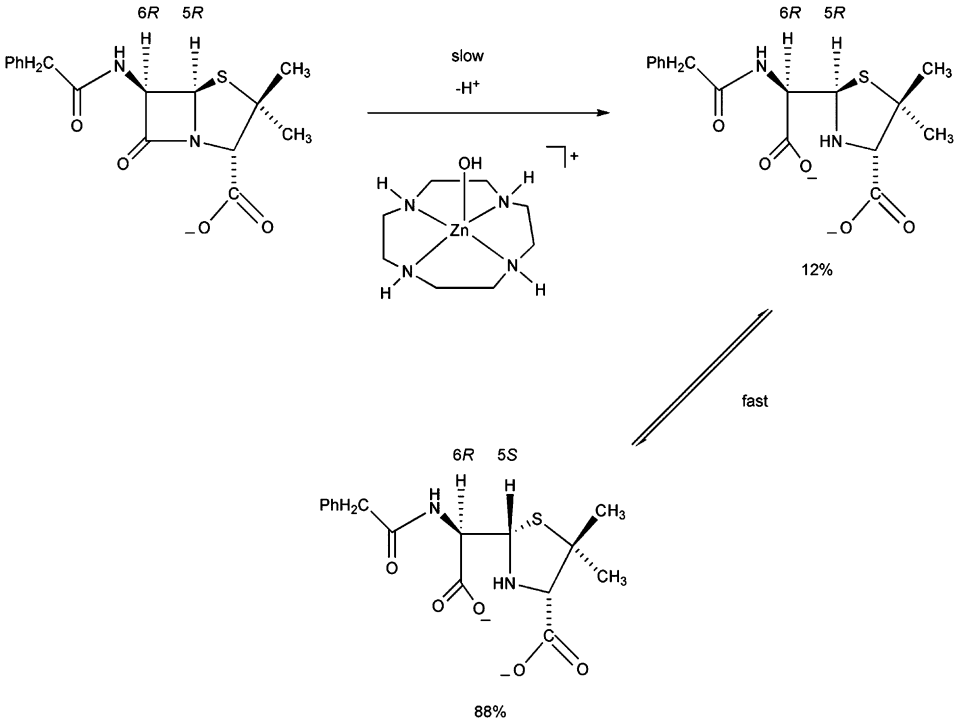


**Scheme 24** Reaction of $[([12]aneN_4)Zn–OH]^+$ with penicillin G.

$49 \pm 2\,kJ\,mol^{-1}$. In a companion study, the aqueous $OH^-$-catalyzed penicillin G hydrolysis reaction was found to have an activation energy of $61 \pm 2\,kJ\,mol^{-1}$. Interestingly, comparison of these two activation energies indicates that the zinc complex lowers the activation barrier for penicillin G hydrolysis by $\sim 12\,kJ\,mol^{-1}$. This is likely due to stabilization of the anionic tetrahedral intermediate by the divalent metal center.[99]

Mechanistic studies of the reaction catalyzed by the metallo-β-lactamase from *Bacteroides fragilis* have been performed using nitrocefin (Scheme 25) as a substrate.[127,131,132] Several theoretical studies pertinent to possible steps in the mechanistic pathway have also been reported.[133–139] Issues stemming from these studies that remain unresolved include whether the nucleophilic hydroxide is bridging or terminal, and the chemical nature of an intermediate that is detected during the hydrolysis of nitrocefin.

Mechanistic studies of nitrocefin hydrolysis catalyzed by $[Zn_2(BPAN)(\mu\text{-}OH)(\mu\text{-}O_2PPh_2)](ClO_4)_2$ (Fig. 21) have provided insight into a reaction pathway of β-lactam hydrolysis involving a binuclear zinc motif.[140] Treatment of $[Zn_2(BPAN)(\mu\text{-}OH)(\mu\text{-}O_2PPh_2)](ClO_4)_2$, which retains a binuclear cationic structure in water, with nitrocefin in a 9:1 mixture of 0.50 M HEPES buffer (in $H_2O$) and dimethyl sulphoxide (DMSO) results in characteristic spectroscopic changes consistent with the

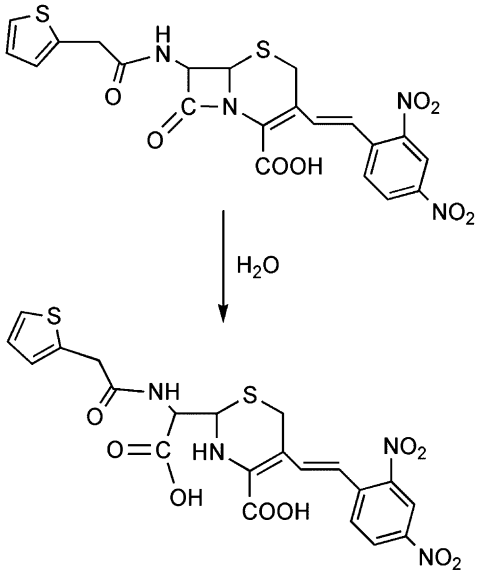


**Scheme 25** Structure of nitrocefin and its hydrolysis product.

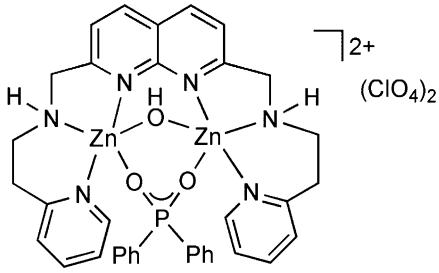


**Fig. 21** $[Zn_2(BPAN)(\mu\text{-}OH)(\mu\text{-}O_2PPh_2)](ClO_4)_2$.

hydrolytic ring opening of the lactam ring. Specifically, an absorption feature that is present for nitrocefin at 390 nm ($\varepsilon = 21{,}000\,M^{-1}\,cm^{-1}$) shifts to 486 nm ($\varepsilon = 10{,}000\,M^{-1}\,cm^{-1}$) in the ring-opened product. This reaction proceeds with a rate enhancement of $2.8 \times 10^3$ relative to the uncatalyzed hydrolysis of the lactam. The rate of the reaction depends on the concentration of substrate, and increases with the presence of increasing amounts of $[Zn_2(BPAN)(\mu\text{-}OH)(\mu\text{-}O_2PPh_2)](ClO_4)_2$, but not in a linear fashion. Overall, saturation kinetic behavior is observed and was fit by invoking a proposed mechanism wherein substrate coordination to the bizinc cation precedes lactam hydrolysis. Using this mechanism, the experimental data was fit to Equation (2) (Scheme 26), which yielded $K = (1.1 \pm 0.2) \times 10^3\,M^{-1}$ and $k_2 = (3.2 \pm 1.0) \times 10^{-3}\,min^{-1}$.

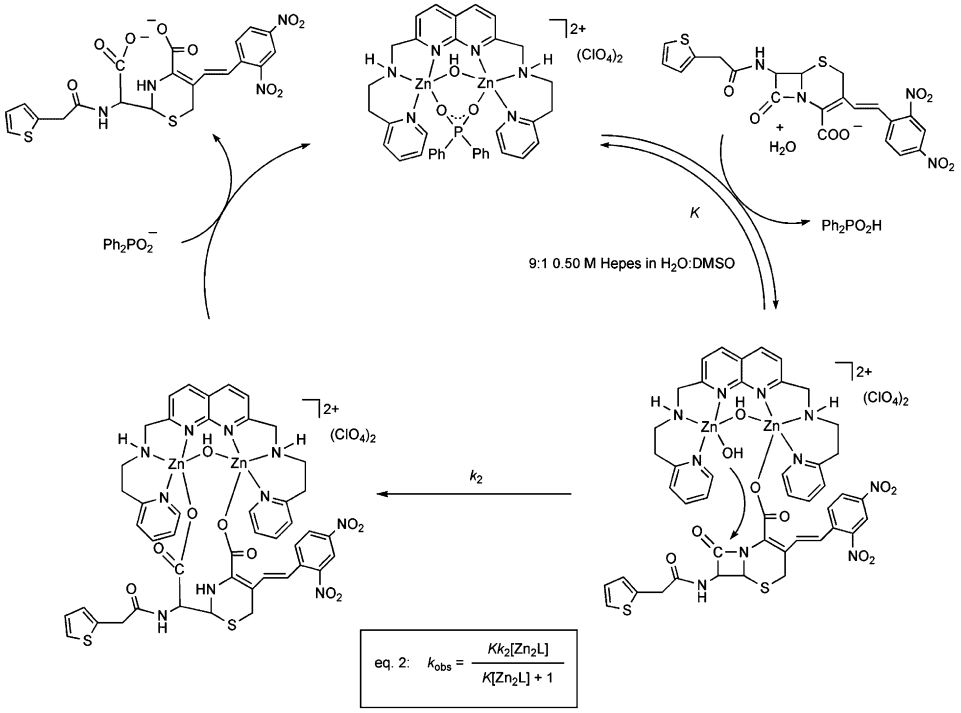


**Scheme 26** Proposed mechanism for nitrocefin hydrolysis catalyzed by $[Zn_2(BPAN)(\mu\text{-}OH)(\mu\text{-}O_2PPh_2)](ClO_4)_2$.

The involvement of a terminal zinc hydroxide moiety in the hydrolysis of nitrocefin (Scheme 26), and not the bridging hydroxide ligand present in $[Zn_2(BPAN)(\mu\text{-}OH)(\mu\text{-}O_2PPh_2)](ClO_4)_2$, was determined on the basis of pH-rate studies. The rate of hydrolysis of nitrocefin catalyzed by $[Zn_2(BPAN)(\mu\text{-}OH)(\mu\text{-}O_2PPh_2)](ClO_4)_2$ increases as the pH increases, suggesting the involvement of a zinc hydroxide species. However, considering the possible involvement of either a zinc aqua or zinc hydroxide moiety as the reactive species for the lactam hydrolysis reaction, the experimental pH-rate data were fit to Equation (3) (Scheme 27). This yielded rate constants for hydrolysis by the $LZn_2\text{–}OH_2$ ($7.5 \times 10^{-4}\,min^{-1}$) and $LZn_2\text{–}OH$ ($3.4 \times 10^{-2}\,min^{-1}$) species, and a kinetic $pK_a$ value of $8.7 \pm 0.2$. Notably, this $pK_a$ value is identical to that measured for a terminal $LZn_2\text{–}OH_2$ moiety on the $[Zn_2(BPAN)(H_2O)(\mu\text{-}OH)(\mu\text{-}O_2PPh_2)](ClO_4)_2$ complex framework.[141] Overall, these results indicate that: (1) a zinc hydroxide species is significantly more reactive than a zinc aqua moiety for nitrocefin hydrolysis and (2) the reactive $LZn_2\text{–}OH$ species in this system is derived from a terminal $LZn_2\text{–}OH_2$ moiety, and the bridging hydroxide ligand is not involved in nitrocefin hydrolysis.

Further evidence for the proposed mechanistic pathway shown in Scheme 26 was derived from independent $^{13}C$ NMR and infrared spectroscopic studies of the

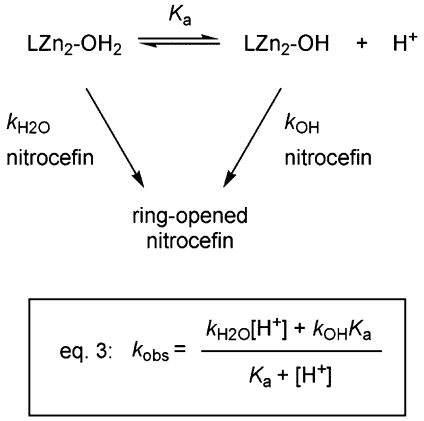


**Scheme 27** Proposed mechanism and rate law for pH-dependence of nitrocefin hydrolysis.

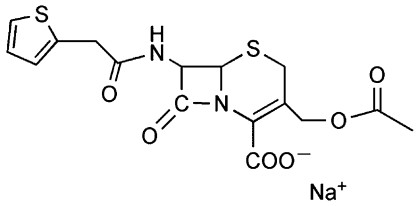


**Fig. 22** Sodium salt of cephalothin.

β-lactam binding properties of $[Zn_2(BPAN)(\mu\text{-}OH)(\mu\text{-}O_2PPh_2)](ClO_4)_2$ in pure DMSO.[140] These studies revealed evidence for the interaction of the carboxylate moiety of cephalothin (Fig. 22), a nitrocefin analog, with the binuclear zinc center. Specifically, the carboxylate carbonyl carbon signal is shifted downfield in the presence of this zinc complex, which is indicative of metal coordination.[142] In addition, the presence of a $\nu_{COO}$ band at $1626\,cm^{-1}$ is consistent with monodentate coordination of the cephalothin carboxylate to Zn(II).[143–145] The amide carbonyl oxygen atom of the β-lactam ring does not interact with a zinc center, as evidenced by the fact that no significant shift in the $\nu_{C=O}$ vibration of the lactam was identified. This coordination motif, in which only the carboxylate moiety of cephalothin interacts with a zinc center, contrasts with studies of divalent metal ion-promoted hydrolysis of penicillin G, wherein bidentate coordination of the lactam to the metal center occurs via the carboxylate and the nitrogen β-lactam atom.[146] Other coordination motifs have also been proposed in reactive systems involving metal ions, including Cu(II)-coordination of the non-lactam deprotonated amide nitrogen.[147]

Additional kinetic studies performed under conditions wherein less water was present (1:9 DMSO: acetone containing 0.28 M $H_2O$) yielded $K = (8.9 \pm 0.3) \times 10^3\,M^{-1}$. The difference between the equilibrium binding constant $K$ for the nitrocefin hydrolysis reaction catalyzed by $[Zn_2(BPAN)(\mu\text{-}OH)(\mu\text{-}O_2PPh_2)](ClO_4)_2$ under

these conditions, versus the same reaction performed in aqueous buffer solution ($K = (1.1 \pm 0.2) \times 10^3\,M^{-1}$), indicates that water competes with the nitrocefin substrate for coordination to the binuclear zinc complex. However, the presence of varying amounts of water does not significantly impact $k_2$ ($(3.2 \pm 1.0) \times 10^{-3}\,min^{-1}$ in 9:1 0.50 M HEPES (in $H_2O$): DMSO versus $k_2 = (6.6 \pm 1.6) \times 10^{-3}\,min^{-1}$ in 1:9 DMSO containing 0.28 M $H_2O$), which is consistent with a mechanism involving intramolecular attack of a Zn–OH nucleophile on a coordinated nitrocefin molecule.

Variable temperature kinetic studies of the nitrocefin hydrolysis reaction catalyzed by $[Zn_2(BPAN)(\mu\text{-}OH)(\mu\text{-}O_2PPh_2)](ClO_4)_2$ in aqueous solution (9:1 0.50 M HEPES buffer (in $H_2O$):DMSO) yielded $\Delta H^{\ddagger} = 62.7 \pm 3.2\,kJ\,M^{-1}$ and $\Delta S^{\ddagger} = -130 \pm 10\,J\,M^{-1}\,K^{-1}$.[140] In the absence of water (1:9 DMSO:acetone), studies of the same reaction yielded activation parameters of $\Delta H^{\ddagger} = 96.1 \pm 5.2\,kJ\,M^{-1}$ and $\Delta S^{\ddagger} = -22.4 \pm 12\,J\,M^{-1}\,K^{-1}$. The dramatic difference between these two sets of parameters suggests that diverse mechanisms are operative depending on the nature of the solvent. In water, a catalytic reaction involving intramolecular attack of a terminal $LZn_2$–OH moiety on a monodentate-coordinated nitrocefin substrate seems plausible (Scheme 26). However, in non-aqueous solution (1:9 DMSO:acetone), where a water molecule is not available for formation of the terminal $LZn_2$–OH moiety, the bridging hydroxide may shift to a terminal position prior to attack on the β-lactam, or may act as the nucleophile from the bridging position. In both of these scenarios, significant reorganization of the cation is required, which is consistent with the slower reaction ($k_{obs}$ (DMSO:acetone) $= 2.0 \times 10^{-3}\,min^{-1}$; $k_{obs}$ ($H_2O$:DMSO) $= 3.4 \times 10^{-2}\,min^{-1}$) and higher activation enthalpy for the β-lactam hydrolysis reaction. Additional factors that could influence the non-aqueous reaction include the alignment of the coordinated substrate and the hydroxide moiety, and/or the nucleophilicity of a bridging hydroxide, which would be reduced due to its interactions with two metal centers.

To gain further insight into the nature of the zinc hydroxide moiety operative for β-lactam hydrolysis in metallo-β-lactamases, studies of bizinc complexes of differing supporting chelate ligand structure were undertaken.[148] Dissolving of the bizinc complex $[Zn_2L3(\mu\text{-}NO_3)(NO_3)_2]$ in water results in the formation of $[Zn_2L3(\mu\text{-}OH)(NO_3)_2]$ (Fig. 23), which was characterized by X-ray crystallography. In this complex, the bridging hydroxide moiety and terminal bidentate nitrate ligands occupy adjacent *cis* coordination positions. Potentiometric pH titrations performed in aqueous solution yielded a $pK_a$ value of $7.40 \pm 0.10$ for the bridging water ligand in $[Zn_2L3(\mu\text{-}OH_2)(NO_3)_n(sol)_{2-n}]^{(2-n)+}$.

Treatment of $[Zn_2L3(\mu\text{-}NO_3)(NO_3)_2]$ with nitrocefin in 1:9 DMSO:$H_2O$ at pH = 7.5 results in hydrolysis of the β-lactam with $k_{obs} = 6.0 \pm 1.0\,min^{-1}$ at 313 K. This reaction is first order in nitrocefin. Similar to the reactivity displayed by $[Zn_2(BPAN)(\mu\text{-}OH)(\mu\text{-}O_2PPh_2)](ClO_4)_2$, the rate of nitrocefin hydrolysis increases with increasing concentration of $[Zn_2L3(\mu\text{-}NO_3)(NO_3)_2]$, but not in a linear fashion. The $k_{obs}$ versus $[Zn_2L3(\mu\text{-}NO_3)(NO_3)_2]$ data for this reaction is best fit using an approach akin to that outlined in Scheme 26, which yielded $K = 107 \pm 20\,M^{-1}$. A kinetic $pK_a$ value of $7.5 \pm 0.2$ was determined as outlined in Scheme 27. The nearly identical $pK_a$ value to that measured via potentiometric titration for $[Zn_2L3(\mu\text{-}OH_2)(NO_3)_n(sol)_{2-n}]^{(2-n)+}$

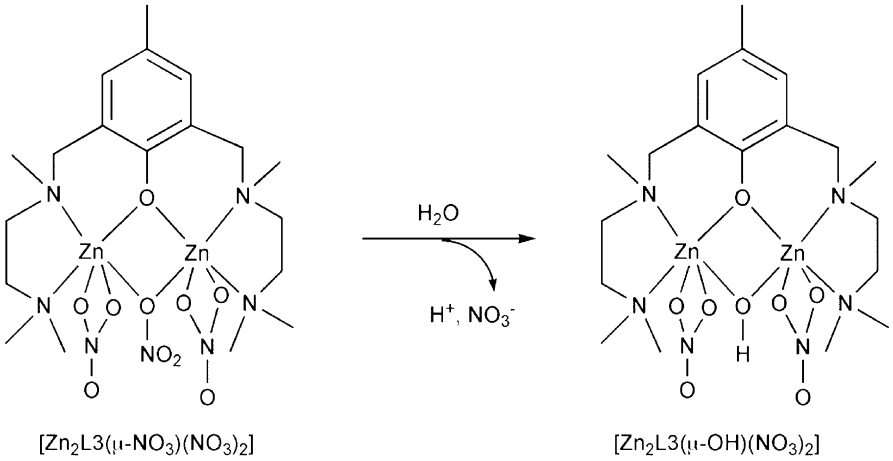


**Fig. 23** Formation of $[Zn_2L_3(\mu\text{-OH})\ (NO_3)_2]$ in water.

$(7.40 \pm 0.10)$ indicates that the bridging hydroxide moiety in $[Zn_2L3(\mu\text{-OH})(NO_3)_2]$ is the nucleophile responsible for nitrocefin hydrolysis in 1:9 DMSO:$H_2O$ solution. The poor nucleophilic character of this bridging hydroxide is indicated by the fact that the rate constant derived for nitrocefin hydrolysis by the aqua complex $[Zn_2L3\text{-}(\mu\text{-}OH_2)(NO_3)_n(sol)_{2-n}]^{(2-n)+}$ ($k_{obs} = 1.0 \times 10^{-3}\,m^{-1}$) is only 10 times less reactive than $[Zn_2L3(\mu\text{-OH})(NO_3)_2]$ ($k_{obs} = 1.0 \times 10^{-2}\,min^{-1}$).

Evidence for cephalothin (Fig. 22) or penicillin G (benzylpenicillin, Scheme 24) coordination to $[Zn_2L3(\mu\text{-}NO_3)(NO_3)_2]$ in DMSO and water solution, prior to hydrolysis, was obtained using $^{13}C$ NMR and infrared spectral data. Specifically, a downfield shift of the carboxylate carbon resonance, coupled with a blue shift of the $\nu_{as}(COO)$ vibration, provided evidence for monodentate coordination of the carboxylate group of the antibiotic to Zn(II) in both aqueous and organic solution. In the latter environment (1:9 DMSO:acetone) containing only a small amount of water (0.112 M), the substrate binds more tightly, with $K = (3.1 \pm 0.5) \times 10^4\,M^{-1}$.

Variable temperature kinetic studies for the hydrolysis of nitrocefin catalyzed by $[Zn_2L3(\mu\text{-OH})(NO_3)_2]$ in acetone:DMSO yielded $\Delta H^{\ddagger} = 88.4 \pm 5.3\,kJ\,M^{-1}$ and $\Delta S^{\ddagger} = -45.3 \pm 16.0\,J\,M^{-1}K^{-1}$. These values are similar to those found for nitrocefin hydrolysis catalyzed by $[Zn_2(BPAN)(\mu\text{-OH})(\mu\text{-}O_2PPh_2)](ClO_4)_2$ in 1:9 DMSO:acetone ($\Delta H^{\ddagger} = 96.1 \pm 5.2\,kJ\,M^{-1}$ and $\Delta S^{\ddagger} = -22.4 \pm 12\,J\,M^{-1}K^{-1}$) and are consistent with intramolecular attack by the bridging hydroxide on the coordinated β-lactam substrate in the rate-determining step.[140]

Comparison of the rate the hydrolysis of nitrocefin catalyzed by $[Zn_2L3(\mu\text{-OH})\text{-}(NO_3)_2]$ versus $[Zn_2L3(\mu\text{-OD})(NO_3)_2]$ gave an inverse solvent isotope effect ($k_H/k_D$) of 0.204.[148] Taking into consideration that free $OD^-$ is a better nucleophile than free $OH^-$,[149] it was concluded that Zn–OD will be more reactive than Zn–OH and that the finding of an inverse solvent isotope effect in this reaction is consistent with rate-limiting nucleophilic attack and subsequent rapid protonation of the leaving group.

An intermediate has been spectroscopically identified in the reaction of [$Zn_2$L3-(μ-OH)$(NO_3)_2$] with a 10-fold excess of nitrocefin in wet DMSO.[148,150] This intermediate is relevant to an intermediate detected by stopped-flow experiments in the hydrolysis of nitrocefin catalyzed by the metallo-β-lactamase from *Bacteroides fragilis*.[127,132] UV–visible spectroscopic results and kinetic data suggest that this intermediate is anionic and has a deprotonated nitrogen atom resulting from ring opening of the lactam. The fact that this intermediate can be observed in the enzyme system suggests that protonation of the leaving group is rate determining in the enzymatic β-lactam hydrolysis reaction.[132] In the model system, the intermediate exhibits an absorption maximum at 640 nm ($\varepsilon \sim 38{,}900\ M^{-1}\,cm^{-1}$), whereas the enzyme intermediate shows an absorption at 665 nm ($\varepsilon \sim 30{,}000\ M^{-1}\,cm^{-1}$). The similarity of these two features suggests that structurally similar species are being produced. Addition of acid to the intermediate generated from [$Zn_2$L3(μ-OH)-$(NO_3)_2$] results in immediate spectroscopic changes consistent with the formation of the final nitrocefin hydrolysis product. This reaction is reversible, as addition of base results in the regeneration of the 640 nm feature. $^{13}$C NMR and infrared measurements were used to further characterize this intermediate, and a structure was proposed on the basis of these spectroscopic studies (Fig. 24).

Using pyridinium triflate, the deprotonated amide intermediate was estimated to have $pK_a = 4.20$. This low value is consistent with Zn(II) ion stabilization of the deprotonated amide. The formation of this deprotonated amide intermediate occurs in wet DMSO with a microscopic rate constant that corresponds to the intramolecular hydrolysis of coordinated nitrocefin catalyzed by [$Zn_2$L3(μ-OH)$(NO_3)_2$]. Activation parameters for this reaction ($\Delta H^{\ddagger} = 77.6 \pm 8.0\ kJ\,M^{-1}$ and $\Delta S^{\ddagger} = -62.7 \pm 20.0\ J\,M^{-1}\,K^{-1}$) are within error of those found for the same reaction in acetone:DMSO

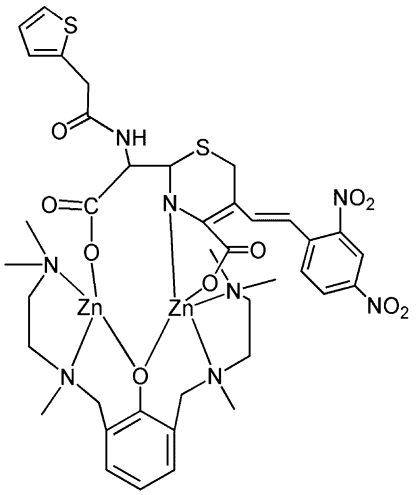


**Fig. 24** Proposed structure of spectroscopically observable deprotonated intermediate in the hydrolysis of nitrocefin catalyzed by [$Zn_2$L3(μ-OH)$(NO_3)_2$].

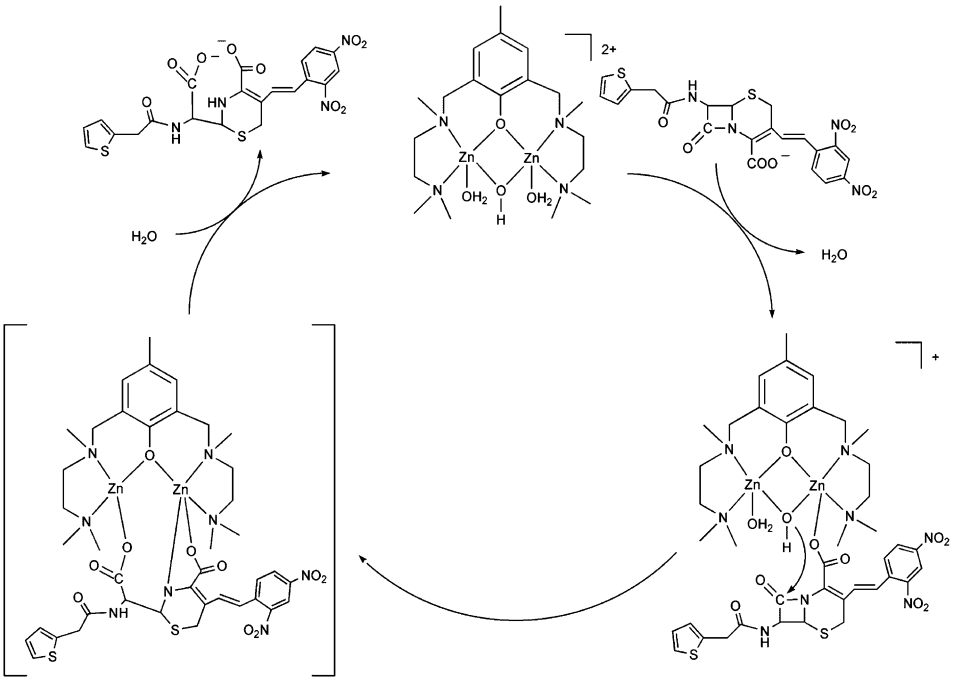

**Scheme 28** Proposed mechanism for nitrocefin hydrolysis catalyzed by [$Zn_2$L3(μ-OH)$(NO_3)_2$] in wet DMSO. The coordinated $NO_3^-$ ligands in the complex are replaced by water under these conditions.

($\Delta H^{\ddagger} = 88.4 \pm 5.3\ \mathrm{kJ\,M^{-1}}$ and $\Delta S^{\ddagger} = -45.3 \pm 16.0\ \mathrm{J\,M^{-1}\,K^{-1}}$). Thus, the intermediate is formed as the product of the rate-determining step as shown in Scheme 28. Overall, this mechanism has similarity to that proposed for nitrocefin hydrolysis catalyzed by the metallo-β-lactamase from *Bacteroides fragilis*.[127,131]

The nitrocefin hydrolysis reactivity of mononuclear zinc complexes has also been studied for comparison to the results obtained from the binuclear systems.[140,148] Treatment of [(bpta)Zn]$(X)_2$ (X = $NO_3$ or OTf, Fig. 25) with nitrocefin in aqueous solution results in hydrolysis of the β-lactam ring. The pH-dependence of the rate of the [(bpta)Zn$(H_2O)$]$(NO_3)_2$-catalyzed reaction yielded a kinetic $pK_a = 7.84 \pm 0.2$. This low value is consistent with the involvement of a mononuclear Zn–OH moiety as the nucleophile in the β-lactam hydrolysis reaction. At low concentration, this reaction is first-order in [(bpta)Zn–OH]$NO_3$, but at higher concentrations a leveling-off of the rate occurs, indicative of saturation behavior and nitrocefin coordination to the zinc complex. Fitting of the data to Equation (2) (Scheme 26) yielded the binding constant $K = 1140 \pm 106\ \mathrm{M^{-1}}$ at $[H_2O] = 13.9$ M and pH = 7.50. Increasing of the water concentration to 27.8 M resulted in a lower binding constant ($K = 425 \pm 90\ \mathrm{M^{-1}}$). This indicates that water competes with nitrocefin for coordination to the mononuclear zinc complex. At both water concentrations, the nitrocefin binding constant for [(bpta)Zn$(H_2O)$]$(NO_3)_2$ is notably higher than that found

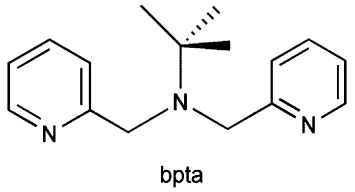


**Fig. 25** Structure of the bpta ligand.

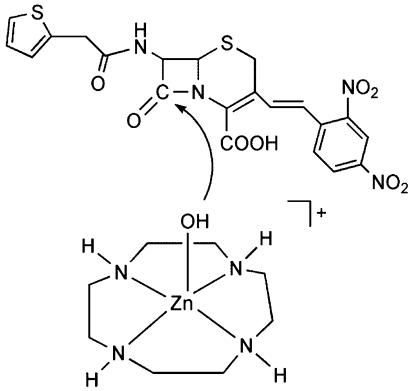


**Fig. 26** Bimolecular reaction of $[([12]aneN_4)Zn(OH)]NO_3$ with nitrocefin.

for nitrocefin coordination to $[Zn_2L3(\mu\text{-}OH)(NO_3)_2]$ ($K = 107 \pm 20\,M^{-1}$). This is likely a consequence of the weaker Lewis acidity of the zinc centers in $[Zn_2L3(\mu\text{-}OH)(NO_3)_2]$ due to the presence of the anionic phenolate donor (Fig. 23) in the supporting chelate ligand.

Hydrolysis of nitrocefin catalyzed by $[([12]aneN_4)Zn(H_2O)](NO_3)_2$ (Fig. 5)[99] proceeds via a pathway that does not involve substrate coordination to the zinc center. Specifically, as the zinc center in the hydroxide species $[([12]aneN_4)Zn(OH)]NO_3$ is coordinatively saturated, the reaction proceeds via a bimolecular pathway (Fig. 26).

An important conclusion from these comparative studies is that mononuclear Zn(II) complexes can be as efficient for nitrocefin hydrolysis as binuclear systems, thus providing evidence that the second zinc center ($Zn_2$) in metallo-β-lactamases is not required for nucleophile activation or catalytic activity.

Studies of the hydrolysis of penicillin G promoted by a series of binuclear Zn(II) complexes (Fig. 27) have been reported.[151] These complexes, which are supported by pyrazolate-containing chelate ligands, have varying Zn···Zn distances.[152–154] In the complexes having a shorter Zn···Zn distance (**1** and **3**), a single bridging hydroxide is present. However in complexes of this series having a longer Zn···Zn distance (**2** and **4**), a terminal hydroxide ligand participates in a strong hydrogen-bonding interaction with a water molecule that is coordinated to the other zinc center. This secondary interaction produces a lower $pK_a$ value for the aqua analogs of **2** and **4**

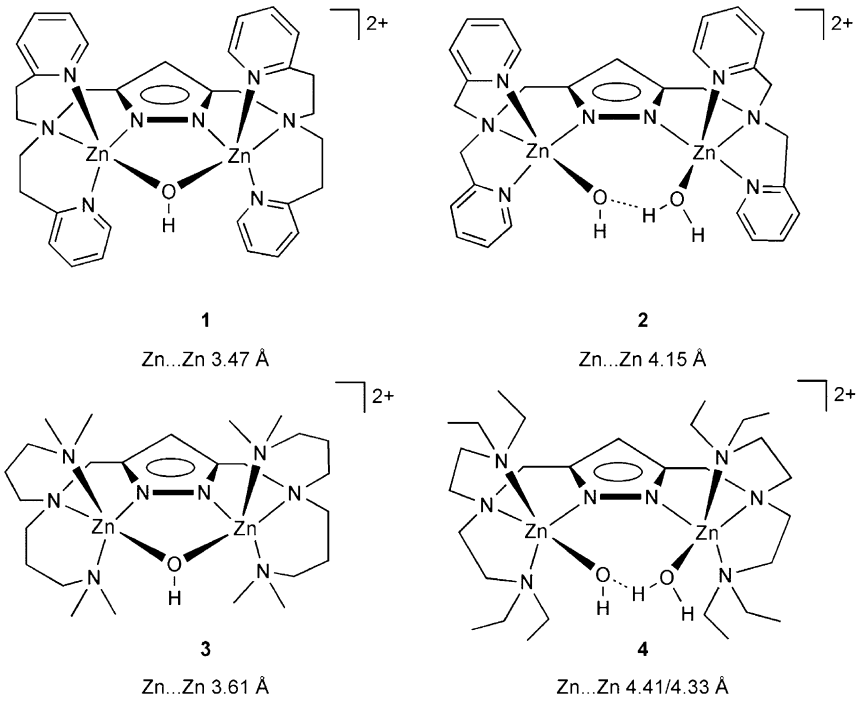


**Fig. 27** Cationic portions of pyrazolate-bridged binuclear zinc hydroxide complexes.

(7.60 and 7.57, respectively) versus the p$K_a$ value found for the aqua analog of **1** (7.96).[153–155]

Treatment of **1–3** with excess penicillin G (benzylpenicillin) in DMSO:$H_2O$ (9:1) results in hydrolytic ring opening of the lactam. The rate of this reaction differs depending on the structural features of the zinc complex, with the reaction rate increasing in the order **2** < **1** < **3**. Complex **4** is unreactive toward penicillin G. For **3**, approximately three equivalents of the substrate are hydrolyzed in 20 min at ambient temperature. Complexes **1** and **3** show significantly enhanced reactivity relevant to $Zn(NO_3)_2 \cdot H_2O$ and $Zn(ClO_4)_2 \cdot 6H_2O$, whereas **2** and **4** show reduced reactivity. Thus, the binuclear zinc complexes produce either enhanced or diminished β-lactam hydrolysis activity depending on the structure of the cation.

X-ray crystallographic studies of the reaction products generated via admixture of the supporting chelate ligands found in **3** and **4** with $Zn(ClO_4)_2 \cdot 6H_2O$, base, and the simple β-lactam oxazetidinylacetate (oaa) provide insight into how substrate coordination may influence the structural features of the binuclear zinc complex. As shown in Fig. 28a, the binuclear zinc–oaa complex supported by the chelate ligand found in **3** contains the β-lactam coordinated in an anisobidentate fashion (Zn(1)–O(1) 2.006(3) Å, Zn(1)–O(2) 2.358(4) Å).[156] At each zinc center, one of the dimethylamino donor atoms is not coordinated, and the zinc center exhibits a

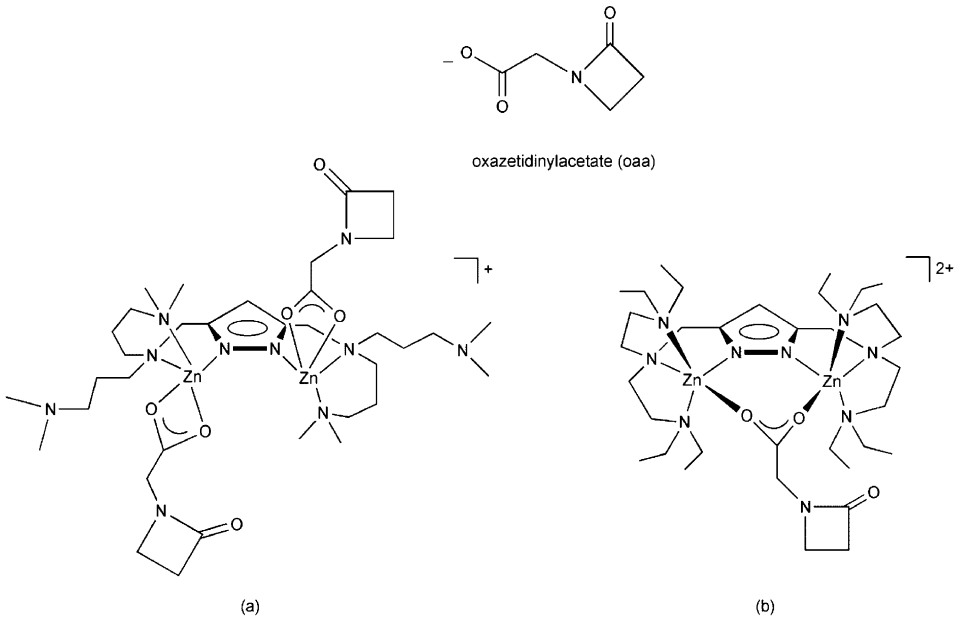


**Fig. 28** Structural features of oxazetidinylacetate adducts.

distorted square pyramidal geometry.[157] The Zn···Zn distance in this complex is 4.328(1) Å. The dissociation of the amine donor in this structure may result from low stability for the six-membered chelate ring.[158,159] Using the chelate ligand found in **4** in the same type of reaction, an adduct of oaa is formed wherein the carboxylate moiety bridges the two zinc centers (Fig. 28b). In this complex, each zinc center exhibits a distorted trigonal bipyramidal geometry ($\tau = 0.86/0.79$).[157] Notably, in both of these complexes, the β-lactam carbonyl does not interact with a Zn(II) center.

The differing chelate ligand coordination properties exhibited by the β-lactam adduct complexes shown in Fig. 28 may provide evidence of why complexes **1** and **3** (Fig. 27) exhibit enhanced reactivity relative to **2** for β-lactam hydrolysis involving penicillin G, and why **4** is unreactive. In **1** and **3**, the presence of unstable six-membered chelate rings may enable dissociation of multiple N-donors, thus providing coordination sites for penicillin G coordination, including perhaps β-lactam carbonyl coordination, as well as possible binding sites for water and the formation of a Zn–OH nucleophile. $^1$H NMR studies of equimolar mixtures of **1** (Fig. 27) and penicillin G in $d_6$-acetone/$D_2O$ (8:1) at 300 K at early reaction times revealed resonances at chemical shifts intermediate between those of the free ligand and **1**, suggesting that a dynamic process may be occurring in solution wherein N-donors dissociate from the Zn(II) centers in the presence of penicillin G. When the same type of $^1$H NMR experiment was performed using **2** and penicillin G, only minor signal broadening was observed, indicating that the zinc complex likely retains

coordination of all ligand appendages in solution. Overall, these combined studies provide evidence that the low reactivity of **2** and **4** may be due to the fact that once substrate binds to the binuclear zinc center, in a similar motif to that shown in Fig. 28b, there may not be any available Zn(II) coordination sites for β-lactam carbonyl and/or water activation.

For the structures shown Schemes 26 and 28, and in Fig. 28, coordination of the β-lactam substrate to a binuclear zinc center involves the carboxylate moiety and not the β-lactam amide carbonyl oxygen. Evidence for carboxylate coordination, and against β-lactam amide oxygen coordination in these complexes, was obtained via $^{13}C$ NMR and infrared spectroscopic studies, and/or by X-ray crystallography. It is worth noting that recent structural investigations of β-lactam adduct compounds have revealed that Zn(II) coordination of a β-lactam carbonyl oxygen can occur under specific conditions.[151,160] As shown in Fig. 29a, a binuclear zinc complex having bridging oxazetidinylacetate ligands has been isolated using a supporting chelate ligand having only three nitrogen donors to each zinc center.[151] Notably, the Zn–O(amide) distance in this compound (2.005(2) Å) is shorter than both Zn–O(carboxylate) distances (2.093(3) and 2.060(2) Å). Consistent with this strong interaction is the fact that the amide C–O bond in this complex is longer (1.242(4) Å) than in complexes wherein the amide oxygen does not interact with the Zn(II) center (e.g. complexes shown in Fig. 28 which exhibit C–O distances of 1.210(6) and 1.218(4) Å, respectively). The amide C–N bond is also shorter in the complexes shown in Fig. 29 than in complexes wherein the amide oxygen does not interact with the Zn(II) ion. These combined structural parameters indicate that the β-lactam amide moiety is significantly polarized upon coordination to Zn(II) center. However, these complexes are not reactive toward hydrolysis, presumably because of the anionic nature of the *N*-deprotonated β-lactam.

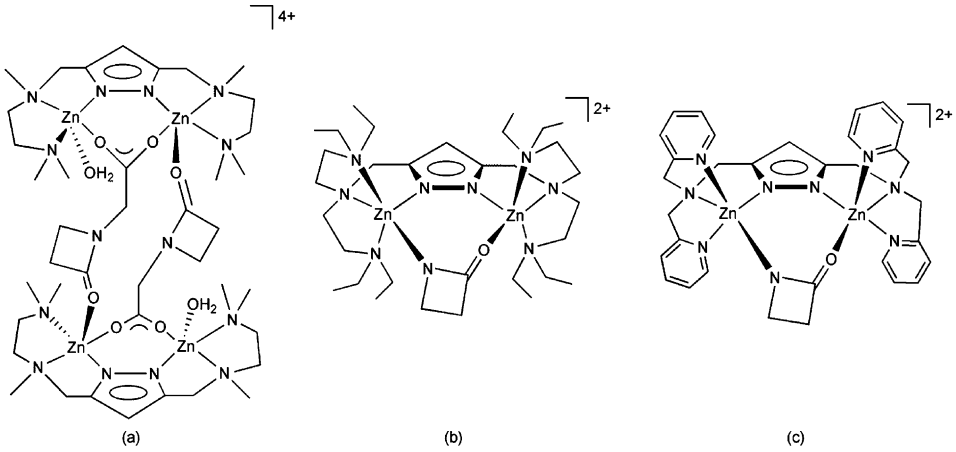


**Fig. 29** Structurally characterized binuclear zinc β-lactam complexes having β-lactam carbonyl coordination.

PEPTIDE HYDROLYSIS

Metalloaminopeptidases use an active site motif containing one or two metal ions to cleave the *N*-terminal residue of a polypeptide chain.[161] The catalytic mechanism of the aminopeptidase from *Aeromonas proteolytica* (ApAP) has been outlined in great detail.[162] The active site co-catalytic zinc centers in ApAP are ligated by a mixture of carboxylate and histidine donors, with bridging hydroxide and aspartate ligands (Fig. 30). In a proposed catalytic mechanism for this enzyme, the amide carbonyl moiety of the substrate is proposed to initially bind to $Zn_1$ (Scheme 29). Upon substrate binding, the bridging hydroxide moiety becomes terminal on $Zn_1$. This process may be assisted by the formation of an interaction between the *N*-terminal amino group and $Zn_2$, as well as by the formation of a new hydrogen bond between this amino group and the carbonyl oxygen of a $Zn_2$-bound carboxylate ligand. Attack of the $Zn_1$–OH moiety on the activated amide carbonyl carbon yields a tetrahedral intermediate that decomposes upon protonation of the leaving group. This C–N bond-breaking is proposed as the rate-limiting step.[163]

A few model systems have been reported which mediate the hydrolysis of peptide substrates.[164–168] For example, treatment of a macrocyclic bizinc complex of the OBISDIEN (1,4,7,14,16,19-hexaaza-10,22-dioxcyclotetracosane) ligand (Scheme 30) with glycylglycine (Gly–Gly) at varying p*D* values in $D_2O$ results in hydrolysis to produce two equivalents of glycine.[164] At 343 K, and p*D* values of 8.37 and 8.72, values for the hydrolysis rate constant ($k_H$) of $2.6(2) \times 10^{-7}\,s^{-1}$ and $3.5(2) \times 10^{-7}\,s^{-1}$, respectively, were obtained. Coupled with speciation studies performed as a function of pH, it was determined that three zinc hydroxide species, $[LZn_2(OH)Gly–Gly]^{2+}$, $[LZn_2(OH)_2Gly–Gly]^{+}$, and $[LZn_2(OH)_3Gly–Gly]$ (L = OBISDIEN) have similar rate constants ($k_H \sim 5 \times 10^{-7}\,s^{-1}$) for the hydrolysis reaction. These hydroxide derivatives are approximately five times more active than a similar complex having no hydroxide component (e.g. $[LZn_2(Gly–Gly)]^{3+}$, $k_H = 1.0(2) \times 10^{-7}\,s^{-1}$). A proposed mechanism for glycylglycine hydrolysis promoted by the bishydroxo complex is shown in Scheme 30.

The binuclear zinc complex $[(LH^{+})_2Zn_2(Gly–Gly)_2](ClO_4)_4$ (Fig. 31, L = 1-methyl-4-(6-amino-2-pyridylmethyl)-piperazine) was characterized by X-ray crystallography.[168] In this structure, a water molecule is positioned close (O(water)···C(carbonyl) 3.050 Å)

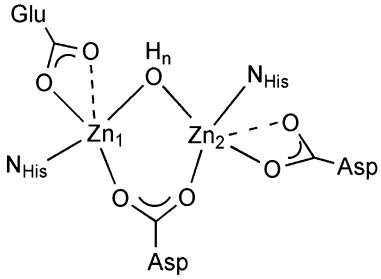


**Fig. 30** Active site co-catalytic zinc centers in ApAP.

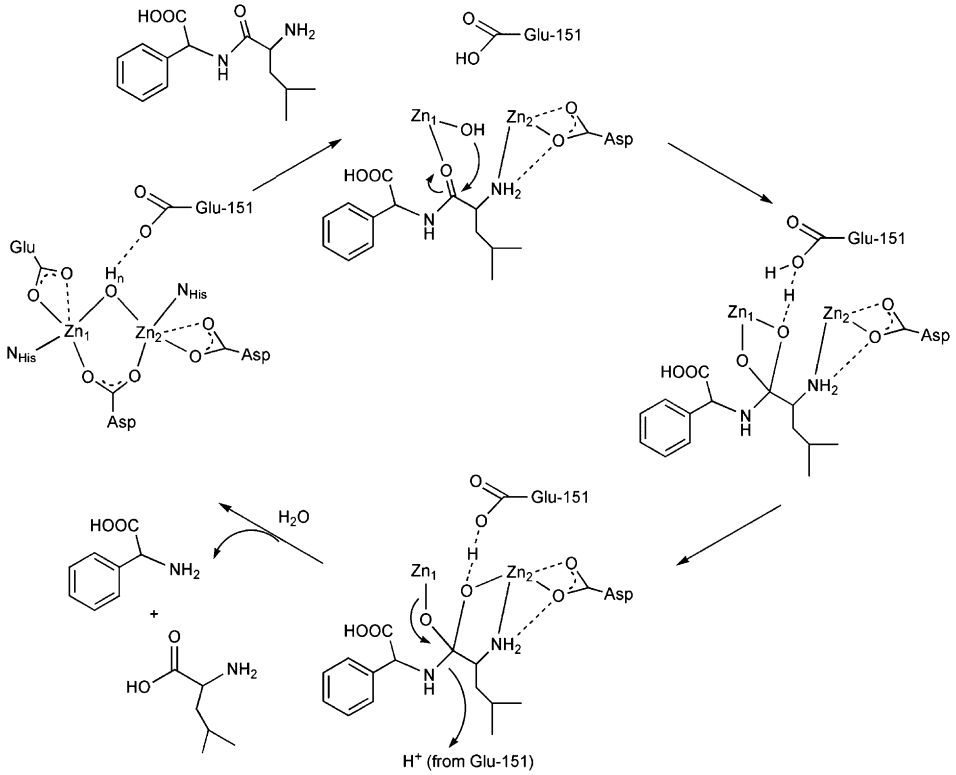


**Scheme 29** Selected transformations in the proposed mechanistic pathway for peptide hydrolysis by ApAP. The zinc-coordinated amino acid ligands are shown only on the resting state structure (left) for clarity.

to the amide carbonyl carbon of Gly–Gly, the oxygen atom of which is coordinated to the zinc center. At 70 °C and pH = 7.0(1) (50 mM HEPES) the coordinated Gly–Gly in $[(LH^+)_2Zn_2(Gly–Gly)_2](ClO_4)_4$ undergoes hydrolysis over the course of days (~28% Gly–Gly hydrolysis after 5 days). The structural and reactivity properties of this complex have relevance to the monozinc peptidase aminopeptidase A.[169]

Binuclear zinc complexes have been shown to mediate the hydrolysis of the activated peptide model substrate L-leucine–*p*-nitroanilide (LNA, Fig. 32) with the reactions being followed spectroscopically by the formation of *p*-nitroaniline ($\lambda_{max}$~400 nm).[165–167] This model substrate has also been used in studies of ApAP.[170] The hydrolysis of LNA mediated by the zinc complex $[(bomp^-)]Zn_2(CH_3CO_2)_2]BPh_4$ (Fig. 33a; H(bomp): 2,6-bis[bis(2-methoxyethyl)aminomethyl]-4-methylphenol) in water/DMF (6:4) occurs via a reaction that is first-order in complex and substrate, with a second-order rate constant $k = 2.3(1) \times 10^{-3}\,M^{-1}\,s^{-1}$ at 25 °C. At best, a yield of ~65% for a single turnover reaction was obtained, indicating that

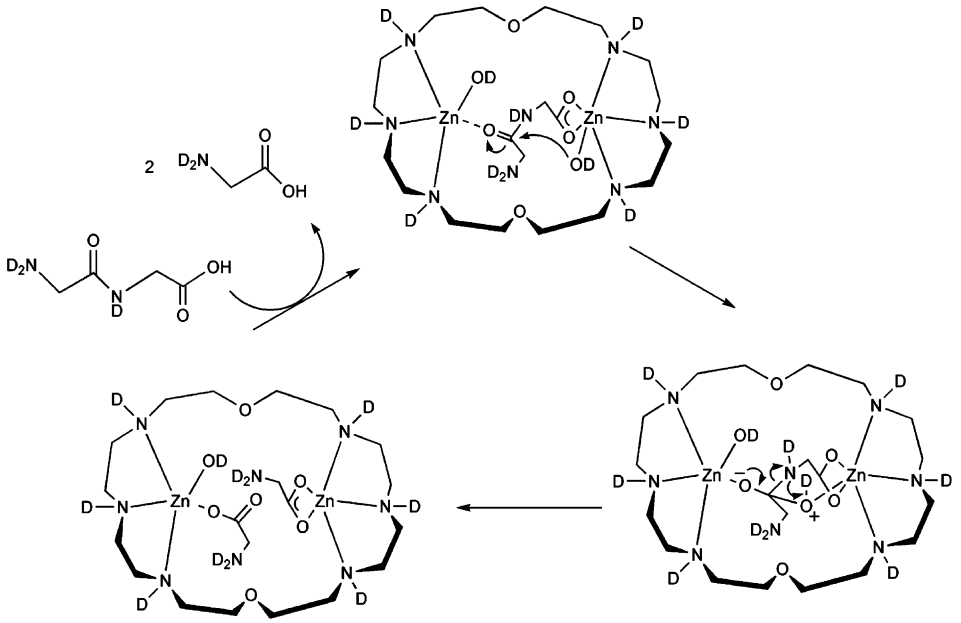

**Scheme 30** Proposed mechanism for Gly–Gly hydrolysis promoted by a bizinc complex of the OBISDIEN chelate ligand.

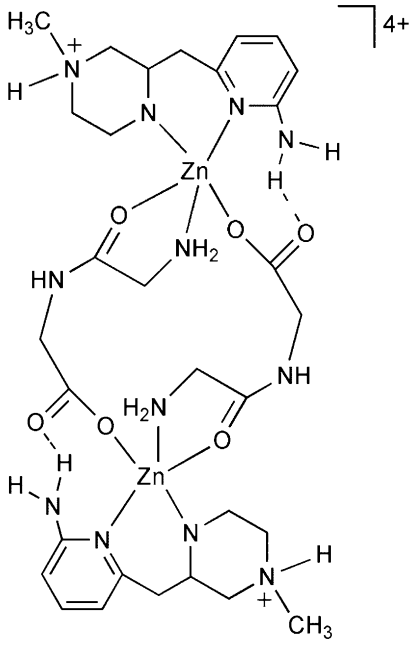

**Fig. 31** Cationic portion of $[(LH^+)_2Zn_2(Gly–Gly)_2](ClO_4)_4$.

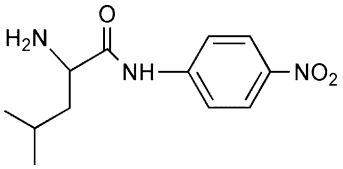


**Fig. 32** L-leucine–*p*-nitroanilide (LNA).

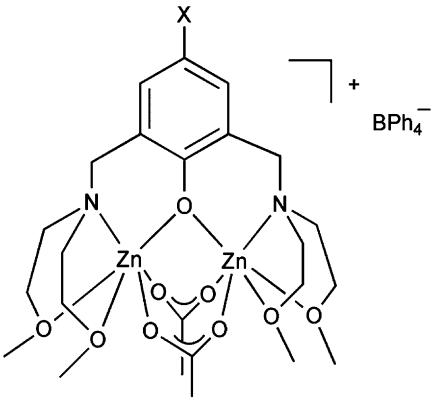


(a) X = -$CH_3$ ($bomp^-$)
(b) X = -$NO_2$ ($bonp^-$)
(c) X = -Cl ($bocp^-$)

**Fig. 33** Binuclear zinc complexes that mediate the hydrolysis of *N*-*p*-nitrophenyl- L-leucine in water-containing solutions.

the zinc complex becomes inactive following substrate hydrolysis. The actual active zinc complex for the amide hydrolysis reaction in this system is not known.

Analogs of the $bomp^-$ ligand, $bonp^-$ (H(bonp): 2,6-bis[bis(2-methoxyethyl) aminomethyl]-4-nitrophenol) and $bocp^-$ (H(bocp): 2,6-bis[bis(2-methoxyethyl) aminomethyl]-4-chlorophenol) have been used to assemble zinc complexes for comparative model aminopeptidase reactivity studies.[166] Using the method of initial rates, the second-order rate constants for the hydrolysis of LNA promoted by $[(bonp^-)]Zn_2(CH_3CO_2)_2]BPh_4$ and $[(bocp^-)]Zn_2(CH_3CO_2)_2]BPh_4$ (Fig. 33b and c) at 25 °C in DMF:tricine buffer were found to be $5.9(5) \times 10^{-1}\,M^{-1}\,s^{-1}$ and $2.7(1) \times 10^{-2}\,M^{-1}\,s^{-1}$, respectively. Comparison of these rate constants to that obtained for the hydrolysis of the same substrate promoted by $[(bomp^-)]Zn_2(CH_3CO_2)_2]BPh_4$ ($2.3(1) \times 10^{-3}\,M^{-1}\,s^{-1}$) under identical conditions reveals that the inclusion of an electron withdrawing substituent on the phenolate ring increases the rate of the LNA hydrolysis reaction. Studies of the rate of this reaction as a function of pH for the $[(bomp^-)]Zn_2(CH_3CO_2)_2]BPh_4$- and $[(bocp^-)]Zn_2(CH_3CO_2)_2]$

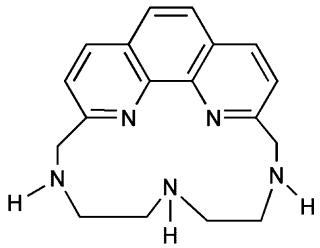

L4

**Fig. 34** Phenanthroline-containing polyamine macrocyclic ligand.

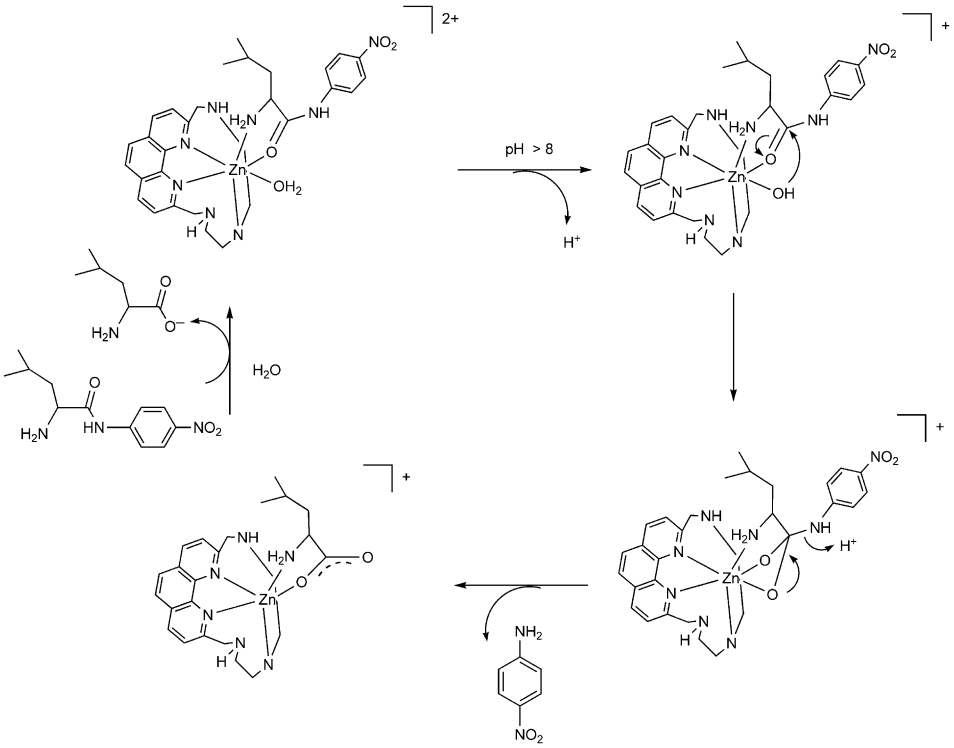

**Scheme 31** Proposed mechanism for LNA hydrolysis mediated by a zinc complex of a phenanthroline-containing polyamine ligand.

$BPh_4$-promoted reactions yielded kinetic $pK_a$ values of 9.4 and 9.1, respectively. Both values are suggested to correspond to the deprotonation of a $Zn–OH_2$ moiety to produce a reactive zinc hydroxide species.

A zinc complex of a phenanthroline-containing macrocycle (L4, Fig. 34) binds LNA with a log $K$ value of 5.55 (308 K) to form $[(L4)Zn(LNA)]^{2+}$, as determined by

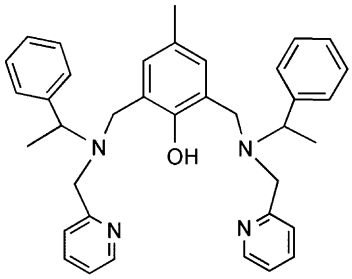


**Fig. 35** H(bppmp) ligand.

potentiometric titration and $^1$H NMR studies.[167] This complex undergoes a monodeprotonation at pH > 8, a reaction that results in either the formation of a zinc hydroxide species ($[(L4)Zn(LNA)(OH)]^+$) or a complex having a deprotonated $LNA^-$ ligand ($[(L4)Zn(LNA^-)]^+$). This deprotonated complex is active for LNA hydrolysis to produce L-leucine and *p*-nitroaniline. When corrected for the amount of deprotonated complex in solution, this reaction proceeds with a pseudo first-order rate constant of $3.0 \times 10^{-6}\,s^{-1}$. An intramolecular mechanism is proposed for this reaction wherein a zinc-bound hydroxide attacks the coordinate LNA ligand (Scheme 31).

Zinc complexes of optically resolved forms of the dinucleating ligand H(bppmp) (2,6-bis[{(*R*/*S*)-1-phenylethyl-2-pyridylmethyl}aminomethyl]-4-methylphenol, Fig. 35) exhibit differing second-order rate constants (*R*: $3.3(7) \times 10^{-2}\,M^{-1}\,s^{-1}$; *S*: $7.6(5) \times 10^{-2}\,M^{-1}\,s^{-1}$) for the hydrolysis of LNA in DMF:$H_2O$ (2:3) at pH = 8.0.[171] The enhanced reactivity of [(*S*-bppmpZn$_2$)(MeCO$_2$)$_2$]BPh$_4$ versus that of [(*R*-bppmpZn$_2$)(MeCO$_2$)$_2$]BPh$_4$ is attributed to better recognition of the LNA substrate by the former complex.

Outside the scope of coverage of this work are synthetic systems involving the catalytic or stoichiometric alcoholysis of esters or amides promoted by zinc ions or complexes.[172–177]

## 5 Phosphate ester hydrolysis

### PHOSPHATE MONOESTER HYDROLYSIS

Alkaline phosphatase is one of a number of zinc-containing enzymes and nucleases that catalyze in the hydrolysis of a phosphate ester linkage.[178–186] The catalytic mechanism of *Escherichia coli* alkaline phosphatase has been extensively investigated and involves initial coordination of the phosphate monoester substrate (e.g. 4-nitrophenyl phosphate) in a bridging position between two active site zinc centers (Scheme 32).[187] A deprotonated active site serine residue then acts as a nucleophile to attack the phosphoryl group which results in cleavage of the P–O bond to the 4-nitrophenolate leaving group. In this reaction, a phosphorylserine group is formed

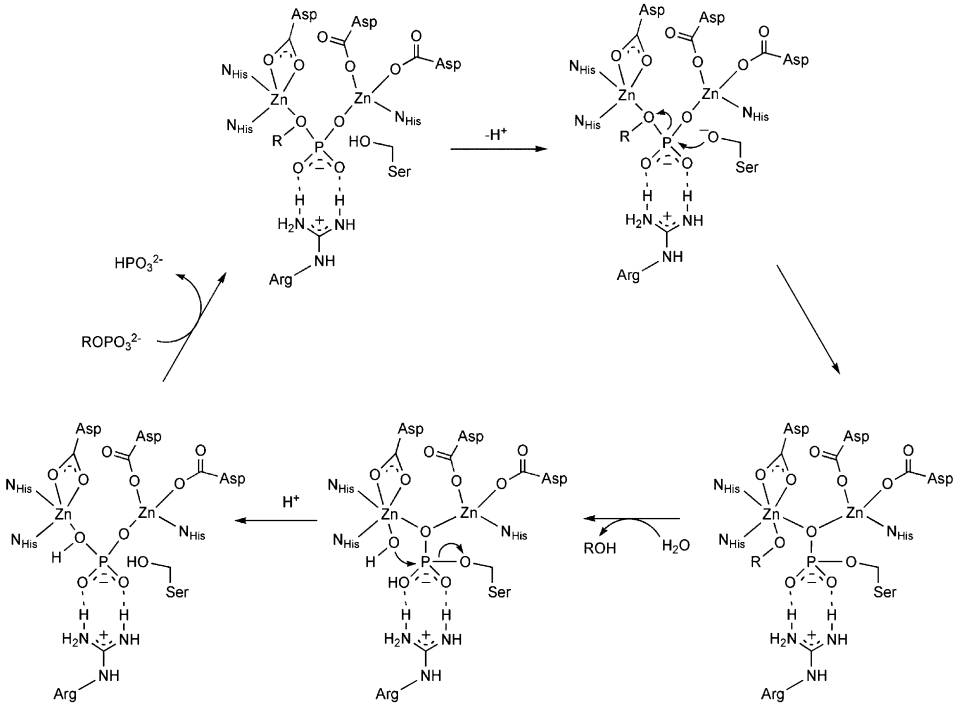


**Scheme 32** Phosphate monoester hydrolysis catalyzed by alkaline phosphatase.

that remains coordinated to the binuclear zinc center. In addition, one of the two zinc ions provides stabilization for the anionic 4-nitrophenolate leaving group. Hydrolysis of the phosphorylserine group occurs via attack of a Zn–OH moiety to yield $HPO_4^{2-}$, which is subsequently released from the active site. As shown in Scheme 32, hydrogen-bonding interactions involving an arginine residue (Arg-166 in *E. coli*) are important throughout the catalytic cycle.

Phosphate ester hydrolysis can occur via three possible limiting mechanisms.[187] A dissociative mechanistic pathway involves an $S_N1$-type reaction in which a stable metaphosphate ion ($PO_3^-$) is formed, which then undergoes reaction with a hydroxide nucleophile to yield the final products. In an associative pathway, a stable five-coordinate phosphorane intermediate forms prior to departure of the leaving group. In a concerted pathway for phosphate ester hydrolysis, nucleophilic attack and P–O(H) bond formation occur simultaneously with P–O(R) bond cleavage involving the leaving group.

As with amide hydrolysis reactions, extensive mechanistic studies of metal-mediated phosphate monoester hydrolysis reactions have been performed using exchange inert mononuclear Co(III) complexes.[9,188–202] To date, only a few zinc complexes that promote phosphate monoester hydrolysis have been reported. A binuclear zinc complex supported by a macrocyclic cryptate ligand (Fig. 36)

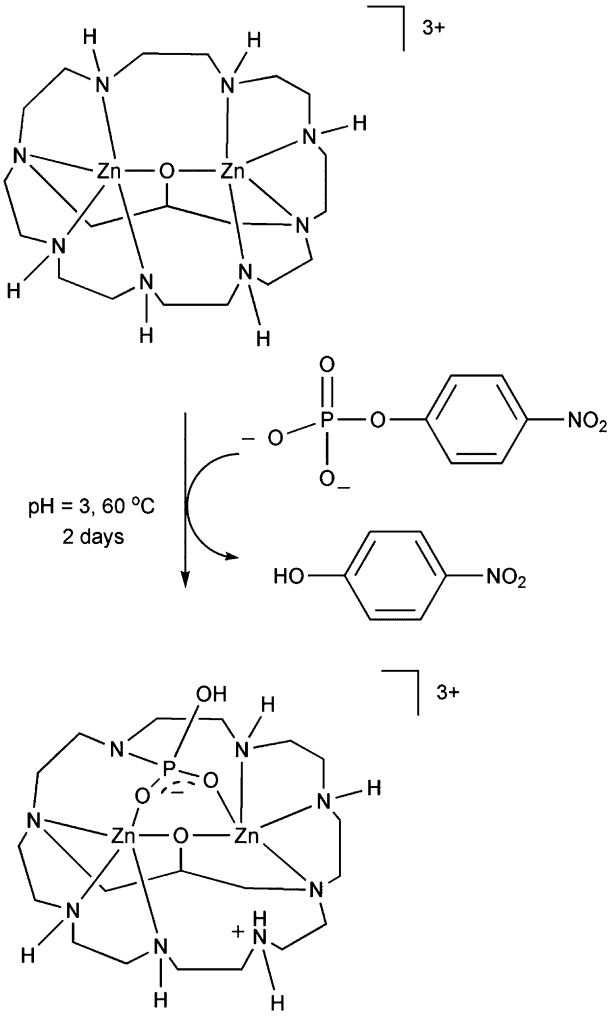


**Fig. 36** Phosphate monoester hydrolysis promoted by a bizinc cryptand complex.

promotes the cleavage of 4-nitrophenyl phosphate dianion in aqueous solutions via attack of an internal amine nucleophile.[14,203] This complex contains two zinc ions separated by a distance of 3.24 Å and bridged by an alkoxide anion. Each zinc center exhibits a distorted trigonal bipyramidal geometry, with secondary and tertiary amine nitrogen donors in the axial positions. The product of the 4-nitrophenyl phosphate hydrolysis reaction is a phosophoramide derivative (Fig. 36). Kinetic studies of this reaction yielded a maximum second-order rate constant for 4-nitrophenyl phosphate hydrolysis of $(1.52 \pm 0.05) \times 10^{-3}\,M^{-1}\,s^{-1}$ at pH = 5.9 and 35 °C. Rate studies as a function of pH yielded a bell-shaped curve with $pK_1 = 5.2$ and $pK_2 = 6.3$. These values correspond to protonation constants for the substrate

($NPP^{2-} + H^+ = HNPP^-$; $NPP^{2-}$ = 4-nitrophenyl phosphate dianion) and supporting chelate ligand ($NH + H^+ = NH_2^+$, NH = donor of macrocycle).

Treatment of bizinc complexes of a series of aryl-bridged ligands (Fig. 37a–d) with 4-nitrophenyl phosphate in DMSO and buffered water (tris (pH 8.36) or HEPES (pH 8.13)) at 55 °C results in phosphate ester hydrolysis with pseudo first-order rate constants as shown in Fig. 37.[204] Mononuclear analogs (Fig. 37e and f) also exhibit phosphate monoester hydrolysis reactivity, albeit significantly lower than that of the binuclear systems. Studies of the rate of 4-nitrophenyl phosphate hydrolysis versus pH for the reaction promoted by the binuclear zinc complex ligated by *S*,*S*′-bis (10-(1,4,7-triazacyclododecyl))-1′,3′-dithiobenzene (Fig. 37a) yielded a kinetic p$K_a$ of 7.8. This value was attributed to deprotonation of a bridging $H_2O$ ligand between the zinc ions. A mechanistic pathway involving attack of the bridging hydroxide on a coordinated phosphate monoester dianion has been proposed for this system.

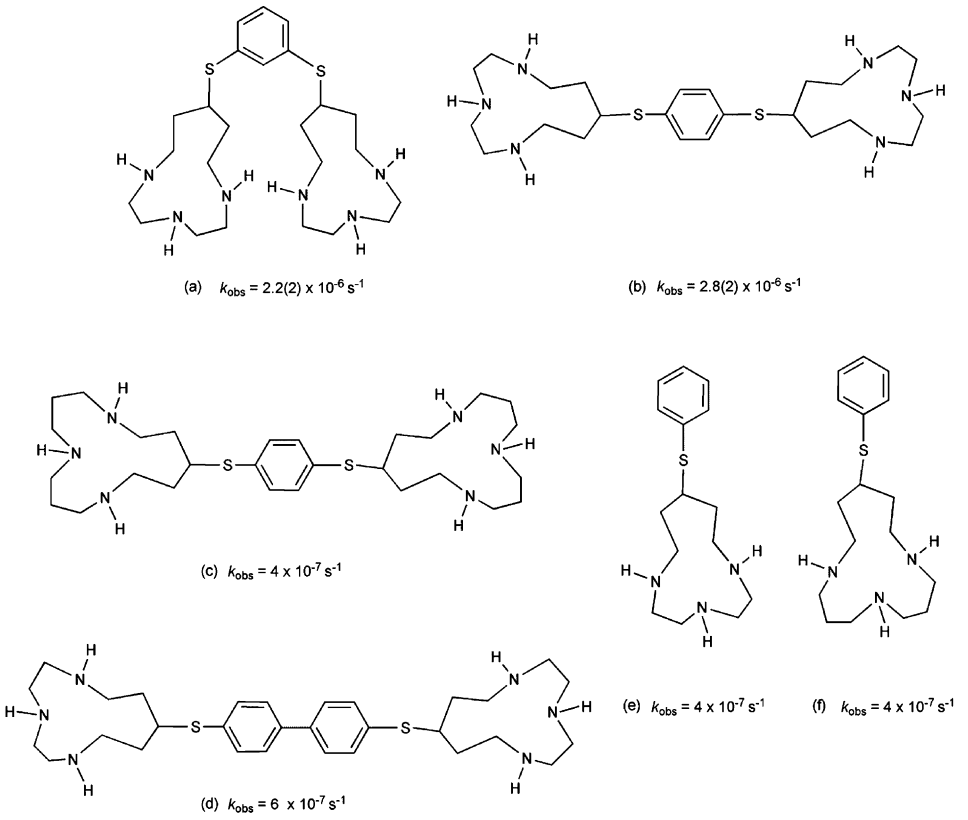


**Fig. 37** Aryl-bridged ligands and pseudo first-order rate constants for the hydrolysis of 4-nitrophenyl-phophate promoted by the zinc complex of each ligand. Pseudo first-order rate constants were determined using 227 mM (dimer) or 454 mM (monomer) solutions.

The mononuclear four-coordinate zinc hydroxide complex [($Tp^{iPr2}$)Zn–OH] does not promote the hydrolysis of 4-nitrophenylphosphate in $Et_2O$ solution.[205] Instead, the phosphate ester is deprotonated to give a binuclear μ-phosphate complex, [($Tp^{iPr2}Zn)_2$(μ-$O_2P$(O–$C_6H_4$–*p*-$NO_2$)].

Outside the scope of coverage of this contribution are Zn(II)-promoted reactions involving ATP hydrolysis.[203]

## PHOSPHATE DIESTER AND TRIESTER HYDROLYSIS

Hydrolysis reactions involving phosphate diester and triester substrates, particularly bis(4-nitrophenyl) phosphate and tris(4-nitrophenyl) phosphate, have often been examined as model reactions phosphate ester cleaving enzymes. The hydrolysis of phosphotriesters is also relevant to the chemistry of phosphotriesterases, zinc-containing enzymes found in soil bacteria.[206,207] The active site of the phosphotriesterase from *Pseudomonas diminuta* contains two zinc centers ligated by a mixture of oxygen and nitrogen donors (Fig. 38).[208,209] A proposed mechanism for this enzyme involves attack of the bridging hydroxide on the coordinated phosphotriester substrate.[210]

Similar to studies of phosphate monoester hydrolysis reactions, extensive kinetic and mechanistic investigations involving exchange inert Co(III) compounds have yielded insight into the pathways of these reactions.[9,192,194,197,198,200,211–220]

Several synthetic mononuclear zinc complexes have been shown to exhibit stoichiometric or catalytic hydrolysis reactivity involving phosphate di- and/or triester substrates. For example, a mononuclear zinc complex supported by the

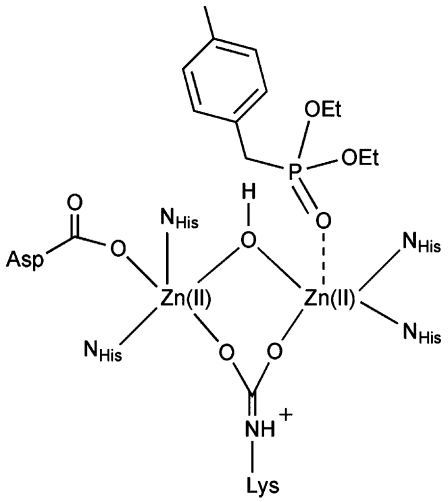


Fig. 38Structure of active site binuclear zinc cluster in the phosphotriesterase from *P. diminuta* in the presence of the competitive inhibitor diethyl-4-methylbenzyl phosphonate.

$Me_2$pyo[14]trien$eN_4$ (CR) ligand (Fig. 6a) catalyzes the hydrolysis of the triester diphenyl 4-nitrophenyl phosphate in aqueous acetonitrile solution.[221] This reaction is first-order in zinc complex and phosphate ester. On the basis of pH-rate studies, which revealed a kinetic p$K_a$ value of 8.7,[40] the active zinc complex is proposed to be $[(CR)Zn–OH]^+$. A hybrid mechanism in which the zinc center of $[(CR)Zn–OH]^+$ serves to provide the hydroxide nucleophile, and also electrophilically activates the phosphoryl P–O bond, is favored for this system. This type of bifunctional mechanism was proposed based on the fact that the second-order rate constant for the $[(CR)Zn–OH]^+$-catalyzed reaction ($2.8 \times 10^{-1}$ $M^{-1}s^{-1}$) is an order of magnitude larger than that of free hydroxide ion-catalyzed hydrolysis ($2.8 \times 10^{-2}\,M^{-1}s^{-1}$). As $OH^-$ is a better nucleophile than the zinc-coordinated hydroxide, Lewis acid activation of the substrate is also operative in this system.

Attachment of a cyclodextrin unit to an N–$CH_3$ form of the CR macrocycle (Fig. 39) yielded a zinc complex with only modestly improved effectiveness ($k_2 = 21.7 \times$ $10^{-2}\,M^{-1}s^{-1}$) over the mononuclear system ($k_2 = (3.80 \pm 0.05) \times 10^{-2}\,M^{-1}s^{-1}$) for the hydrolysis of diphenyl 4-nitrophenyl phosphate under identical conditions.[109] This enhancement is proposed to be due to binding of 4-nitrophenolate moiety in the cyclodextrin cavity.

Bifunctional analogs of the $[(CR)Zn]^{2+}$ (Fig. 6a) structure in which an auxiliary catalytic imidazole or thiophenol group has been incorporated (Fig. 40) exhibit enhanced reactivity for the intramolecular transesterification reaction of 2-hydroxypropyl 4-nitrophenyl phosphate (HPNP) relative to the parent complex.[222]

Zinc complexes of the cyclen ([12]ane$N_4$ = 1,4,7,10-tetraazacyclododecane) ligand have been extensively studied in terms of phosphate ester hydrolysis reactivity. For example, a proposed binuclear Zn(II) hydroxide complex of cyclen was reported to enhance the rate of hydrolysis of ethyl(2,4-dinitrophenyl)-methylphosphonate and diethyl(2,4-dinitrophenyl) phosphate.[223,224] It should be noted that the nuclearity of the zinc–cyclen complex in solution was not conclusively identified in this work.

The mononuclear zinc complexes $[([12]aneN_3)Zn(OH_2)](ClO_4)_2$ (Fig. 4) and $[([12]aneN_4)Zn(OH_2)](ClO_4)_2$ (Fig. 5) promote the hydrolysis of the triester tris(4-nitrophenyl) phosphate and the diester bis(4-nitrophenyl) phosphate.[225] For these

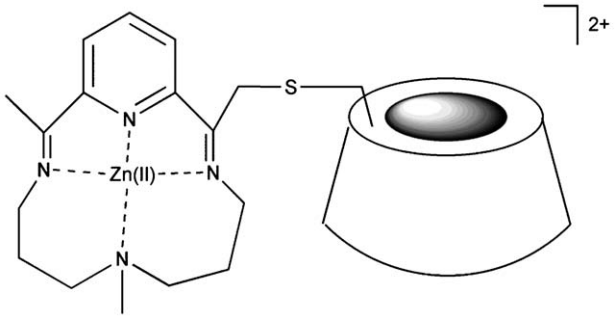


**Fig. 39** Cationic portion β-cyclodextrin-appended zinc complex.

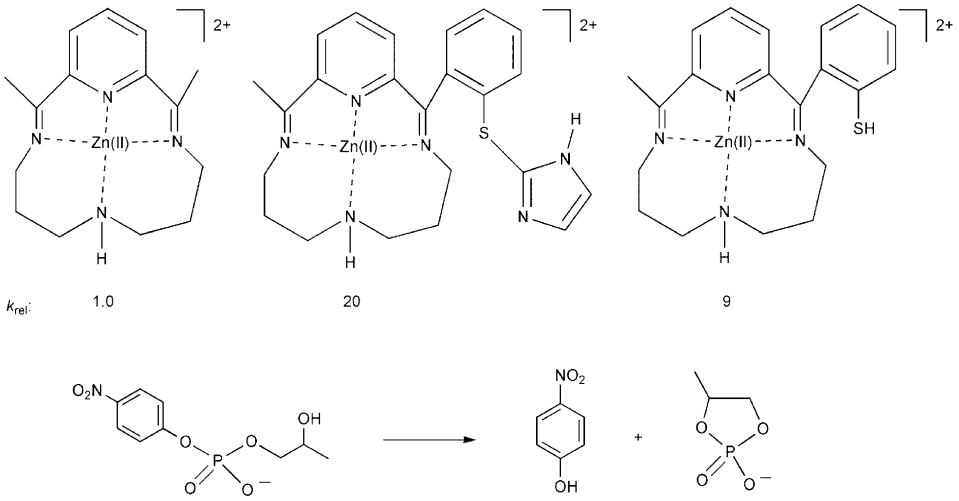


**Fig. 40** (top) Cationic portion of bifunctional zinc complexes and relative second-order rate constant values and (bottom) intramolecular transesterification reaction of 2-hydroxypropyl 4-nitrophenyl phosphate (HPNP).

reactions, pH-rate profiles indicate that the active species are the zinc hydroxide derivatives [([12]ane$N_3$)Zn(OH)]$ClO_4$ and [([12]ane$N_4$)Zn(OH)]$ClO_4$. For the phosphate triester hydrolysis reactions, the second-order rate constants at 25 °C and $I = 0.20$ for free $OH^-$, [([12]ane$N_3$)Zn(OH)]$ClO_4$, and [([12]ane$N_4$)Zn(OH)]$ClO_4$ are $10.7 \pm 0.2$, $7.0 \pm 0.2$, and $3.7 \pm 0.2\ M^{-1}\,s^{-1}$, respectively. Thus, free $OH^-$ ion is the most reactive species for the hydrolysis of tris(4-nitrophenyl) phosphate. However, for the hydrolysis of bis(4-nitrophenyl) phosphate, [([12]ane$N_3$)Zn(OH)]$ClO_4$ ($k = (8.5 \pm 0.2) \times 10^{-5}\ M^{-1}\,s^{-1}$) is approximately four times more reactive than [([12]ane$N_4$)Zn(OH)]$ClO_4$ ($k = (2.1 \pm 0.2) \times 10^{-5}\ M^{-1}\,s^{-1}$) and free $OH^-$ ($k = (2.4 \pm 0.1) \times 10^{-5}\ M^{-1}\,s^{-1}$) at 35 °C and $I = 0.20$ ($Na^+$). The differing hydrolytic reactivity of [([12]ane$N_3$)Zn(OH)]$ClO_4$ (relative to free $OH^-$) for activated phosphate triester versus diester hydrolysis has been explained in terms of differing mechanistic pathways. Specifically, in the triester hydrolysis reaction, the Zn(II) center of [([12]ane$N_3$)Zn(OH)]$ClO_4$ is primarily proposed to provide the nucleophile, with little or no interaction with the P = O group of the substrate (Fig. 41). However, in the phosphate diester hydrolysis reaction, a hybrid-type mechanism is proposed wherein the zinc center is suggested to provide the hydroxide nucleophile as well as electrophilic activation of the P = O moiety of the monoanionic diester substrate.

Insight into the role of the serine nucleophile in the catalytic cycle of alkaline phosphatase was gained through studies of the bis(4-nitrophenyl) phosphate reactivity of a mononuclear Zn(II) complex supported by the (*S*)-1-(2-hydroxy-2-phenylethyl)- 1,4,7,10-tetrazacyclodecane ligand (Scheme 33).[226] In aqueous solution, this complex exhibits a $pK_a$ value for the zinc-bound alkoxide moiety of $7.30 \pm 0.02$.

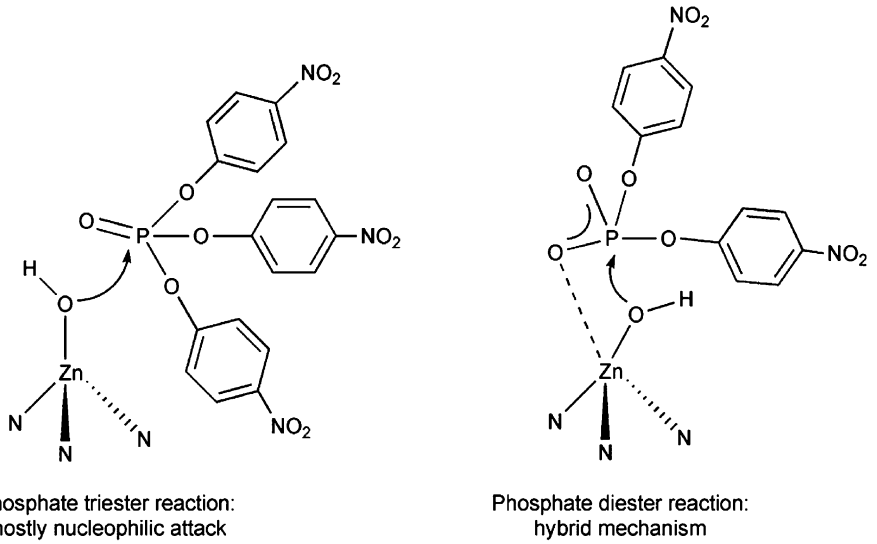


**Fig. 41** Proposed mechanisms for phosphate triester and diester hydrolysis promoted by [([12]aneN$_3$)Zn(OH)]ClO$_4$.

A phosphoryl transfer reaction from bis(4-nitrophenyl) phosphate to the zinc-bound alkoxide moiety is promoted by this complex in aqueous solution (pH = 6.0–10.3) at 35°C and $I = 0.10$ M ($NaNO_3$). A pH-rate profile for this reaction yielded a sigmoidal curve and a kinetic p$K_a$ value of 7.4. As this value corresponds to that measured for the Zn–OR moiety by potentiometric titration, the zinc-bound alkoxide was confirmed as the reactive nucleophile for phosphoryl transfer. The rate of this reaction is 125 times greater than for the bis(4-nitrophenyl) phosphate hydrolysis reaction promoted by [([12]aneN$_4$)Zn(OH)]ClO$_4$.[225] Following phosphoryl transfer to the alkoxide moiety, a second reaction occurs wherein the pendant phosphorylated alcohol undergoes hydrolysis to yield a coordinated phosphate monoester product. This intramolecular reaction involves water activation by the mononuclear zinc center to produce a reactive Zn–OH nucleophile (Scheme 33). The final product is unreactive toward further hydrolysis. Similar studies were performed using a zinc complex of a $N_2O$ (alkoxide) ligand. These studies revealed a $10^4$ rate enhancement for the hydrolysis of the phosphotriester diethyl(4-nitrophenyl) phosphate.[227] Involvement of a zinc-bound alkoxide nucleophile to form a phosphorylated ligand intermediate was proposed for this reaction.

Kinetic studies of reactions of three tris(pyrazolyl)borate-ligated zinc hydroxide complexes ([(Tp$^{R,Me}$)Zn–OH], Fig. 42, top) with triorganophosphate ester substrates in chloroform provided evidence for a concerted or hybrid-type mechanism.[96] The reactions under study in this case are stoichiometric (Fig. 42, bottom) and involve generation of 4-nitrophenol (R‴ = OC$_6$H$_4$–*p*-NO$_2$). Notably, this acidic phenol rapidly undergoes reaction with the starting [(Tp$^{R,Me}$)Zn–OH] complex to yield [(Tp$^{R,Me}$)Zn–OC$_6$H$_4$–*p*-NO$_2$] derivatives. This second reaction is at least

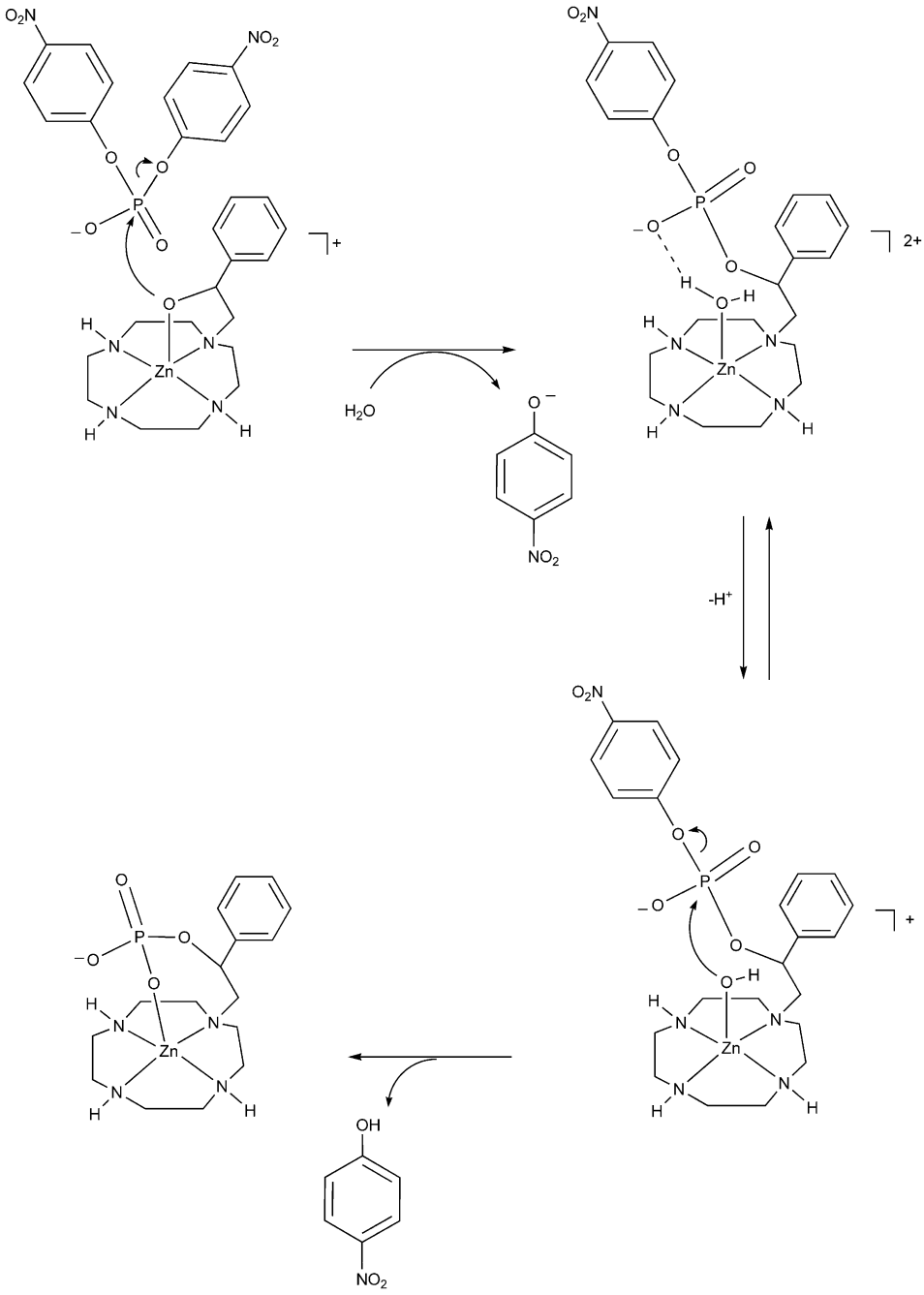


**Scheme 33** Proposed reaction pathway for phosphate ester hydrolysis involving an internal alkoxide nucleophile.

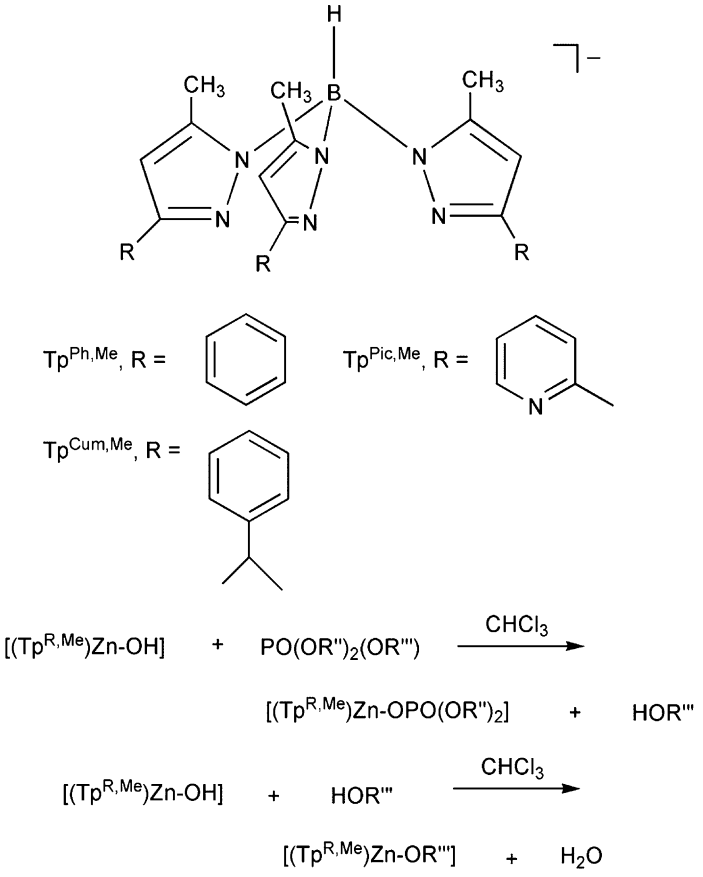


**Fig. 42** Phosphate triester hydrolysis reactivity of [(Tp$^{R,Me}$)Zn–OH] compounds.

two orders of magnitude faster than the initial phosphate triester hydrolysis reaction and is thus not a problem in kinetic studies. The phosphate triester cleavage reactions are first-order both in the zinc complex and phosphate ester. Determination of the second-order rate constant for reaction of each zinc complex with the phosphate triester substrate as a function of temperature in the range of 17.5–47.5 °C enabled the construction of Arrhenius and Eyring plots. Activation energies were determined and ranged from 46 to 69 kJ mol$^{-1}$. The activation entropies ranged from −54 to −126 J mol K$^{-1}$ and were suggested to indicate a degree of ordering in the transition state. A hybrid-type mechanism was proposed in which a four-centered arrangement is present in the activated complex. These reactions are proposed to follow a trajectory (Scheme 18) as outlined previously for amide hydrolysis. It should be noted that a similar phosphate ester hydrolysis reaction had been previously reported involving [(Tp$^{iPr2}$)Zn–OH], albeit kinetic studies were not performed.[205]

Kinetic studies of the reaction of a mononuclear $N_2S$(thiolate)-ligated zinc hydroxide complex (PATH)Zn–OH with tris(4-nitrophenyl) phosphate in 33% ethanol–water and $I = 0.10$ ($NaNO_3$) also point to a hybrid-type mechanism (Fig. 43).[228] Overall, this reaction is second order and a pH-rate profile indicates that the zinc hydroxide species (PATH)Zn–OH is involved in the reaction. The maximum rate constant for this reaction ($16.1(7)\,M^{-1}\,s^{-1}$) is higher than that reported for free hydroxide ion ($10.7 \pm 0.2\,M^{-1}\,s^{-1}$).[225] This implies that a simple mechanism involving nucleophilic attack is not operative, as free $OH^-$ is a better nucleophile. Studies of the temperature dependence of the second-order rate constants for this reaction yielded activation parameters of $\Delta H^{\ddagger} = 36.9(1)\,kJ\,mol^{-1}$ and $\Delta S^{\ddagger} = -106.7(4)\,J\,mol\,K^{-1}$. The negative entropy is consistent with considerable order in the transition state and a hybrid-type mechanism (Fig. 43, bottom).

The reactivity of zinc complexes supported by a variety of tridentate amine donor ligands (Fig. 44) with diphenyl 4-nitrophenyl phosphate in 20% (v/v) acetonitrile–water, and with 2,4-dinitrophenyl diethyl phosphate in 1% (v/v) in methanol–water, has been investigated.[229,230] For the former reaction, the second-order rate constant for the hydrolysis of 2,4-dinitrophenyl diethyl phosphate correlates linearly with the $-\Delta H$ value for the formation of the $[(ligand)Zn(OH_2)]^{2+}$ complex from free chelate ligand and aqueous zinc ion. This indicates that in this series of complexes, faster hydrolysis of 2,4-dinitrophenyl diethyl phosphate corresponds to weaker chelate

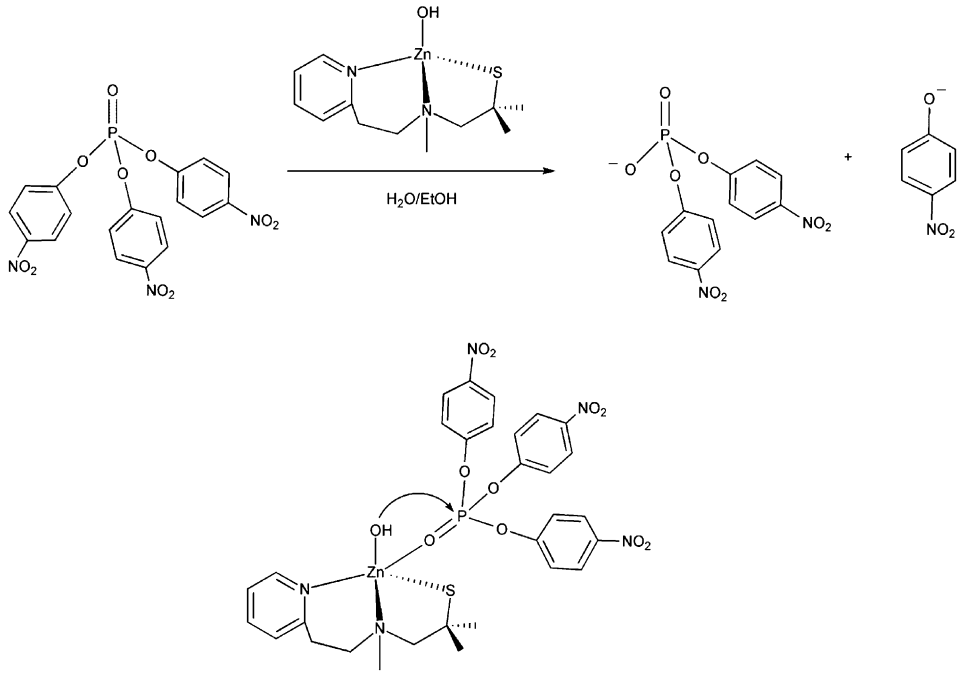


**Fig. 43** (top) Tris(4-nitrophenyl) phosphate reaction involving (PATH)Zn–OH and (b) proposed reactive species in a hybrid-type mechanistic pathway.

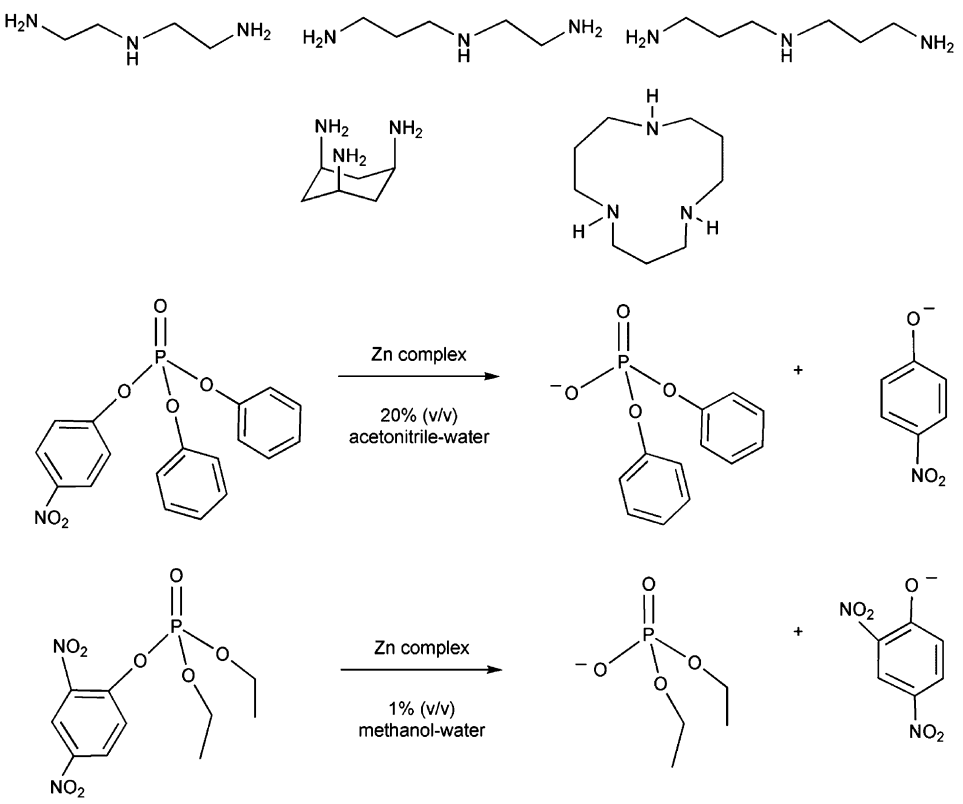


**Fig. 44** (top) Tridentate amine donor ligands and (bottom) phosphate triester hydrolysis reactions promoted by zinc complexes of these ligands.

ligand binding to the zinc center. This weaker coordination in turn correlates with a more Lewis acidic zinc ion, and a lower p$K_a$ value for the zinc-bound water molecule. Similar results have been obtained for the hydrolysis reaction of 2,4-dinitrophenyl diethyl phosphate.[230] These reactions are proposed to take place via a mechanism wherein a zinc-coordinated hydroxide ion attacks the coordinated phosphate triester.

In a separate study, zinc complexes of a variety of macrocyclic and linear polyamines (Fig. 45) have been probed for transesterification reactivity involving 2-hydroxypropyl 4-nitrophenyl phosphate (HPNP, Fig. 40, bottom) and for hydrolysis reactivity involving the phosphate diester bis(4-nitrophenyl) phosphate.[231] As outlined below, for the ligands shown in Fig. 45, tridentate donors that coordinate to the zinc center in a facial or tripodal coordination mode produce the most reactive complexes. This is because the lower coordination number of these ligands (relative to tetradentate donor analogs) allows for coordination positions to be available for interactions between the zinc center and the phosphate ester. Examination of the pH-dependence of the HPNP-transesterification reaction involving Zn(II) complexes of L5–L7 and L9–L12 revealed a sigmoidal curves

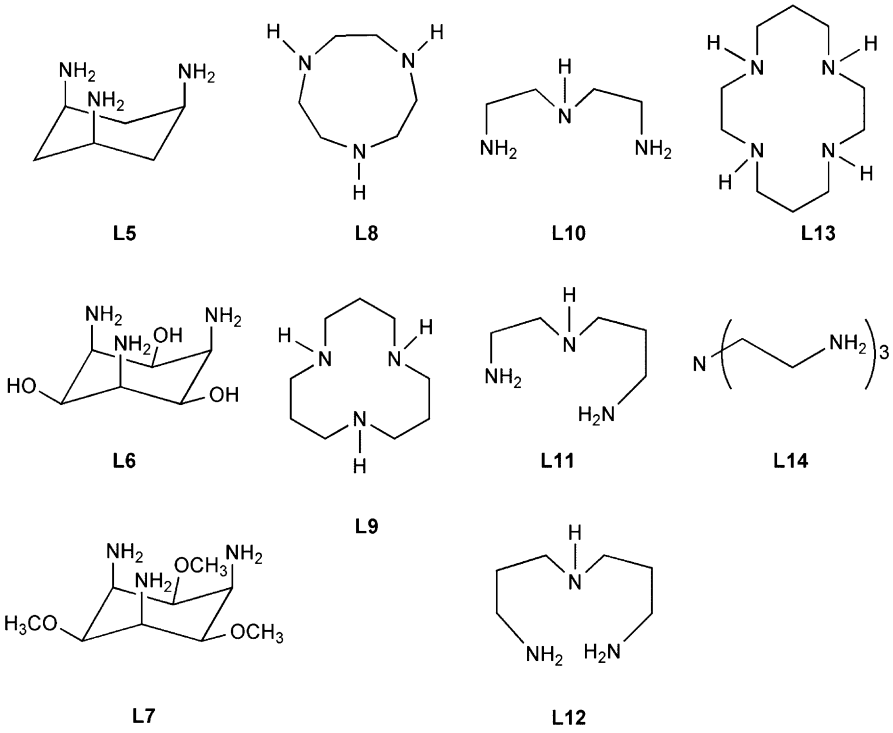


**Fig. 45** Macrocyclic and linear polyamine ligands.

and kinetic p$K_a$ values that are similar to the p$K_a$ values determined by potentiometric titration for a zinc-coordinated water molecule. Working at a pH high enough to ensure full deprotonation of the Zn–$OH_2$ moiety in each complex, variable concentration studies indicated a first-order dependence on zinc complex concentration and overall second-order reactions for HPNP transesterification. Analysis of the range of second-order rate constants obtained for zinc complexes of ligands L5–L9 in a Brønsted plot (log $K$ versus p$K_a$ (kinetic)) at 25 °C yielded a linear correlation and $\beta_{nuc}$ value of 0.75. Interpretation of this value is discussed below in comparison to that obtained in reactions involving the hydrolysis of bis-4-nitrophenylphosphate. A solvent deuterium isotope effect value ($^{D}k = 1.43$) was determined for the transesterification reaction involving the L6-ligated zinc complex at pH = 10.5. This $^{D}k$ value is consistent with nucleophilic attack involving the Zn–OR species of the coordinated substrate (Fig. 46) and not general base catalysis.

For the hydrolysis of bis-4-nitrophenylphosphate hydrolysis promoted by zinc complexes of L5–L14, kinetic studies were carried out at pH = 11 to ensure full deprotonation of the Zn–$OH_2$ moiety of the complexes. Rate constants obtained at 25 °C were used in the preparation of a Brønsted plot. In this plot, reactivity differences as a function of the type of chelate ligand present are clearly evident. Zinc complexes supported by L5–L7 and L9 exhibit the highest reactivity and the

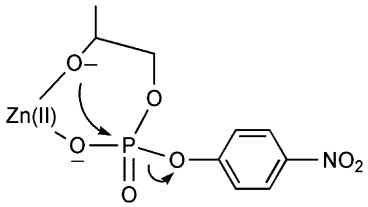


**Fig. 46** Proposed intramolecular nucleophilic attack in the transesterification of HPNP.

rate constants for these reactions exhibit a linear correlation in the Brønsted plot ($\beta_{nuc} = 0.20$). The complexes of L13 and L14 exhibit the lowest bis-4-nitrophenylphosphate hydrolysis reactivity, whereas the complexes supported by a tridentate linear ligand (L10–L12, Fig. 45) exhibit intermediate efficiency, albeit with no linear correlation in the log $K$ versus p$K_a$ plot.

The $\beta_{nuc}$ values obtained for the reactions involving zinc complexes of L5–L9 (HPNP transesterification) and L5–L7 and L9 (bis-4-nitrophenylphosphate (diester) hydrolysis) are an indication of two opposing effects of the zinc center, specifically the involvement of the metal center in substrate activation, and the loss of efficiency of the nucleophile due to zinc coordination. These $\beta_{nuc}$ values differ notably from the value ($\beta_{nuc} = -0.15$) determined for phosphate triester hydrolysis promoted by zinc complexes of the ligands shown in Fig. 44.[230] This difference has been interpreted to indicate that for HPNP transesterification and BNP hydrolysis, the efficiency of the zinc-bound nucleophile is more important in determining intrinsic complex reactivity than is substrate activation, whereas for the hydrolysis of phosphate triesters, activation of the substrate is more important. This difference is attributed to the fact that for HPNP and BNP reactivity, negative charge build-up during the reaction is localized on an oxygen atom that is not directly bound to the zinc center. However, for phosphate triester hydrolysis, anionic charge build-up occurs on the zinc-bound oxygen atom and is stabilized by the metal center. Therefore, for the HPNP and BNP reactions, the zinc center is less able to stabilize the increasing negative charge on the substrate and the reactivity of the zinc-bound nucleophile instead plays a major role.

Mononuclear zinc hydroxide complexes supported by tripodal tetradentate ligands, some of which contain hydrophobic bulky appendages (tris(2-aminoethyl) amine (L15), *N*,*N*′,*N*″-tris(2-benzylaminoethyl)amine (L16), and *N*,*N*′,*N*″-tris(imbenzyl-L-histidylethylaminoethyl)amine (L17) ligands (Fig. 47)), have been identified via pH-rate profile studies as the reactive species involved in hydrolysis reactions of bis-4-(nitrophenyl) phosphate and tris(4-nitrophenyl) phosphate in 33% methanol/water.[232] The Zn(II) hydroxide complex of L17 exhibits higher efficiency in both phosphate diester and triester hydrolysis reactions than the zinc complexes of the other two tripodal tetradentate ligands. This is despite a lower p$K_a$ (7.43) value for the $[(L17)Zn(OH_2)]^{2+}$ species ($[(L15)Zn(OH_2)]^{2+}$: 10.72; $[(L16)Zn\ (OH_2)]^{2+}$: 9.61) suggesting that the phosphate ester cleavage reactivity of the zinc complex of L17 is not determined solely by the nucleophilicity of the Zn–OH moiety. Some properties of the L17 ligand that may come into play in influencing the reaction pathway for

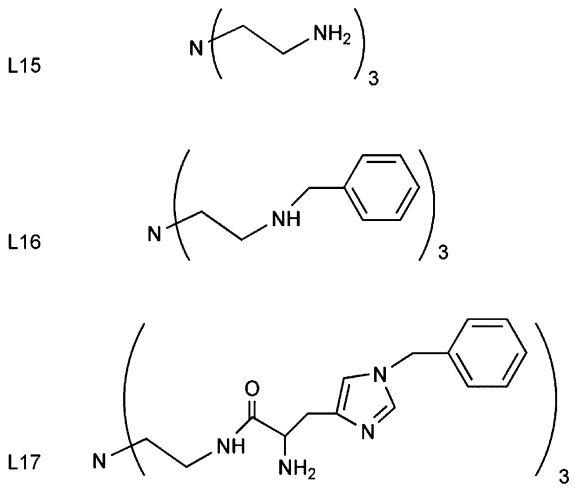


**Fig. 47** Tripodal tetradentate ligands.

phosphate ester hydrolysis include the more labile nature of the imidazole donors, the nature of the chelate ring size formed in zinc complexes, and an overall increased flexibility within the chelate ligand structure.

Mononuclear zinc complexes of *N*,*N*′,*N*″′-tris(3-aminopropyl)amine ligands having either hydrogen atoms or methyl groups as the substituents on the coordinating nitrogen atoms exhibit slight catalytic activity for the hydrolysis of the phosphotriester 2,4-dinitrophenyl diethyl phosphate.[233] A zinc hydroxide complex is proposed as the reactive species that promotes phosphotriester hydrolysis.

Binuclear zinc complexes wherein each metal center is supported by a tripodal tetradentate ligand environment involving a bridging phenolate donor are reactive toward tris(4-nitrophenyl) phosphate and bis(4-nitrophenyl) phosphate in ethanol/water.[234] The pH-rate profile studies of these reactions are consistent with a mechanism that involves the formation of a reactive mononuclear zinc hydroxide species via cleavage of the binuclear solid-state structure. This mononuclear Zn–OH species is proposed to act as the nucleophile toward the phosphate ester substrate.

Chelate tetradentate tripodal ligands having internal hydrogen-bond donors (L18–L20, Fig. 48) produce zinc complexes with enhanced phosphate diester transesterification and hydrolysis reactivity relative to analogs that lack secondary hydrogen-bonding interactions.[20] Comparison of the bis(4-nitrophenyl) phosphate reactivity of zinc complexes of a series of $N_3O$-donor ligands (Fig. 48) revealed that zinc complexes of the L18 and L19 ligands produced transesterification products (4-nitrophenol and the *O*-phosphorylated chelate ligand) whereas the L20 ligand produced only phosphate ester hydrolysis products. For the transesterification reaction of the L19-ligated zinc complex, the second-order rate constant is $9.7 \times 10^{-2}\,M^{-1}\,s^{-1}$ at pH = 7.0 and 25 °C. This rate is approximately six orders of magnitude faster than the spontaneous hydrolysis of bis(4-nitrophenyl) phosphate

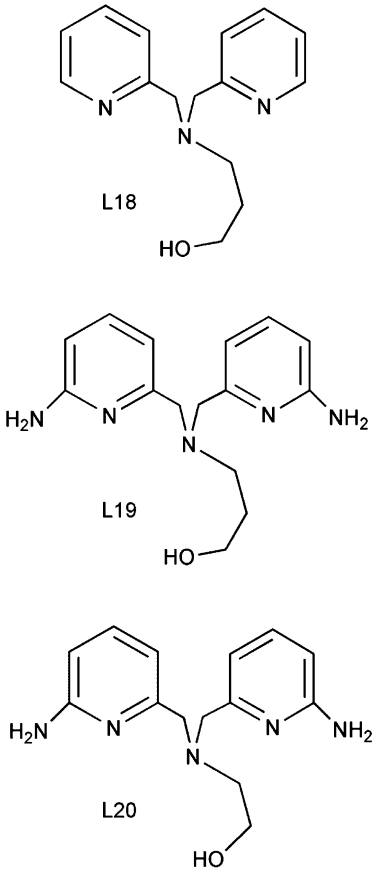


**Fig. 48** Tripodal tetradentate ligands having internal hydrogen-bond donor amine substituents.

under identical conditions. The rate enhancement is attributed to the enhanced nucleophilicity of an alkoxide (versus hydroxide) and the presence of secondary hydrogen-bonding interactions. In addition to the zinc center, the hydrogen bonds can provide additional Lewis acid activation for the phosphate diester substrate, and may assist in the stabilization of a dianionic intermediate. Additional evidence of the influence of secondary hydrogen-bonding interactions was derived from comparison of the bis(4-nitrophenyl) phosphate transesterification reactivity of the zinc complexes of L18 and L19, which revealed a 230-fold reactivity increase for the latter complex. For the hydrolysis reaction involving the L20-ligated zinc complex, the rate acceleration is $\sim 10^5$ over that of the uncatalyzed reaction.

Comparative studies of the HPNP-transesterification reactivity (Fig. 40, bottom) of $[(tapa)Zn(H_2O)]^{2+}$ and $[(tpa)Zn(H_2O)]^{2+}$ (Fig. 49) revealed that the rate of cyclization of the substrate is accelerated by a factor of $3 \times 10^6$-fold for the former

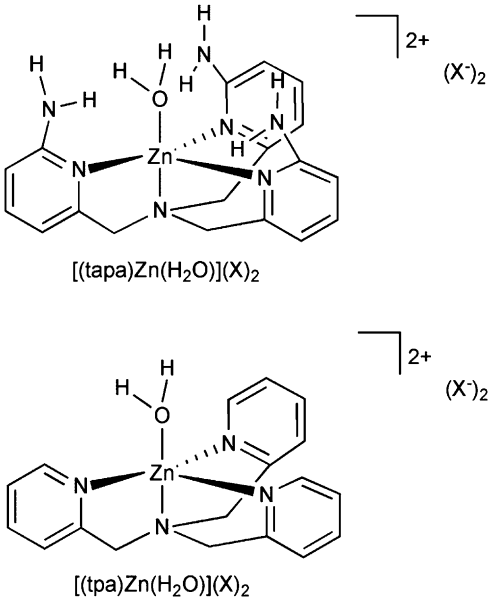


**Fig. 49** Structural drawings of $[(tapa)Zn(H_2O)]^{2+}$ and $[(tapa)Zn(H_2O)]^{2+}$.

complex and $4 \times 10^3$-fold for the latter complex over the uncatalyzed reaction.[235] The difference between these rate enhancements is attributed to enhanced stabilization of a dianionic intermediate in HPNP hydrolysis via secondary hydrogen-bonding interactions.

Several multinuclear zinc complexes that exhibit phosphate diester and triester reactivity have been reported. A binuclear analog of $[(CR)Zn]^{2+}$ (Fig. 6a) in which two $[(CR)Zn]^{2+}$ units are linked by an aromatic spacer was found to be ~4.4 times more effective in terms of the hydrolysis of diphenyl 4-nitrophenyl phosphate in $CH_3CN$:$H_2O$ at 25 °C than its mononuclear analog.[204]

The phosphate diester hydrolysis (using bis(4-nitrophenyl) phosphate) and transesterification (using 2-hydroxypropyl 4-nitrophenyl phosphate) reactivity of the family of binuclear zinc complexes shown in Fig. 37 was examined in studies directed at elucidating how the nature of the ligand bridge influences reactivity.[204] The complex supported by a ligand having a biphenyl linker (Fig. 37d) exhibited the highest reactivity for both substrates. A proposed pathway for the reaction involving bis(4-nitrophenyl) phosphate is shown in Fig. 50. In this reaction, substrate activation is proposed to occur at one zinc center, whereas the nucleophile is generated at the other zinc center. Consistent with this proposed pathway is the identification of a p$K_a$ value of 8 in the pH-rate profile of the reaction. This value is consistent with deprotonation of a terminal Zn–$OH_2$ moiety.

Mono- and binuclear Zn(II) nitrate complexes of the bis(1-methylimidazol-2-ylmethyl)ethylamine and *N*,*N*,*N*′,*N*′-tetrakis(1-methylimidazol-2-ylmethyl)pentane-1,5-diamine ligands (Fig. 51) catalyze the hydrolysis of tris-4-nitrophenyl phosphate

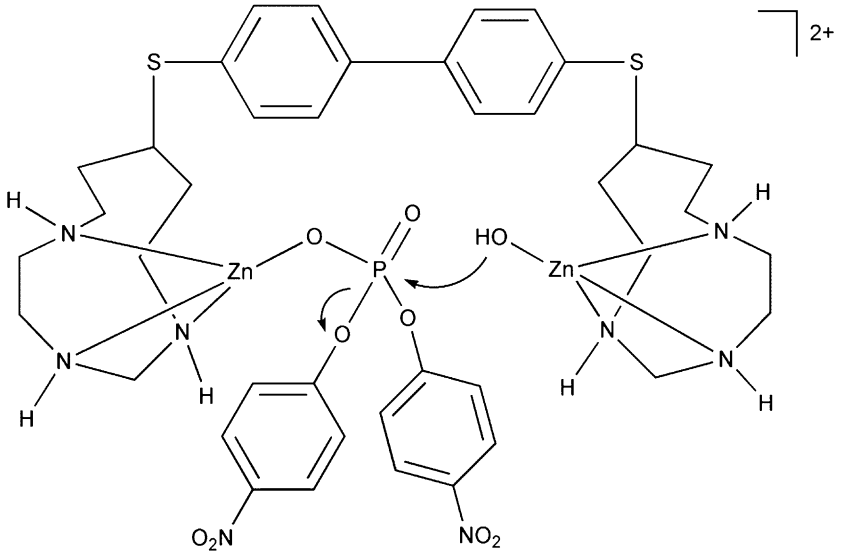


**Fig. 50** Proposed reaction pathway for the hydrolysis of bis(4-nitrophenyl) phosphate promoted by a biphenyl-bridged complex.

to produce bis(4-nitrophenyl) phosphate in 33% ethanol–water solution.[236] No further reaction with the phosphate diester product occurs in this system. Acidic (e.g. aqua) and basic (e.g. hydroxo) forms of both complexes catalyze the hydrolysis of the phosphate triester, with the activity increasing for both types of complexes with increasing pH, which is consistent with the formation of a reactive zinc hydroxide species that may be acting as a nucleophile or general base. The mononuclear complex exhibits higher reactivity, which is consistent with the higher $pK_a$ value (8.16), and formation of a terminal Zn–OH moiety in this complex, whereas a bridging $Zn_2(\mu\text{-OH})$ ($pK_a = 6.99$) is formed in the binuclear derivative. No evidence was found for pre-equilibrium formation of a substrate adduct in these reactions.

Zinc complexes of macrocyclic N- and N/O-donor ligands (L21–L24, Fig. 52) promote the hydrolysis of bis(4-nitrophenyl) phosphate to produce 4-nitrophenyl phosphate and 4-nitrophenol via varying mechanistic pathways.[105,237–241] For example, comparison of the bis(4-nitrophenyl) phosphate reactivity of mono- and binuclear zinc monohydroxo complexes of the L21 ligand revealed that the mononuclear zinc hydroxide complex is more effective at hydrolyzing the phosphate diester substrate than the binuclear monohydroxo complex.[237] Important differences between the reactions involving the mono- versus binuclear complexes include the nature of the nucleophile (terminal Zn–OH versus bridging Zn–OH) and possible differences in recognition of the substrate by the metal complex. In the monozinc complex (Fig. 53), a better nucleophile is present (terminal Zn–OH), but the substrate can interact with only a single Zn(II) center. In the bizinc complex, a poorer

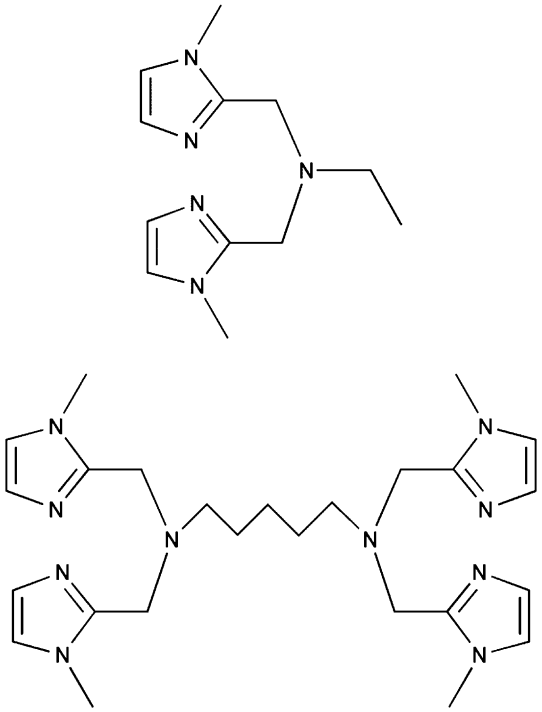

**Fig. 51** Bis(1-methylimidazol-2-ylmethyl)ethylamine; (top) and *N*,*N*,*N*′,*N*′-tetrakis(1-methylimidazol-2-ylmethyl)pentane-1,5-diamine (bottom) ligands.

nucleophile (bridging Zn–OH) is present but better Lewis activation of the substrate is likely achieved as the phosphate diester can bridge the two zinc centers.

The rate of hydrolysis of bis(4-nitrophenyl) phosphate is approximately 10-fold higher for a binuclear $Zn_2(OH)_2$ complex of the L22 ligand (Fig. 52) versus a mononuclear zinc hydroxide complex of the L23 ligand at 308 K.[105] In this system, a monohydroxide binuclear zinc complex ($Zn_2(\mu$-OH)) does not promote phosphate diester hydrolysis. The 10-fold rate enhancement found for the reaction involving the binuclear $Zn_2(OH)_2$ complex was explained via cooperative interaction between the zinc centers. As shown in Fig. 54, the reaction is proposed to take place via attack of a terminal Zn–OH moiety on a phosphate diester substrate that is interacting with both zinc centers. This suggests a cooperative role for the two zinc centers in the phosphate diester hydrolysis reaction.

Inclusion of an alcohol appendage in the L24 ligand framework (Fig. 52) results in a reaction pathway for bis(4-nitrophenyl) phosphate hydrolysis that involves initial nucleophilic attack of a zinc-bound alkoxide moiety on the substrate to give a phosphorylated intermediate (Scheme 34).[239] This intermediate, similar to the phosphorylated serine intermediate proposed in the catalytic cycle of alkaline phosphatase, is subsequently attacked by a Zn–OH moiety to yield 4-nitrophenyl

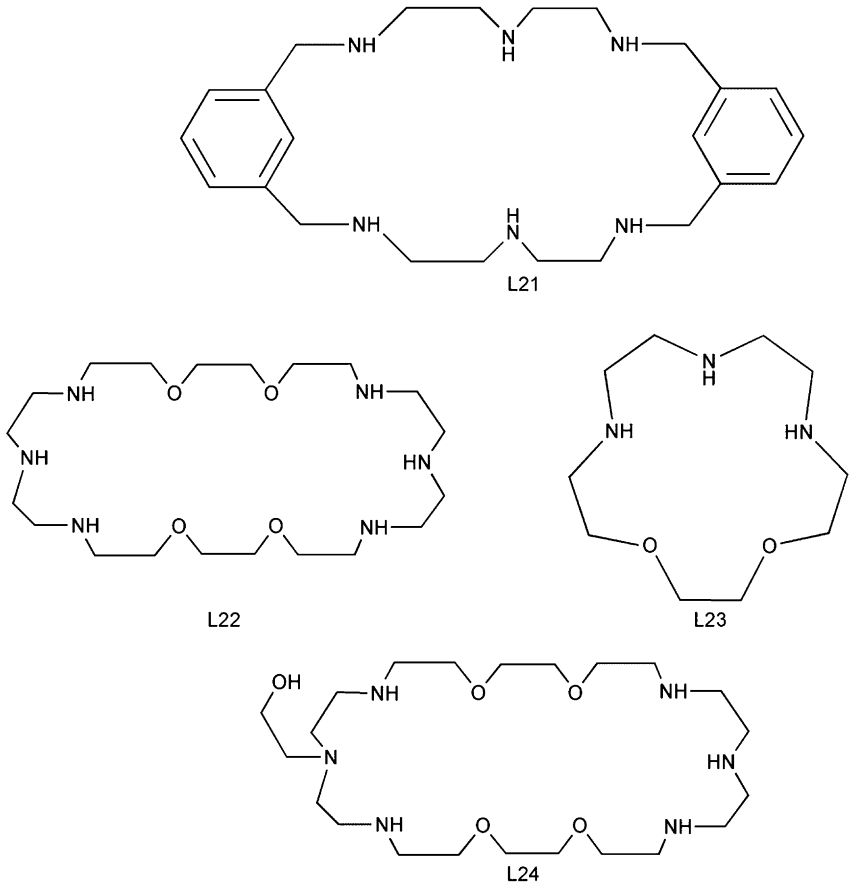


**Fig. 52** Macrocyclic N- and N/O-donor ligands.

phosphate as the final product. Evidence for the initial formation of a new phosphoryl species in the L24-ligated system comes from $^{31}$P NMR where a new resonance appears at 7.3 ppm in aqueous solution as the signal for bis(4-nitrophenyl) phosphate at −8.2 ppm decays. The final phosphate-appended product is subsequently detected by the appearance of a resonance at 7.8 ppm ($J_{H-P} = 11.2$ ppm).

Introduction of a phenanthroline moiety into a chelating macrocyclic ligand (L25, Fig. 55) yields a $[LZn_2(OH)_2]^{2+}$ complex with enhanced bis(4-nitrophenyl) phosphate ester hydrolysis reactivity in aqueous solution relative to $[LZn_2(OH)_2]^{2+}$ complexes of structurally similar ligands (L26 and L27, Fig. 55).[238] The second-order rate constants for these reactions are $62 \times 10^{-5}\,M^{-1}\,s^{-1}$ (L25), $8 \times 10^{-5}\,M^{-1}\,s^{-1}$ (L26), and $4 \times 10^{-5}\,M^{-1}\,s^{-1}$ (L27), respectively. A hybrid-type mechanism akin to that shown in Fig. 54 is proposed wherein the phosphate diester substrate binds to both zinc centers of the $[LZn_2(OH)_2]^{2+}$ complex followed by intramolecular attack of a terminal Zn–OH moiety. The enhanced reactivity of $[L25Zn_2(OH)_2]^{2+}$ is

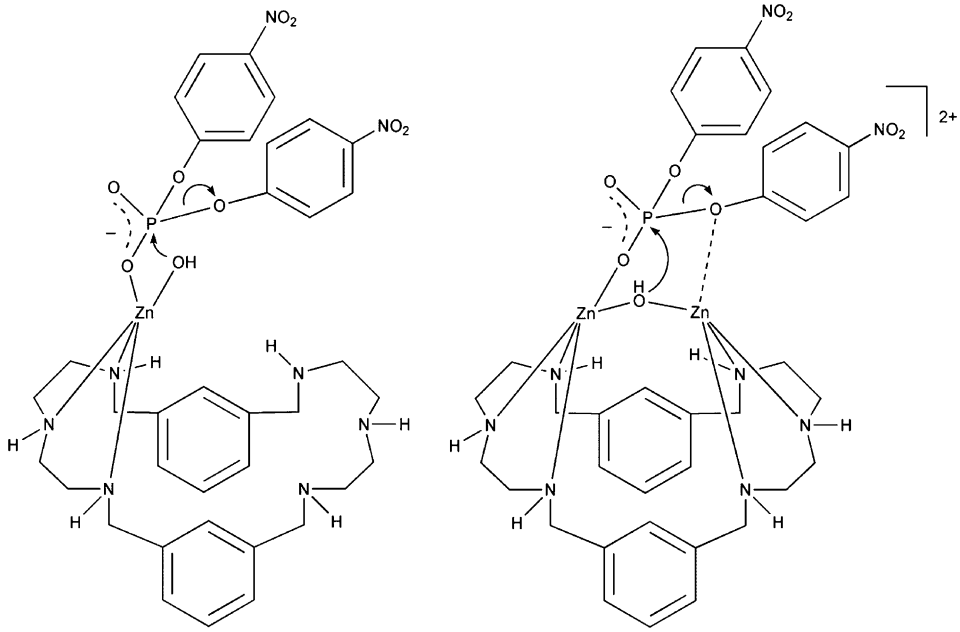

**Fig. 53** Proposed mechanistic pathways for bis(4-nitrophenyl) phosphate hydrolysis reactivity of mono- and bizinc complexes of the L21 ligand.

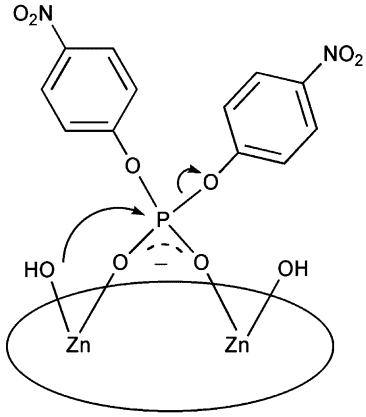

**Fig. 54** Proposed reaction pathway of bis(4-nitrophenyl) phosphate hydrolysis promoted by a binuclear zinc complex of the L22 macrocyclic ligand.

attributed to the presence of the phenanthroline moiety, which may promote coordination of bis(4-nitrophenyl) phosphate via π-stacking and hydrophobic interactions with the aromatic rings of the substrate, and cooperative effects between the zinc centers.

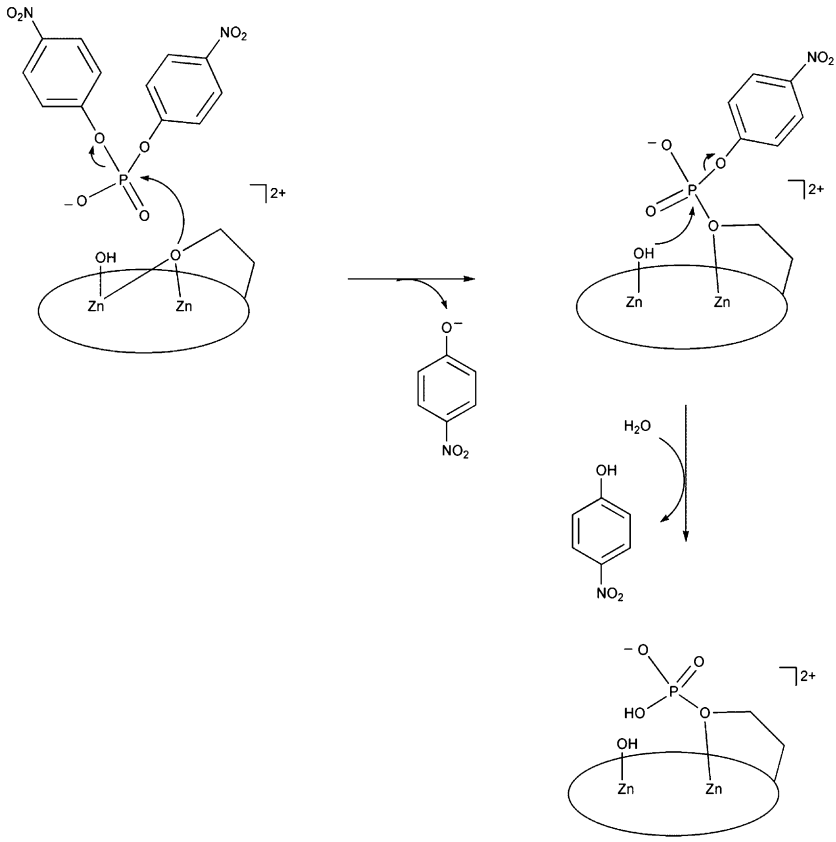


**Scheme 34** Proposed reaction pathway for bis(4-nitrophenyl)phosphate hydrolysis promoted by a bizinc complex of the L24 macrocyclic ligand.

Dipyridine-containing macrocyclic ligands (L28–L30, Fig. 56) have also been used to prepare zinc complexes for phosphate diester cleavage reactivity studies.[240] Active complexes of these ligands for the hydrolysis of bis(4-nitrophenyl) phosphate have in common the presence of one or more Zn–OH units. A zinc hydroxide complex of L28, $[L28Zn(OH)]^{+}$ exhibits a second-order rate constant ($(1.1 \pm 0.06) \times 10^{-4}\,M^{-1}\,s^{-1}$) that is considerably lower than bizinc complexes of the L29 and L30 ligands ($[L29Zn_2(OH)_2]^{2+}$: $(9.6 \pm 0.3) \times 10^{-4}\,M^{-1}\,s^{-1}$; $[L30Zn_2(OH)]^{3+}$: $(19.3 \pm 1.0) \times 10^{-4}\,M^{-1}\,s^{-1}$). This indicates a cooperative role for the zinc centers in the latter two complexes. For the reaction promoted by $[L29Zn_2(OH)_2]^{2+}$, a mechanistic pathway similar to that shown in Fig. 54 is proposed. This is consistent with the availability of multiple open coordination positions at each zinc center in complexes of the L29 ligand, which provides only three nitrogen donors per zinc center. For the zinc complex of the L30 ligand, the active species is proposed to have monodentate coordination of the substrate at one zinc center, and a terminal zinc hydroxide at the

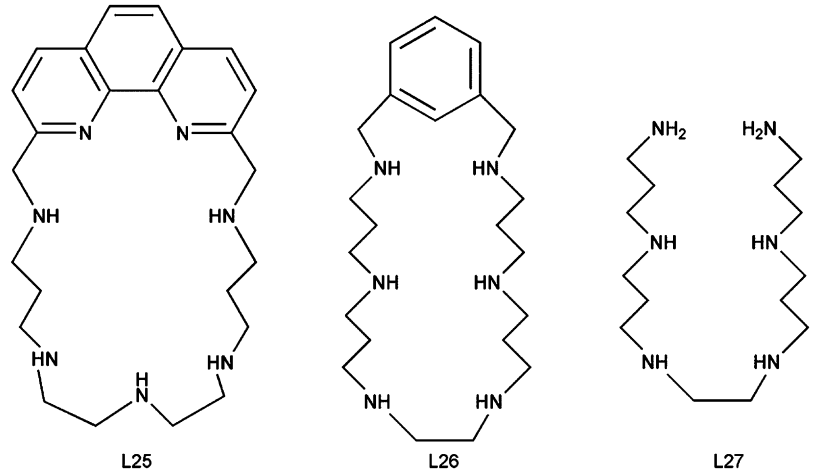


**Fig. 55** L25–L27 ligands.

other zinc center (Fig. 57). As the L30 ligand provides five nitrogen donors per zinc center, this would give each an overall coordination number of six. Hydrophobic and π-stacking interactions involving the pyridyl macrocycles are suggested to enhance substrate coordination to $[L29Zn_2(OH)_2]^{2+}$ and $[L30Zn_2(OH)]^{3+}$ in a similar fashion to that proposed for the phenanthroline containing macrocyclic ligand discussed above.[238]

A binuclear zinc complex of the macrocyclic phenolate-containing ligand BDBPH (Fig. 58) contains zinc centers that are each ligated by three amine donors and bridged by two phenolate oxygen atoms.[242] In a solid-state structure, each zinc center also coordinates a methanol molecule to give an overall distorted octahedral geometry and a Zn–Zn distance of 3.146 Å. In 75% ethanol–water solution, a terminal Zn–OH moiety can be generated at a pH above 9.90. The rate of hydrolysis of tris(4-nitrophenyl) phosphate promoted by this binuclear zinc complex increased in the pH range 9.0–10.5. This reaction is proposed to take place via attack of a terminal Zn–OH moiety on the coordinated tris(4-nitrophenyl) phosphate substrate (Fig. 58). Stabilization of the anionic bis(4-nitrophenyl) phosphate product is suggested to occur by coordination to the binuclear zinc complex.

A similar mechanistic pathway to that shown in the lower portion of Fig. 58 is proposed for tris(4-nitrophenyl) phosophate hydrolysis promoted by binuclear zinc complexes of phenol-based ligands, albeit no kinetic or mechanistic studies were reported for these reactions.[243]

A zinc complex of the BPAN (2,7-bis[2-(2-pyridylethyl)aminomethyl]-1,8-naphthyridine ligand, $[(BPAN)Zn_2(\mu\text{-}OH)(\mu\text{-}Ph_2PO_2)](ClO_4)_2$, Fig. 27) catalyzes the transesterification of the RNA model substrate HPNP (2-hydroxypropyl 4-nitrophenyl phosphate (Fig. 40, bottom) in aqueous buffered solution (HEPES) containing 1% $CH_3CN$.[141] The rate of this reaction was found to be ~7 times fast than the reaction catalyzed by a mononuclear Zn(II) complex of bpta (Fig. 25). A pH-rate

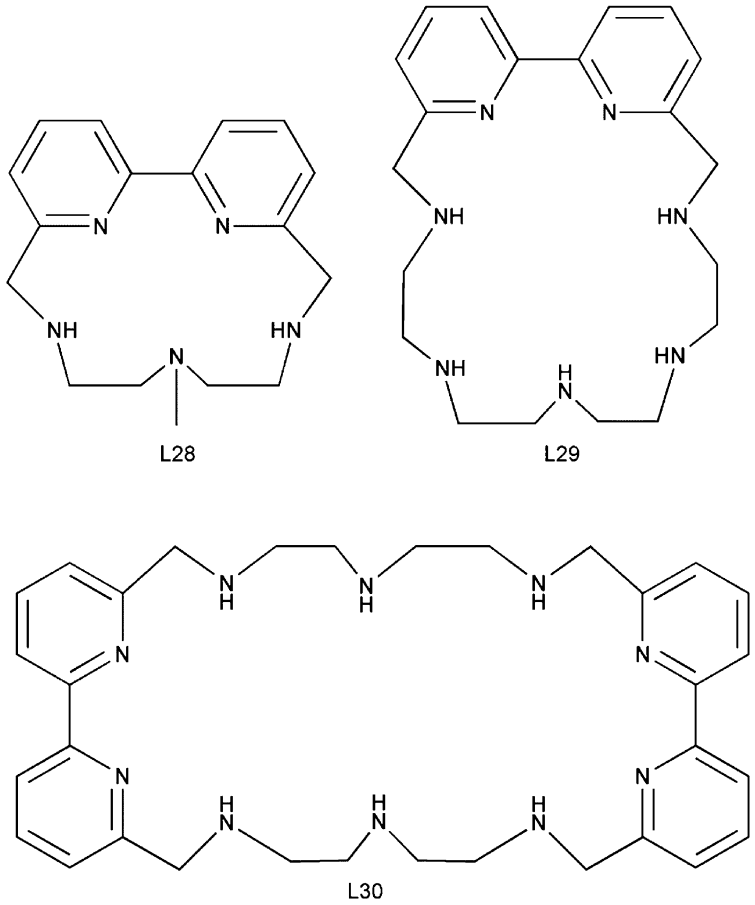


**Fig. 56** L28–L30 ligands.

profile for the reaction involving $[(BPAN)Zn_2(\mu\text{-}OH)(\mu\text{-}Ph_2PO_2)](ClO_4)_2$ revealed an inflection point at pH = 6.97. This value matches a p$K_a$ value determined by potentiometric titration and is assigned to the deprotonation of the bridging water ligand in $([BPAN)Zn_2(\mu\text{-}OH_2)(\mu\text{-}Ph_2PO_2)](ClO_4)_3$. These combined results indicate that the bridging hydroxide moiety in $([BPAN)Zn_2(\mu\text{-}OH)(\mu\text{-}Ph_2PO_2)](ClO_4)_2$ is the base involved in catalyzing the intramolecular transesterification reaction. Further studies indicated that the bridging hydroxide moiety serves as a general base in the HPNP-transesterification reaction.

The $[(BPAN)Zn_2(\mu\text{-}OH)(\mu\text{-}Ph_2PO_2)](ClO_4)_2$ complex also promotes the hydrolysis of bis(4-nitrophenyl) phosphate.[140] This reaction proceeds via initial coordination of the substrate to the binuclear zinc complex ($K = 86 \pm 32\,M^{-1}$). Studies of the effect of pH on this reaction revealed a kinetic p$K_a$ of $7.06 \pm 0.05$, which is consistent with deprotonation of a bridging water molecule. Thus, a bridging hydroxide is the

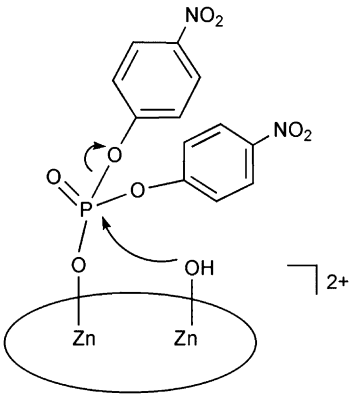


**Fig. 57** Proposed reactive species in the hydrolysis of bis(4-nitrophenyl) phosphate promoted by $[L30Zn_2(OH)]^{3+}$.

reactive species, which could either act as a nucleophile or as a general base. These two possibilities were distinguished by reducing the amount of water present in the reaction mixture, with acetonitrile being used as the cosolvent. This produced a slowing of the rate of phosphate diester hydrolysis indicating that a general base-type mechanism is operative (Scheme 35). Notably, $[(BPAN)Zn_2(\mu\text{-}OH)(\mu\text{-}Ph_2PO_2)](ClO_4)_2$ is only 1.8 times more reactive toward bis(4-nitrophenyl) phosphate than a mononuclear zinc complex of the bpta ligand (Fig. 25).

HPNP transesterification (Fig. 40, bottom) is catalyzed by mono- and bizinc complexes of the *cis*-2,4,6-traminocyclohexane-1,3,5-triol-contaning ligands (L6, L31, and L32) shown in Fig. 59.[244] For the zinc complexes of L31 and L32, bell-shaped pH-rate profiles were obtained for the HPNP-transesterification reaction, indicating deprotonation of two acidic functionalities. The first deprotonation leads to the formation of the reactive species, whereas the second deprotonation results in loss of activity. The mononuclear zinc complex of the L6 ligand exhibits a sigmoidal pH-rate profile, indicating a single deprotonation that leads to reactivity. Overall, the mononuclear zinc complex of L6 is intrinsically more reactive than the bizinc complexes of L31 and L32, as evidenced by comparison of their respective limiting rate constants ($k_{lim}$; $[L6Zn]^{2+}$, $9.7 \times 10^{-3}\,s^{-1}$; $[L31Zn_2]^{4+}$, $1.5 \times 10^{-3}\,s^{-1}$; $[L32Zn_2]^{4+}$, $2.6 \times 10^{-3}\,s^{-1}$). However, the bizinc complexes have a higher affinity for the substrate ($K_b$: $[L6Zn]^{2+}$, $33\,M^{-1}$; $[L31Zn_2]^{4+}$, $107\,M^{-1}$; $[L32Zn_2]^{4+}$, $67\,M^{-1}$). The mechanism for HPNP transesterification catalyzed by the mononuclear $[L6Zn]^{2+}$ complex is suggested to involve simultaneous zinc coordination of the substrate alcohol and phosphate ester groups (Fig. 46). Reactions involving $[L31Zn_2]^{4+}$ and $[L32Zn_2]^{4+}$ may proceed either via the involvement of a zinc-bound hydroxide acting as a base (Fig. 60, left) or via multiple site activation of the substrate and intramolecular attack of a zinc-bound alkoxide moiety (Fig. 60, right). The bell-shaped pH-rate profile for the bizinc systems is attributed to the sequential deprotonation of two zinc-bound water molecules. The first deprotonation reaction

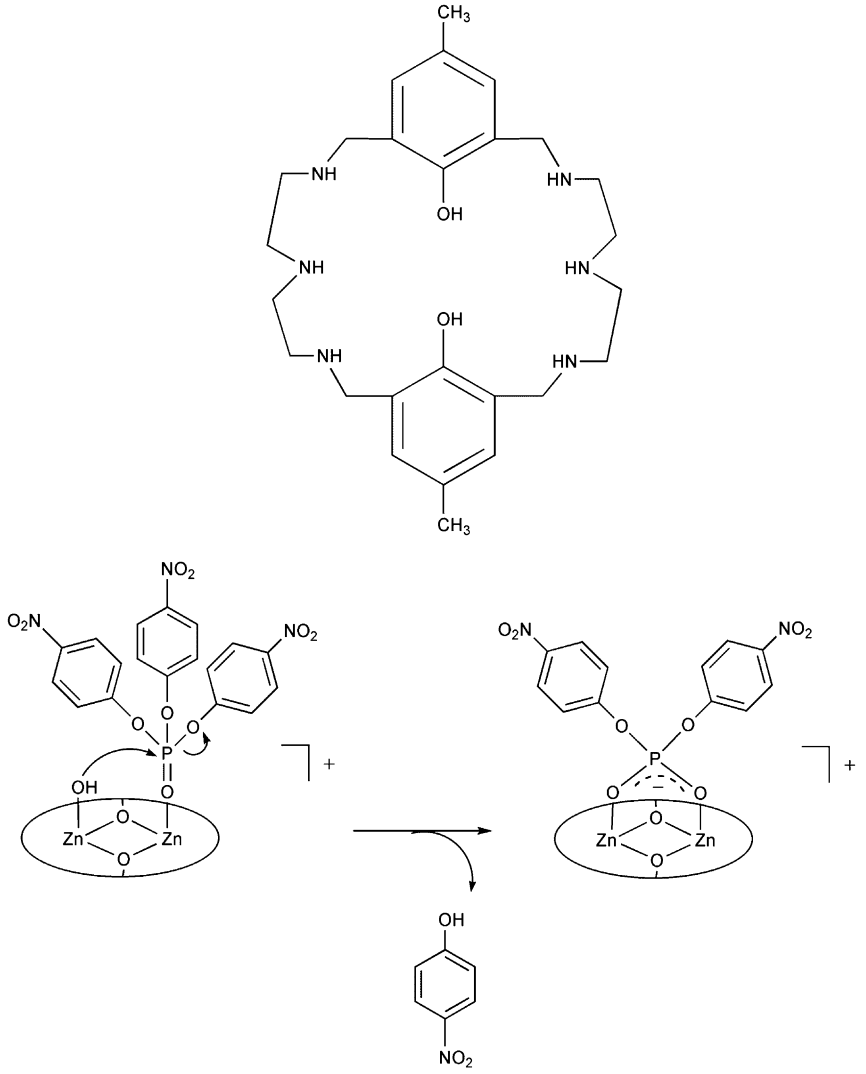


**Fig. 58** (top) BDBPH ligand and (bottom) proposed mechanism for tris(4-nitrophenyl) phosphate hydrolysis.

would yield a Zn–OH species that is active for HPNP transesterification, whereas the second deprotonation would yield a $Zn_2(OH)_2$ species that may interact with the substrate more weakly, perhaps due to blocking of coordination positions as a consequence of bridging hydroxide formation.

Binuclear zinc complexes of pyrazolate-based chelate ligands (Fig. 61) exhibit differing bis(4-nitrophenyl) phosphate hydrolysis reactivity depending on the nature of the supporting chelate ligand.[153] Plots of the pseudo first-order rate constant

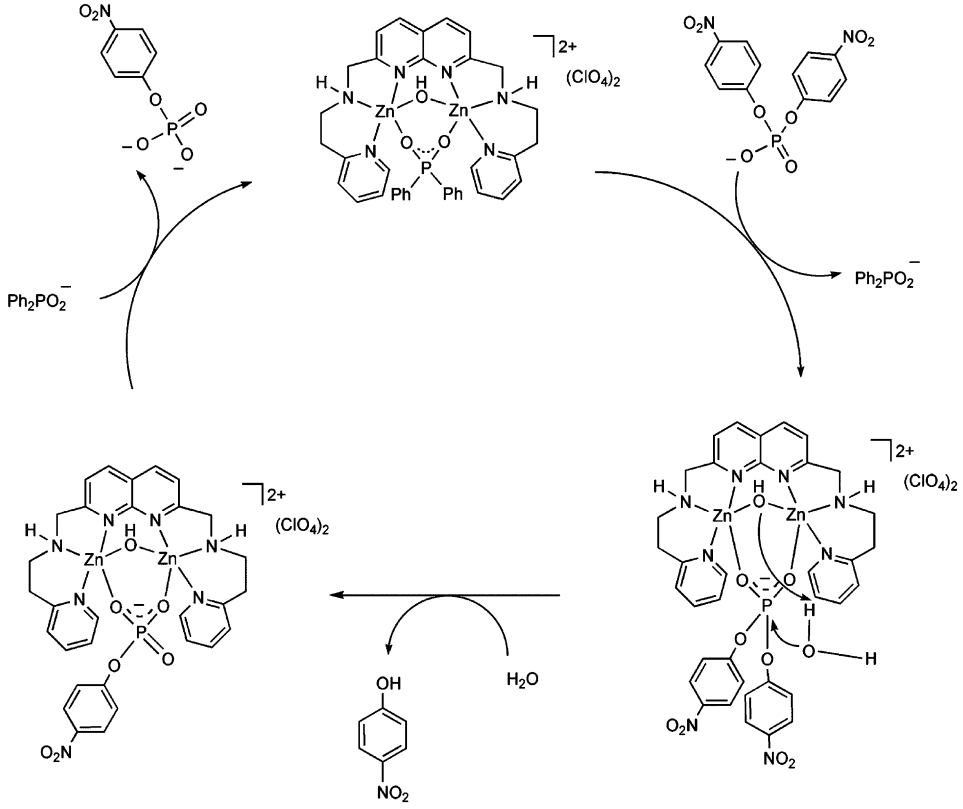

**Scheme 35** Proposed mechanism for bis(4-nitrophenyl) phosphate hydrolysis promoted by $[(BPAN)Zn_2(\mu\text{-}OH)(\mu\text{-}Ph_2PO_2)](ClO_4)_2$.

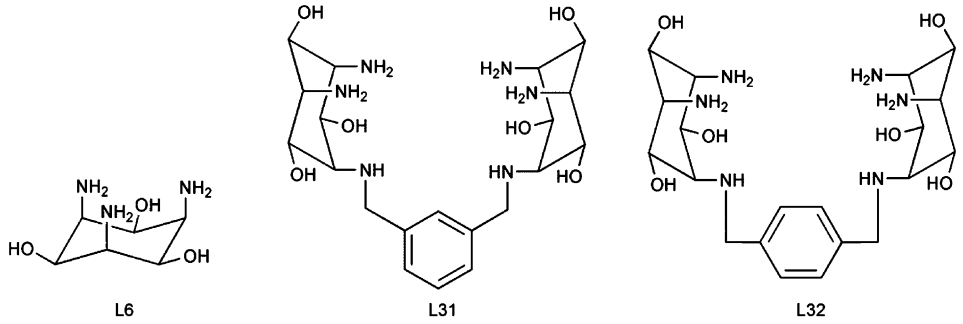

**Fig. 59** The cis-2,4,6-traminocyclohexane-1,3,5-triol-containing ligands.

versus pH for phosphate diester hydrolysis promoted by **5** and **6** yielded kinetic $pK_a$ values consistent with the presence of a reactive zinc hydroxide species. Overall, the reactions are second order and exhibit saturation-type behavior, with **5** ($k = (3.3 \pm 0.3) \times 10^{-5}\,M^{-1}\,s^{-1}$) exhibiting significantly lower reactivity than **6**

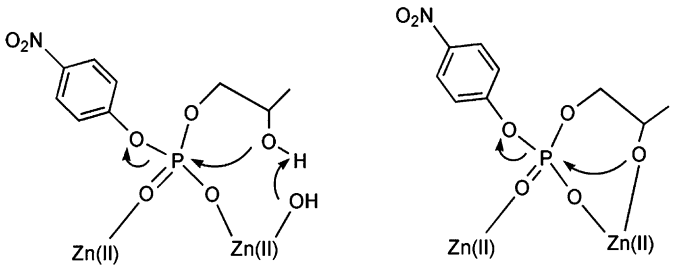


**Fig. 60** Possible mechanistic pathways for HPNP transesterification catalyzed by bizinc complexes of the L31 and L32 ligands.

($(1.1 \pm 0.1) \times 10^{-3}\,M^{-1}\,s^{-1}$) at pH = 8.2, presumably because the hydroxide anion is held more tightly in **5**, which diminishes its nucleophilicity. The proposed mechanism for bis(4-nitrophenyl) phosphate hydrolysis in these systems involves initial equilibrium formation of a zinc complex-substrate adduct followed by phosphate ester hydrolysis. Using this model, substrate binding constants of $K = 24 \pm 3\,M^{-1}$ (**4**) and $18 \pm 1\,M^{-1}$ (**6**) have been determined. These values indicate that the initial substrate coordination is weak, as has been reported for other binuclear zinc complexes.[140,141]

Interestingly, the binuclear zinc $O_2H_3$-bridged species **4** is unreactive toward bis(4-nitrophenyl) phosphate at pH > 7.5. This is attributed to bidentate coordination of the substrate to the binuclear zinc complex with complete displacement of the $O_2H_3$ unit. The zinc centers in the resulting structure each have a coordination number of five, and there is likely not room for coordination and activation of a water molecule. Comparison of the ligand structures in **4** and **6** indicates that while substrate coordination also occurs in **6**, the lower overall coordination number of the supporting chelate ligand enables a coordination position to be available on each zinc center for formation of a Zn–$OH_2$/Zn–OH moiety. In addition, as **6** exhibits enhanced phosphate diester reactivity relative to $Zn(ClO_4)_2$, cooperativity between proximal zinc centers occurs.

Comparison of the bis(4-nitrophenyl) phosphate hydrolysis reactivity of **1** and **2** (Fig. 27) in DMSO:buffered water (1:1) at 50 °C revealed that the complex having the greater Zn···Zn separation is more reactive (**1**: $k = (1.6 \pm 0.1) \times 10^{-4}\,M^{-1}\,s^{-1}$; **2**: $(4.6 \pm 0.1) \times 10^{-4}\,M^{-1}\,s^{-1}$).[154] pH-rate studies are consistent with the involvement of a Zn–OH moiety in these hydrolytic reactions. Saturation-type behavior is observed in terms of substrate concentration for both reactions. Substrate binding constants were determined (**1**: $k = 19.6 \pm 2.1\,M^{-1}$; **2**: $17.9 \pm 1.3\,M^{-1}$) and found to be nearly identical. Notably, $k_{cat}$ values for **1** ($(4.9 \pm 0.4) \times 10^{-6}\,s^{-1}$) and **2** ($(2.3 \pm 0.1) \times 10^{-5}\,s^{-1}$) differ by a factor of approximately 5. Thus, the enhanced hydrolytic efficiency of **2** for the hydrolysis of bis(4-nitrophenyl) phosphate is not due to differing substrate affinities for the complexes, but instead to intrinsically higher reactivity for the system having the larger Zn···Zn separation.

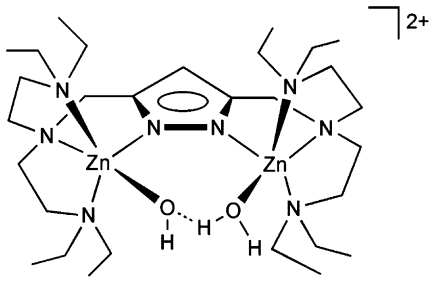


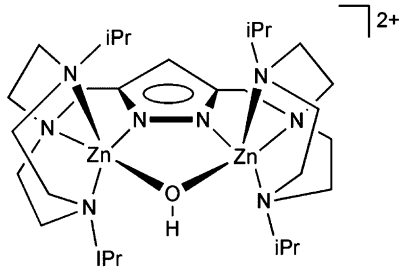


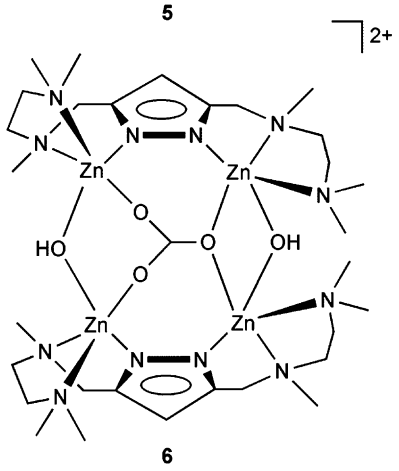


**Fig. 61** Binuclear zinc complex of pyrazolate-based chelate ligands.

The 2-hydroxypropyl 4-nitrophenyl phosphate (HPNP) transesterification reactivity (Fig. 40, bottom) of binuclear zinc complexes of the dianionic ICIMP and trianionic BCIMP ligands (Fig. 62) have been compared.[245] Notably, both of these ligands contain imidazole and carboxylate donors akin to protein-derived residues that are found as ligands to the zinc centers in phosphate-ester-hydrolyzing enzymes such as phosphotriesterase. The initial rate for HPNP transesterification promoted by $[(ICIMP)Zn_2(Ph_2Ac)]ClO_4$ in 50% acetonitrile–water solution (tris buffer) was determined to be five times faster than the reaction promoted by $[(BCIMP)Zn_2(Ph_2Ac)]$.

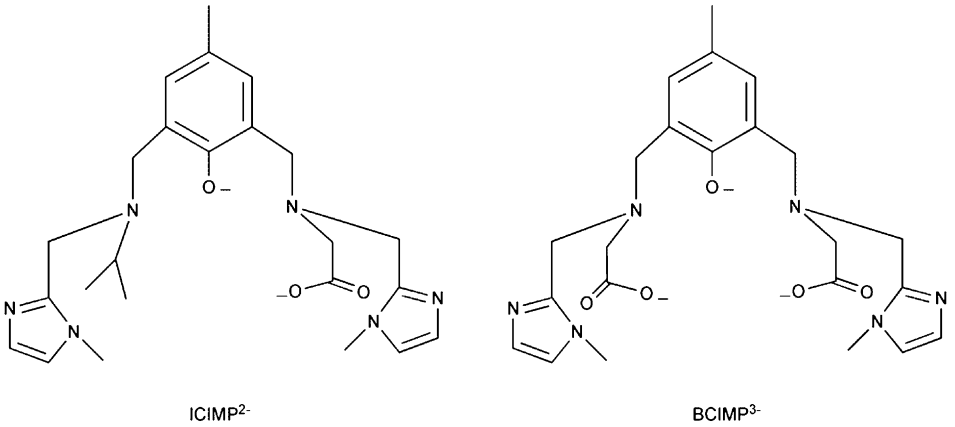


**Fig. 62** Dianionic ICIMP and trianionic BCIMP ligands.

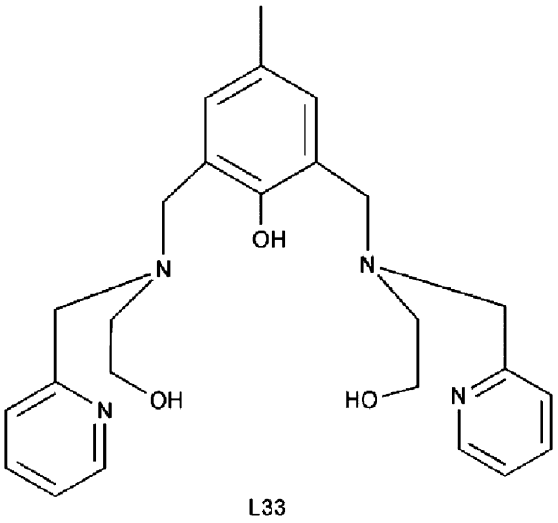


**Fig. 63** L33 ligand.

The difference in reactivity for these two complexes is attributed to the availability of an open coordination position in the ICIMP-ligated complex.

A binuclear zinc complex of the 2,6-bis{[(2-pyridylmethyl)(2-hydroxyethyl) amino]methyl}-4-methylphenol ligand (L33, Fig. 63) catalyzes the hydrolysis of bis(4-nitrophenyl) phosphate in aqueous buffer solution to yield 4-nitrophenol and 4-nitrophenyl phosphate.[246] Analysis of the pH-rate profile revealed a sigmoidal-shaped curve with a $pK_a = 7.13$. This value is similar to a deprotonation event characterized by potentiometric titration and has been assigned to deprotonation of

a ligand alcohol appendage. Additional kinetic and mechanistic studies in DMSO solution indicate that a similar reaction takes place under these conditions, thus providing further evidence that the reactive nucleophile is a zinc alkoxide species. A proposed mechanism for bis(4-nitrophenyl) phosphate hydrolysis catalyzed by this binuclear complex involves initial weak coordination ($K_b = 16.26\,M^{-1}$) of the phosphate diester substrate followed by intramolecular attack of the alkoxide moiety. Cleavage of the P–O bond of the leaving group (4-nitrophenolate) followed by displacement of the phosphate monoester product (4-nitrophenyl phosphate) is proposed to complete the catalytic cycle (Scheme 36).

Binuclear zinc hydroxide complexes of the neutral L34 and L35 (Fig. 64) ligands promote phosphate ester hydrolysis.[247] For L34, dihydroxo ($[(L34)Zn_2(OH)_2]^{2+}$) and trihydroxo ($[(L34)Zn_2(OH)_3]^{+}$) species show similar second-order rate constants ($\sim 6 \times 10^{-5}\,M^{-1}\,s^{-1}$). This level of reactivity is similar to that encountered for mononuclear zinc complexes and suggests that the zinc centers act independently in the phosphate ester hydrolysis reaction. This is consistent with the large distance between the zinc centers imparted by the chelate ligand in these complexes. For the L35 ligand, the trihydroxo derivative complex exhibits a second-order rate constant of $4.2 \times 10^{-3}\,M^{-1}\,s^{-1}$. The enhanced reactivity of $[(L35)Zn_2(OH)_3]^{+}$ is suggested to result from an optimal Zn···Zn distance which enables bridging coordination of the bis(4-nitrophenyl) phosphate substrate in a complex that also contains a nucleophilic terminal Zn–OH moiety.

Catalytic HPNP-tranesterification reactivity (Fig. 40, bottom has been reported for zinc complexes assembled using calix[4]arene ligands (Fig. 65).[172,248–251] Complex **9** induces a 23,000-fold rate enhancement over the uncatalyzed intramolecular cyclization reaction of HPNP.[248] Kinetic and mechanistic studies indicate strong binding of the HPNP substrate to the complex ($K = 5.5 \times 10^{-4}\,M^{-1}$) and a $k_{cat}$ value of $7.7 \times 10^{-4}\,s^{-1}$ at pH = 7.0 in acetonitrile/20 mM HEPES (1:1) at 25 °C. As **9** is 50 times more active for HPNP transesterification than **8**, which contains only one zinc center, cooperativity between metal centers occurs in the former complex. Notably, the monozinc calix[4]arene complex **8** is 6 times more reactive than **7**. This result provides evidence that the hydrophobic calix[4]arene moiety plays an important role in the reaction.

Incorporation of internal dimethylamino groups on the calix[4]arene structure yielded **10**, which exhibits a substrate binding affinity that is 30-fold reduced ($K = 0.19 \times 10^{-4}\,M^{-1}$) and a rate constant that is reduced by a factor of 2 ($k_{cat} = 3.6 \times 10^{-4}\,s^{-1}$).[250] In addition, the pH optimum for **9** (pH = 7.5) is considerably higher than that found for **10** (pH = 6.8) These differences suggest that a different catalytic mechanism may be operative in the transesterification of HPNP catalyzed by **9** and **10**. For **9**, the reaction pathway is proposed to involve activation of the HPNP substrate by one zinc center, whereas the second zinc center may coordinate the hydroxyl appendage of the substrate, thus lowering its $pK_a$ value, or may provide a Zn–OH group to deprotonate the substrate (Fig. 66, top). For the reaction involving **10**, double Lewis activation of the substrate is proposed, with an internal dimethyl amino group serving as the base for deprotonation of the substrate (Fig. 66, bottom).

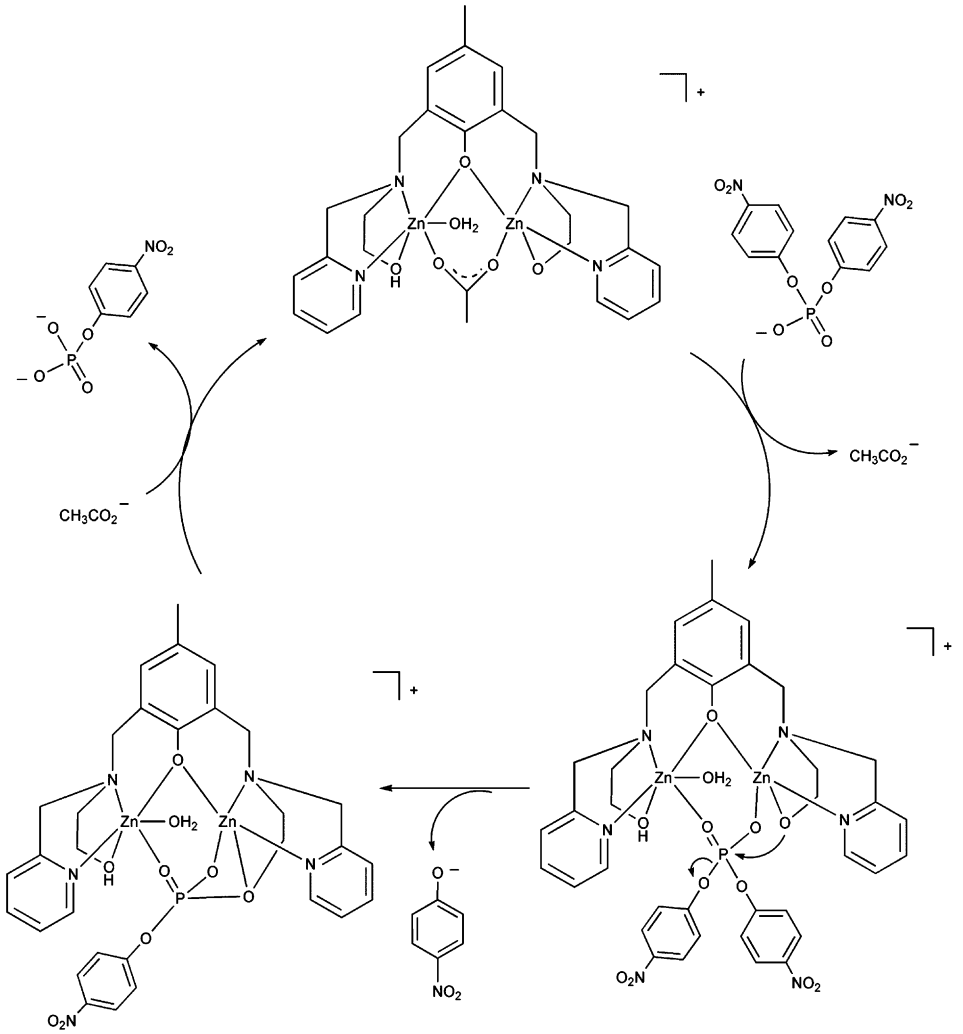

**Scheme 36** Proposed mechanism for the hydrolysis of bis(4-nitrophenyl)phosphate catalyzed by a binuclear zinc complex of the L33 ligand.

Flexibility is important in term of the HPNP reactivity of the calix[4]arene complexes, as evidenced by the fact that the constrained analog **11** (Fig. 65) exhibits both a lower substrate affinity ($K = 0.70 \times 10^{-4}\,M^{-1}$) and catalytic rate ($k_{cat} = 0.95 \times 10^{-4}\,s^{-1}$) than **9**.[249]

Positioning of the zinc centers on the calix[4]arene framework also influences HPNP-tranesterification reactivity.[172] Specifically, the 1,2-vicinal complex **12** is a significantly less effective catalyst for HPNP transesterification than **9**.

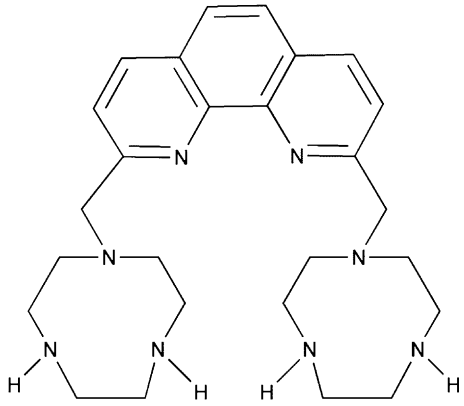


L34

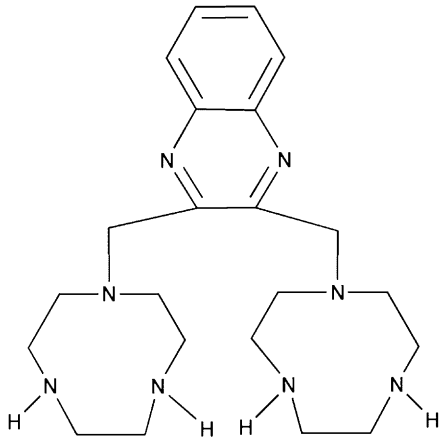


L35

**Fig. 64** L34 and L35 ligands.

A calix[4]arene derivative having three appended zinc centers (Fig. 67) exhibits decreased substrate binding ($K = 0.70 \times 10^{-4}\,M^{-1}$) relative to **9** (Fig. 65), but an increased catalytic rate ($k_{cat} = 24 \times 10^{-4}\,s^{-1}$) for the transesterification of HPNP.[249] The mechanism of this reaction is proposed to involve substrate activation by two zinc centers, with the third providing a Zn–OH moiety to deprotonate the substrate (Fig. 67).

Binuclear zinc hydroxide complexes of the Htdmbpo and Hbdmbbppo ligands (Fig. 68) promote the transesterification of HPNP (Fig. 40, bottom).[252] Binding constants and catalytic rate constants were determined for the respective complexes. The Htdmpo-ligated zinc complex exhibits a slighter higher rate constant ($1.10 \times 10^{-3}\,s^{-1}$) than the Hbdmbbppo-ligated complex ($8.33 \times 10^{-4}\,s^{-1}$). However,

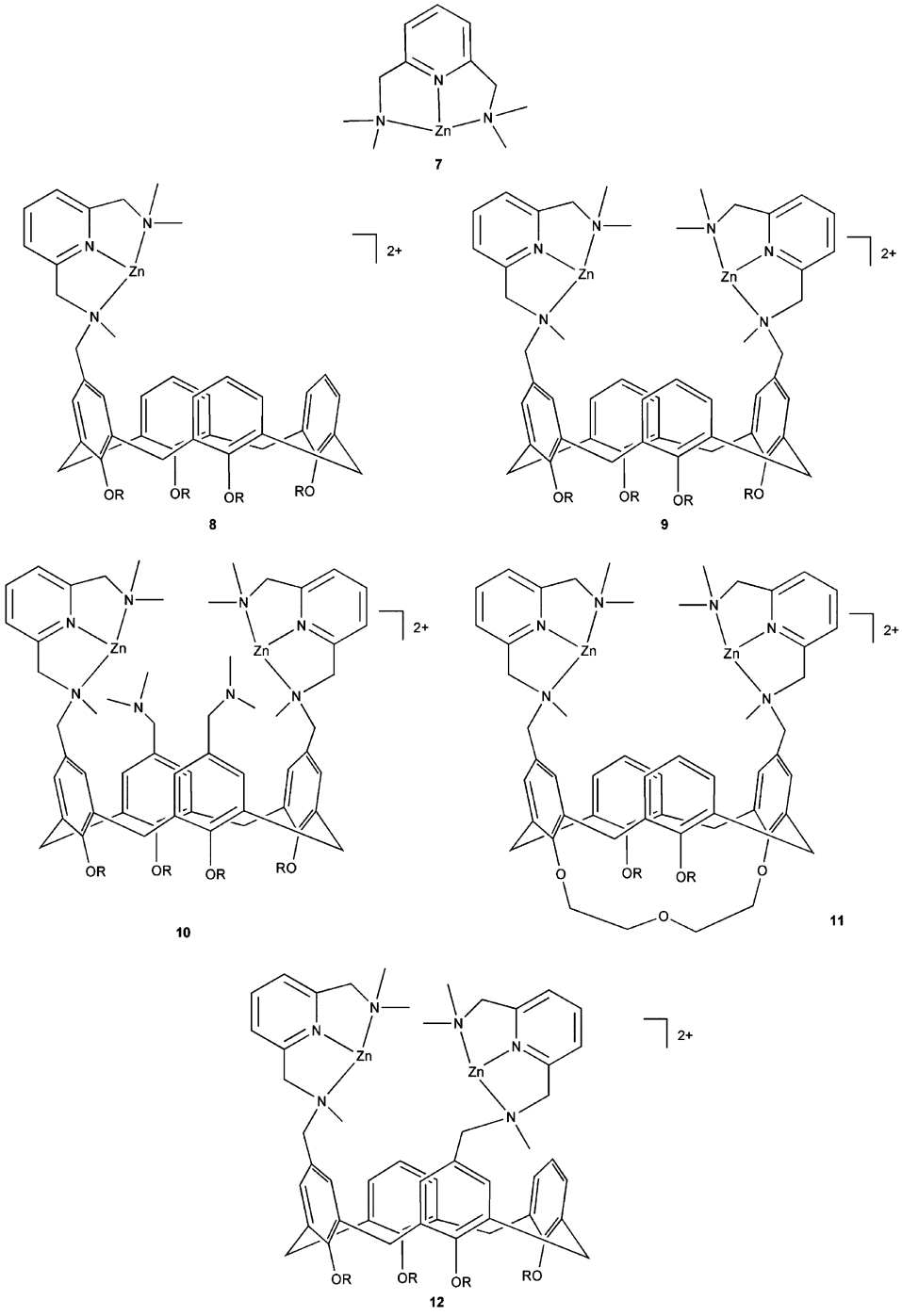


**Fig. 65** Calix[4]arene complexes examined for HPNP-transesterification reactivity.

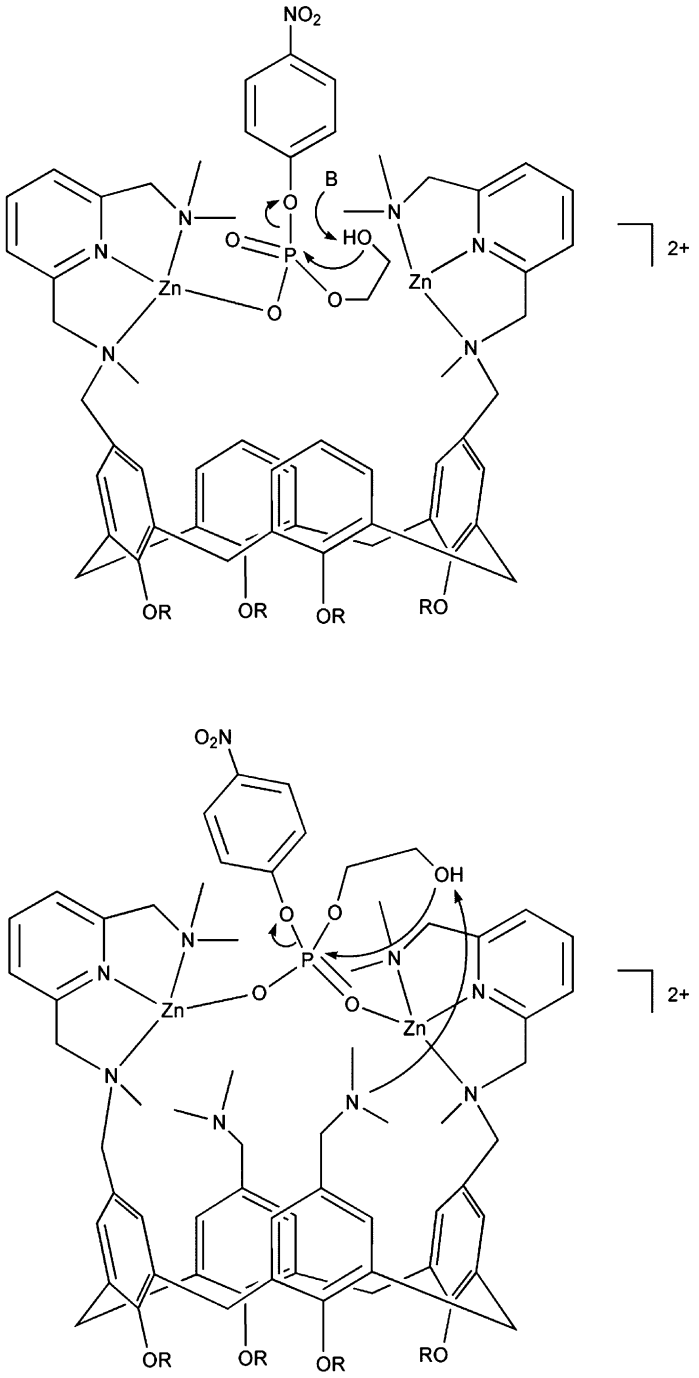


**Fig. 66** Proposed mechanistic pathways for the transesterification of HPNP catalyzed by **9** (top) and **10** (bottom).

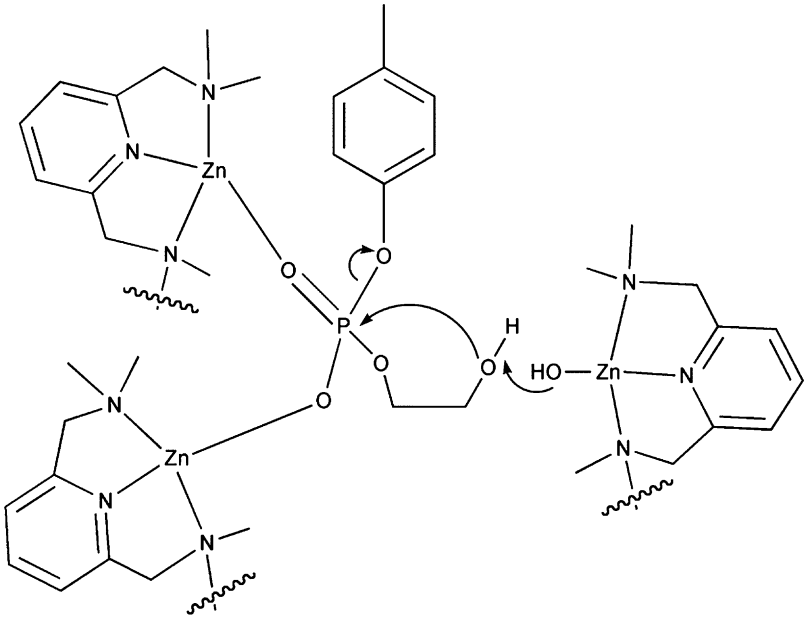


**Fig. 67** Proposed mechanism for HPNP transesterification catalyzed by a trinuclear $(N_3Zn)_3$-appended calix[4]arene complex. The calix[4]arene unit is not shown for clarity.

the later complex exhibits substrate binding that is 2.5 times more effective, which results in a higher overall activity for the complex of the asymmetric Hbdmbbppo ligand. For these complexes, a mechanism for HPNP transesterification is proposed wherein the substrate binds to the binuclear zinc center in a μ-1,3-bridging fashion, with a terminal zinc hydroxide moiety serving as a general base for the deprotonation of the HPNP alcohol hydroxy group. A similar mechanism has been proposed for HPNP transesterification promoted by a binuclear zinc complex of the bimido ligand (Fig. 69, top), and a preorganized mixed imidazole/carboxylate-donor ligand (Fig. 69, bottom).[253,254]

Extensive studies of HPNP transesterification (Fig. 40, bottom) promoted by zinc complexes of 1,4,7-triazacyclononane-containing ligands ($[(L36OH)Zn]^{2+}$ and $[(L(37)O)Zn_2]^{3+}$, Fig. 70) have provided important insight into the role of the metal complex in the reaction.[255,256] As shown in Fig. 70, Zn(II) complexes of the L36OH and L37O ligands can have different protonation states for the alcohol portion of the chelate ligand. For the mononuclear complex, the alcohol remains protonated up to pH = 10.4. However, in the binuclear complex, deprotonation of the alcohol occurs below pH = 6. Ionization of a zinc-bound water molecule occurs with $pK_a = 9.2$ for the $[(L36OH)Zn]^{2+}$ and with $pK_a = 8.0$ for $[(L(37)O)Zn_2]^{3+}$. For both complexes, it is proposed that this ionization results in the formation of a terminal Zn–OH moiety, which acts to deprotonate the HPNP substrate in the transesterification reaction, perhaps through general base catalysis as is shown in Fig. 60 (left).[257,258] Enhanced reactivity for the binuclear $[(L(37)O)Zn_2]^{3+}$ complex

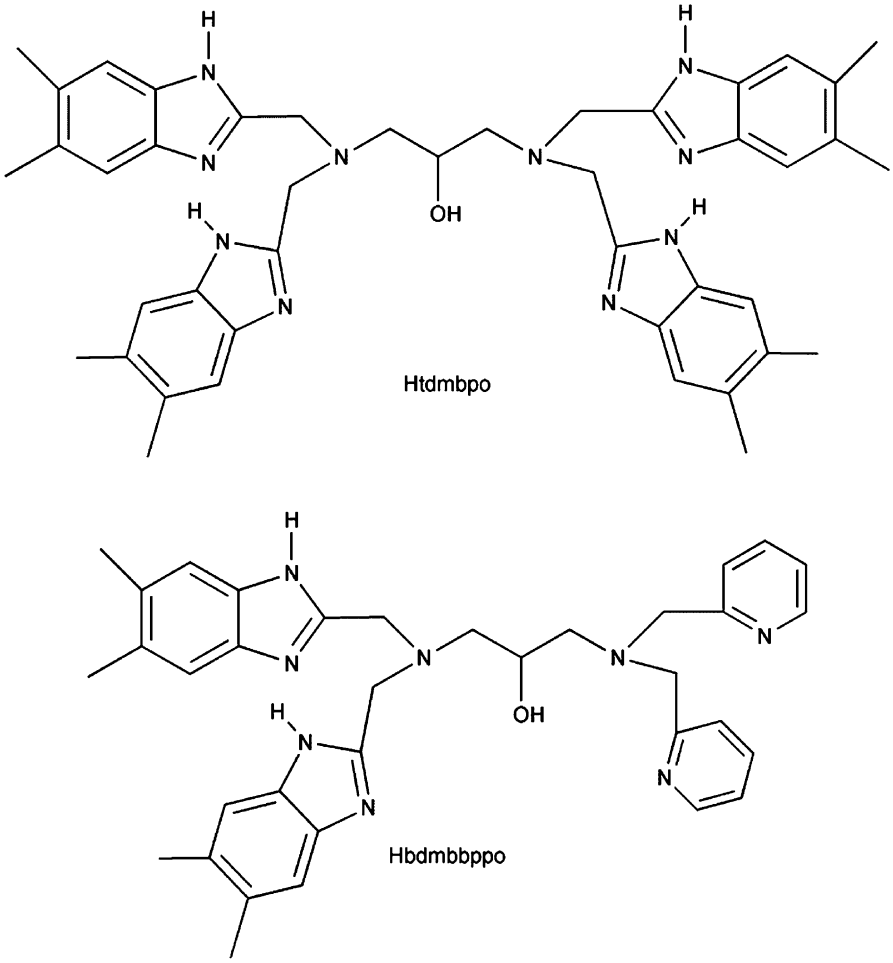


**Fig. 68** Htdmbpo and Hbdmbbppo ligands.

versus the mononuclear $[(L36OH)Zn]^{2+}$ complex in this reaction is rationalized on the basis of cooperative roles for the zinc centers in $[(L(37)O)Zn_2]^{3+}$ in facilitating the loss of a proton from the Michaelis complex between the metal complex and the substrate, and in stabilizing the transition state. Notably, comparison of the second-order rate constant for HPNP transesterification by $[(L(37)O)Zn_2]^{3+}$ ($0.25\,M^{-1}\,s^{-1}$) with the first-order rate constant for the uncatalyzed reaction ($k = 3.8 \times 10^{-8}\,s^{-1}$) at pH = 7.6 indicates that the transition state of the metal-catalyzed reaction is stabilized by 9.3 kcal $mol^{-1}$. From inhibition studies, it was proposed that 2.4 kcal $mol^{-1}$ of this stabilization involves the ground state Michaelis complex whereas the remaining stabilization is achieved as the transition state for HPNP transesterification is approached.

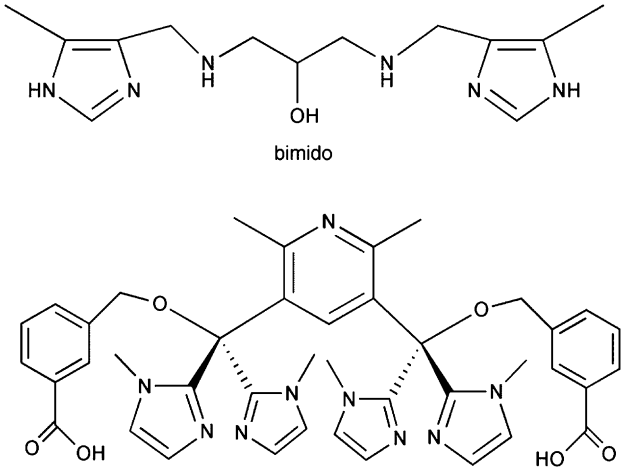


**Fig. 69** (top) Structure of bimido ligand and (bottom) preorganized mixed imidazole/carboxylate-donor ligand.

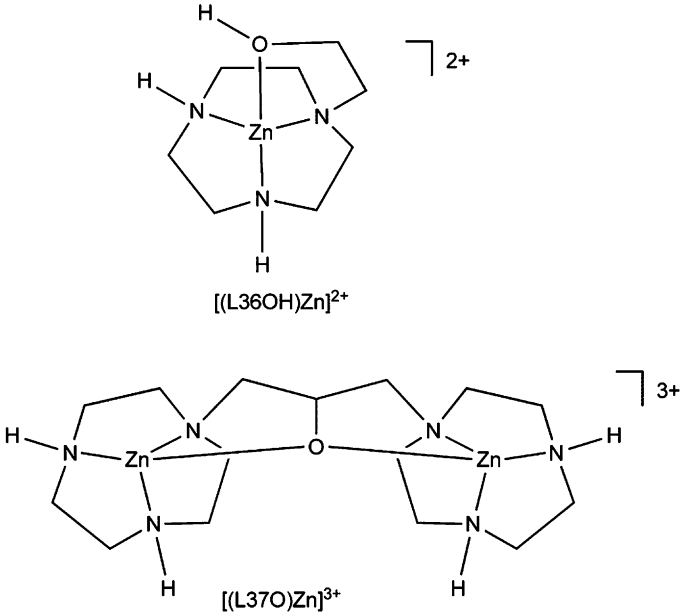


**Fig. 70** $[(L36OH)Zn]^{2+}$ and $[(L37O)Zn_2]^{3+}$.

Binuclear zinc complexes of triazacyclononane-containing ligands having different bridge structures (Fig. 71) exhibit second-order rate constants for HPNP transesterification that are only 3–5 times larger than that exhibited by the mononuclear $[(L36OH)Zn]^{2+}$ complex.[256] This behavior is contrasted by that of

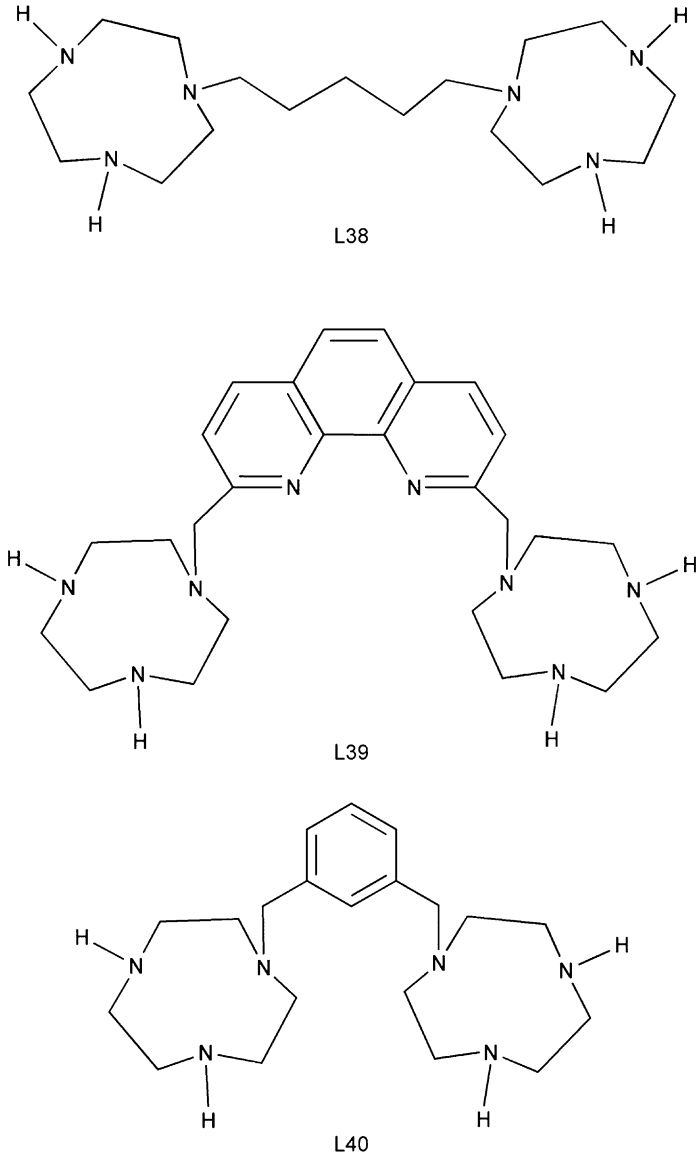


**Fig. 71** L38–L40 ligands.

$[(L(37)O)Zn_2]^{3+}$, which exhibits a second-order rate constant that is 120-fold larger than that found for $[(L36OH)Zn]^{2+}$. This dramatic difference in reactivity for the binuclear complexes is attributed to cooperative interactions in $[(L(37)O)Zn_2]^{3+}$ that are not achievable using the binuclear ligands (L38–L40) shown in Fig. 71. For example, the two centers in $[(L(37)O)Zn_2]^{3+}$ may be an optimal distance to provide

electrostatic stabilization of the transition state. Overall, the catalytic power of $[(L(37)O)Zn_2]^{3+}$ (Fig. 70, bottom) is approximately half of that exhibited by enzyme catalysts, with a rate acceleration of $9.8 \times 10^6$-fold for the transesterification of HPNP. This acceleration is primarily attributed to electrostatic stabilization of the anionic transition state of the reaction by the compact cationic zinc complex.[258] On the basis of these results, it has been argued that electrostatic considerations should be a primary issue in the design of new small molecule catalysts for phosphate diester cleavage.

A few trinuclear zinc complexes have been reported that promote the cleavage of phosphate esters. For example, calix[4]arene systems having three $N_3$-ligated Zn(II) centers, and which promote the transesterification of HPNP, have been previously

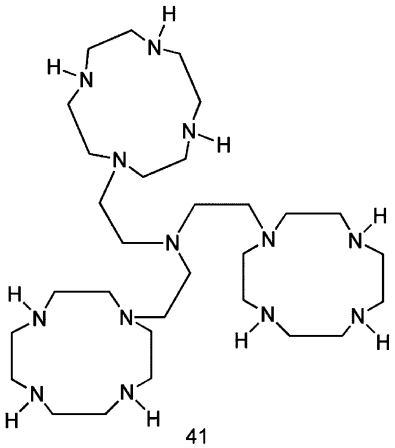

41

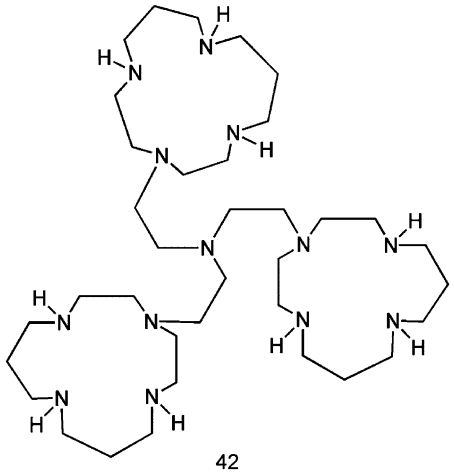

42

**Fig. 72** L41 and L42 ligands.

discussed herein.[249] Trinuclear zinc complexes having $N_4$-donor macrocyclic donors (L41 and L42, Fig. 72) coordinated to each zinc center form mono-, di-, and trihydroxo complexes in aqueous solution. For both ligand types, only the di- and trihydroxo species ($[(L41/42)Zn_3(OH)_2]^{4+}$ and $[(L41/L42)Zn_3(OH)_3]^{3+}$) promote bis(4-nitrophenyl) phosphate hydrolysis.[259] The reactivity found for these multinuclear complexes significantly exceeds that exhibited by the mononuclear complex $[([12]and N_4)Zn(OH)]^{+}$, indicating a cooperative effect between the zinc centers in the trinuclear complexes. For these reactions, an associative mechanism is proposed wherein the bis(4-nitrophenyl) phosphate substrate initially bridges two zinc centers and subsequently undergoes nucleophilic attack from a terminal Zn–OH moiety on the third zinc center. In support of this proposal, it was noted that higher reactivity is found for the L42-ligated system, which has higher $pK_a$ values for the formation of Zn–OH species. Notably, in these systems, similar second-order rate constants are found for the phosphate ester cleavage reactions promoted by the bis- and trihydroxo derivatives. This is likely due to a lower Lewis acidity for the zinc centers in the trihydroxo complex, which would modulate the degree to which the complex can activate the substrate toward nucleophilic attack. Therefore, despite an expected higher nucleophilicity for the Zn–OH units in the trihydroxo complex, similar overall hydrolysis reactivity to the bishydroxo complex is observed.

Outside the scope of coverage of this contribution are studies of zinc complexes having peptide-based ligands[260–262] and Zn(II)-complex-promoted reactions involving RNA or DNA hydrolysis.[261,263–288]

## References


1. Lippard, S.J. and Berg, J.M. (1994). *Principles of Bioinorganic Chemistry*. University Science Books, Mill Valley, CA
2. Karlin, K.D. (1993). *Science* **261**, 701–708
3. Parkin, G. (2000). *Chem. Commun.* 1971–1985
4. Parkin, G. (2001). *Met. Ions Biol. Syst.* **38**, 411–460
5. Parkin, G. (2004). *Chem. Rev.* **104**, 699–768
6. Kimura, E., Koike, T. and Shionoya, M. (1997). *Struct. Bond.* **89**, 1–28
7. Weston, J. (2005). *Chem. Rev.* **105**, 2151–2174
8. Kimura, E. (1994). *Prog. Inorg. Chem.* **41**, 443–491
9. Chin, J. (1991). *Acc. Chem. Res.* **24**, 145–152
10. Bashkin, J.K. (1999). *Curr. Opin. Chem. Biol.* **3**, 752–758
11. Suh, J. (2003). *Acc. Chem. Res.* **36**, 562–570
12. Suh, J. (1992). *Acc. Chem. Res.* **25**, 273–279
13. Breslow, R. (1995). *Acc. Chem. Res.* **28**, 146–153
14. Kimura, E. and Kikuta, E. (2000). *J. Biol. Inorg. Chem.* **5**, 139–155
15. Martin, R.B. (2002). *Inorg. Chim. Acta* **339**, 27–33
16. Gelinsky, M., Vogler, R. and Vahrenkamp, H. (2002). *Inorg. Chem.* **41**, 2560–2564
17. diTargiani, R.C., Chang, S., Salter, M.H., Hancock, R.D. and Goldberg, D.P. (2003). *Inorg. Chem.* **42**, 5825–5836
18. Mareque-Rivas, J.C., Prabaharan, R. and de Rosales, R.T.M. (2004). *Chem. Commun.* 76–77
19. Mareque-Rivas, J.C., Prabaharan, R. and Parsons, S. (2004). *Dalton Trans.* 1648–1655

20. Livieri, M., Mancin, F., Tonellato, U. and Chin, J. (2004). *Chem. Commun*. 2862–2863
21. Vallee, B.L. and Williams, R.J.P. (1968). *Proc. Natl. Acad. Sci.* **59**, 498–505
22. Maret, W. and Vallee, B.L. (1993). *Method. Enzymol.* **226**, 52–71
23. Vallee, B.L. and Auld, D.S. (1992). *Faraday Discuss. Chem. Soc.* **93**, 47–65
24. Vallee, B.L. and Auld, D.S. (1993). *Acc. Chem. Res.* **26**, 543–551
25. Vallee, B.L. and Auld, D.S. (1990). *Biochemistry* **29**, 5647–5659
26. Tripp, B.C., Smith, K. and Ferry, J.G. (2001). *J. Biol. Chem.* **276**, 48615–48618
27. Lindskog, S. (1997). *Pharmacol. Ther.* **74**, 1–20
28. Christianson, D.W. and Cox, J.D. (1999). *Annu. Rev. Biochem.* **68**, 33–57
29. Krebs, J.F., Ippolito, J.A., Christianson, D.W. and Fierke, C.A. (1993). *J. Biol. Chem.* **268**, 27458–27466
30. Hakansson, K., Carlsson, M., Svensson, L.A. and Liljas, A. (1992). *J. Mol. Biol.* **227**, 1192–1204
31. Bertini, I., Luchinat, C., Mangani, S. and Pierattelli, R. (1995). *Comment. Inorg. Chem.* **17**, 1–15
32. Hakansson, K. and Wehnert, A. (1992). *J. Mol. Biol.* **228**, 1212–1218
33. Silverman, D.N. and Lindskog, S. (1988). *Acc. Chem. Res.* **21**, 30–36
34. Liljas, A., Hakansson, K., Jonsson, B.H. and Xue, Y. (1994). *Eur. J. Biochem.* **219**, 1–10
35. Christianson, D.W. and Fierke, C.A. (1996). *Acc. Chem. Res.* **29**, 331–339
36. Kimura, E., Shiota, T., Koike, T., Shiro, M. and Kodama, M. (1990). *J. Am. Chem. Soc.* **112**, 5805–5811
37. Zhang, X., van-Eldik, R., Koike, T. and Kimura, E. (1993). *Inorg. Chem.* **32**, 5749–5755
38. Zhang, X. and van-Eldik, R. (1995). *Inorg. Chem.* **34**, 5606–5614
39. Nakata, K., Shimomura, N., Shiina, N., Izumi, M., Ichikawa, K. and Shiro, M. (2002). *J. Inorg. Biochem.* **89**, 255–266
40. Woolley, P. (1975). *Nature* **258**, 677–682
41. Tabushi, I., Kuroda, Y. and Mochizuki, A. (1980). *J. Am. Chem. Soc.* **102**, 1152–1153
42. Huguet, J. and Brown, R.S. (1980). *J. Am. Chem. Soc.* **102**, 7571–7572
43. Brown, R.S., Curtis, N.J. and Huguet, J. (1981). *J. Am. Chem. Soc.* **103**, 6953–6959
44. Slebocka-Tilk, H., Cocho, J.L., Frakman, Z. and Brown, R.S. (1984). *J. Am. Chem. Soc.* **106**, 2421–2431
45. Xue, Y., Liljas, A., Jonsson, B.H. and Lindskog, S. (1993). *Proteins* **17**, 93–106
46. Kimblin, C., Allen, W.E. and Parkin, G. (1995). *J. Chem. Soc. Chem. Commun*. 1813–1815
47. Alsfasser, R., Trofimenko, S., Looney, A., Parkin, G. and Vahrenkamp, H. (1991). *Inorg. Chem.* **30**, 4098–4100
48. Ruf, M. and Vahrenkamp, H. (1996). *Inorg. Chem.* **35**, 6571–6578
49. Alsfasser, R., Ruf, M., Trofimenko, S. and Vahrenkamp, H. (1993). *Chem. Ber.* **126**, 703–710
50. Bergquist, C. and Parkin, G. (1999). *J. Am. Chem. Soc.* **121**, 6322–6323
51. Looney, A., Han, R., McNeill, K. and Parkin, G. (1993). *J. Am. Chem. Soc.* **115**, 4690–4697
52. Bergquist, C., Fillebeen, T., Morlok, M.M. and Parkin, G. (2003). *J. Am. Chem. Soc.* **125**, 6189–6199
53. Kitajima, N., Hikichi, S., Tanaka, M. and Moro-oka, Y. (1993). *J. Am. Chem. Soc.* **115**, 5496–5508
54. Yamaguchi, S., Tokairin, I., Wakita, Y., Funahashi, Y., Jitsukawa, K. and Masuda, H. (2003). *Chem. Lett.* **32**, 406–407
55. Jeffrey, G.A. (1997). *An Introduction to Hydrogen Bonding*. Oxford University Press, New York, NY
56. Echizen, T., Ibrahim, M.M., Nakata, K., Izumi, M., Ichikawa, K. and Shiro, M. (2004). *J. Inorg. Biochem.* **98**, 1347–1360

57. Eklund, H., Nordstrom, B., Zeppezauer, E., Soderlund, G., Ohlsson, I., Boiwe, T., Soderberg, B.O., Tapia, O., Branden, C.-I. and Akeson, A. (1976). *J. Mol. Biol.* **102**, 27–59
58. Ramaswamy, S., Park, D.-H. and Plapp, B.V. (1999). *Biochemistry* **38**, 13951–13959
59. Agarwal, P.K., Webb, S.P. and Hammes-Schiffer, S. (2000). *J. Am. Chem. Soc.* **122**, 4803–4812
60. Mayer, J.M. (1988). *Comment. Inorg. Chem.* **8**, 125–135
61. Meijers, R., Morris, R.J., Adolph, H.W., Merli, A., Lamzin, V.S. and Cedergren-Zeppezauer, E.S. (2000). *J. Biol. Chem.* **276**, 9316–9321
62. Sartorius, C., Gerber, M., Zeppezauer, M. and Dunn, M.F. (1987). *Biochemistry* **26**, 871–882
63. Kleifeld, O., Rulisek, L., Bogin, O., Frenkel, A., Havias, Z., Burstein, Y. and Sagi, I. (2004). *Biochemistry* **43**, 7151–7161
64. Kimura, E., Shionoya, M., Hoshino, A., Ikeda, T. and Yamada, Y. (1992). *J. Am. Chem. Soc.* **114**, 10134–10137
65. Kimblin, C., Bridgewater, B.M., Churchill, D.G. and Parkin, G. (1999). *Chem. Commun*. 2301–2302
66. Seebacher, J., Shu, M. and Vahrenkamp, H. (2001). *Chem. Commun*. 1026–1027
67. Ramaswamy, S., Eklund, H. and Plapp, B.V. (1994). *Biochemistry* **33**, 5230–5237
68. Bergquist, C. and Parkin, G. (1999). *Inorg. Chem.* **38**, 422–423
69. Bergquist, C., Storrie, H., Koutcher, L., Bridgewater, B.M., Friesner, R.A. and Parkin, G. (2000). *J. Am. Chem. Soc.* **122**, 12651–12658
70. Brombacher, H. and Vahrenkamp, H. (2004). *Inorg. Chem.* **43**, 6042–6049
71. Boerzel, H., Koeckert, M., Bu, W., Spingler, B. and Lippard, S. (2003). *Inorg. Chem.* **42**, 1604–1615
72. Walz, R., Weis, K., Ruf, M. and Vahrenkamp, H. (1997). *Chem. Ber.* **130**, 975–980
73. Brombacher, H. and Vahrenkamp, H. (2004). *Inorg. Chem.* **43**, 6054–6060
74. Walz, W. and Vahrenkamp, H. (2001). *Inorg. Chim. Acta* **314**, 58–62
75. Garner, D.K., Fitch, S.B., McAlexander, L.H., Bezold, L.M., Arif, A.M. and Berreau, L.M. (2002). *J. Am. Chem. Soc.* **124**, 9970–9971
76. Cronin, L. and Walton, P.H. (2003). *Chem. Commun*. 1572–1573
77. Lipscomb, W.N. and Strater, N. (1996). *Chem. Rev.* **96**, 2375–2434
78. Christianson, D.W. and Lipscomb, W.N. (1989). *Acc. Chem. Res.* **22**, 62–69
79. Mangani, S., Carloni, P. and Orioli, P. (1992). *Coord. Chem. Rev.* **120**, 309–324
80. Matthews, B.W. (1988). *Acc. Chem. Res.* **21**, 333–340
81. Mock, W.L. and Stanford, D.J. (1996). *Biochemistry* **35**, 7369–7377
82. Mock, W.L. and Aksamawati, M. (1994). *Biochem. J.* **302**, 57–68
83. Schmid, M.F. and Herriott, J.R. (1976). *J. Mol. Biol.* **103**, 175–190
84. Stark, W., Pauptit, R.A., Wilson, K.S. and Jansonius, J.N. (1992). *Eur. J. Biochem.* **207**, 781–791
85. Bode, W., Gomis-Ruth, F.X. and Stockler, W. (1993). *FEBS Lett* **331**, 134–140
86. Pelmenschikov, V. and Siegbahn, P.E.M. (2002). *Inorg. Chem.* **41**, 5659–5666
87. Sutton, P.A. and Buckingham, D.A. (1987). *Acc. Chem. Res.* **20**, 357–364
88. Schepartz, A. and Breslow, R. (1987). *J. Am. Chem. Soc.* **109**, 1814–1826
89. Groves, J.T. and Baron, L.A. (1989). *J. Am. Chem. Soc.* **111**, 5442–5448
90. Takasaki, B.K., Kim, J.H., Rubin, E. and Chin, J. (1993). *J. Am. Chem. Soc.* **115**, 1157–1159
91. Sayre, L.M. (1986). *J. Am. Chem. Soc.* **108**, 1632–1635
92. Hegg, E.L. and Burstyn, J.N. (1998). *Coord. Chem. Rev.* **173**, 133–165
93. Groves, J.T. and Chambers, R.R. (1984). *J. Am. Chem. Soc.* **106**, 630–638
94. Vahrenkamp, H. (1999). *Acc. Chem. Res.* **32**, 589–596
95. Ruf, M. and Vahrenkamp, H. (1996). *Chem. Ber.* **129**, 1025–1028

96. Rombach, M., Maurer, C., Weis, K., Keller, E. and Vahrenkamp, H. (1999). *Chem. Eur. J.* **5**, 1013–1027
97. Pocker, Y. and Stone, J.T. (1967). *Biochemistry* **6**, 668–678
98. Kimura, E., Nakamura, I., Koike, T., Shionoya, M., Kodama, Y., Ikeda, T. and Shiro, M. (1994). *J. Am. Chem. Soc.* **116**, 4764–4771
99. Koike, T., Takamura, M. and Kimura, E. (1994). *J. Am. Chem. Soc.* **116**, 8443–8449
100. Ozturk, G. and Akkaya, E.U. (2004). *Org. Lett.* **6**, 241–243
101. Wendelstorf, C., Warzeska, S., Kovari, E. and Kramer, R. (1996). *Dalton Trans*. 3087–3092
102. Koike, T., Kajitani, S., Nakamura, I., Kimura, E. and Shiro, M. (1995). *J. Am. Chem. Soc.* **117**, 1210–1219
103. Jencks, W.P. and Gilchrist, M. (1968). *J. Am. Chem. Soc.* **90**, 2622–2637
104. Bazzicalupi, C., Bencini, A., Bencini, A., Bianchi, A., Corana, F., Fusi, V., Giorgi, C., Paoli, P., Paoletti, P., Valtancoli, B. and Zanchini, C. (1996). *Inorg. Chem.* **35**, 5540–5548
105. Bazzicalupi, C., Bencini, A., Bianchi, A., Fusi, V., Giorgi, C., Paoletti, P., Valtancoli, B. and Zanchi, D. (1997). *Inorg. Chem.* **36**, 2784–2790
106. Bazzicalupi, C., Bencini, A., Bianchi, A., Fusi, V., Paoletti, P. and Valtancoli, B. (1994). *J. Chem. Soc. Dalton Trans*. 3581–3588
107. Su, X., Sun, H., Zhou, Z., Lin, H., Chen, L., Zhu, S. and Chen, Y. (2001). *Polyhedron* **20**, 91–95
108. Kiefer, L.L. and Fierke, C.A. (1994). *Biochemistry* **33**, 15233–15240
109. Breslow, R. and Singh, S. (1988). *Bioorg. Chem.* **16**, 408–417
110. Xia, J., Xu, Y., Li, S., Sun, W., Yu, K. and Tang, W. (2001). *Inorg. Chem.* **40**, 2394–2401
111. Huang, J., Li, D., Li, S., Yang, D., Sun, W. and Tang, W. (2004). *J. Inorg. Biochem.* **98**, 502–509
112. Zhu, S., Chen, W., Lin, H., Yin, X., Kou, F., Lin, M. and Chen, Y. (1997). *Polyhedron* **16**, 3285–3291
113. Molenveld, P., Engbersen, J.F.J., Kooijman, H., Spek, A.L. and Reinhoudt, D.N. (1998). *J. Am. Chem. Soc.* **120**, 6726–6737
114. Ge, Q., Guo, Y., Lin, H., Gao, D., Lin, H. and Zhu, S. (2004). *Can. J. Chem.* **82**, 409–417
115. Page, M.I. and Laws, A.P. (1998). *Chem. Commun*. 1609–1617
116. Fisher, J.F., Meroueh, S.O. and Mobashery, S. (2005). *Chem. Rev.* **105**, 395–424
117. Cricco, J.A. and Vila, A.J. (1999). *Curr. Pharm. Des.* **5**, 915–927
118. Wang, Z., Fast, W., Valentine, A.M. and Benkovic, S.J. (1999). *Curr. Opin. Chem. Biol.* **3**, 614–622
119. Walsh, T.R., Toleman, M.A., Poirel, L. and Nordmann, P. (2005). *Clin. Microbiol. Rev.* **18**, 306–325
120. Heinz, U. and Adolph, H.W. (2004). *Cell. Mol. Life Sci.* **61**, 2827–2839
121. Fabiane, S.M., Sohi, M.K., Wan, T., Payne, D.J., Bateson, J.H., Mitchell, T. and Sutton, B.J. (1998). *Biochemistry* **37**, 12404–12411
122. Concha, N.O., Rasmussen, B.A., Bush, K. and Herzberg, O. (1996). *Structure* **4**, 823–836
123. Ullah, J.H., Walsh, T.R., Taylor, I.A., Emery, D.C., Verma, C.S., Gamblin, S.J. and Spencer, J. (1998). *J. Mol. Biol.* **284**, 125–136
124. Wommer, S., Rival, S., Heinz, U., Galleni, M., Frere, J.M., Franceschini, N., Amicosante, G., Rasmussen, B., Bauer, R. and Adolph, H.W. (2002). *J. Biol. Chem.* **277**, 24142–24147
125. Cricco, J.A., Orellano, E.G., Rasia, R.M., Ceccarelli, E.A. and Vila, A.J. (1999). *Coord. Chem. Rev.* **190–192**, 519–535
126. Rasia, R.M. and Vila, A.J. (2002). *Biochemistry* **41**, 1853–1860
127. Wang, Z., Fast, W. and Benkovic, S.J. (1999). *Biochemistry* **38**, 10013–10023

128. Hernandez Valladares, M., Kiefer, M., Heinz, U., Soto, R.P., Meyer-Klaucke, W., Nolting, H.F., Zeppezauer, M., Galleni, M., Frere, J.-M., Rossolini, G.M., Amicosante, G. and Adolph, H.-W. (2000). *FEBS Lett.* **467**, 221–225
129. Gross, F. and Vahrenkamp, H. (2005). *Inorg. Chem.* **44**, 4433–4440
130. Ogawa, K., Nakata, K. and Ichikawa, K. (1998). *Chem. Lett*. 797–798
131. Wang, Z. and Benkovic, S.J. (1998). *J. Biol. Chem.* **273**, 22402–22408
132. Wang, Z., Fast, W. and Benkovic, S.J. (1998). *J. Am. Chem. Soc.* **120**, 10788–10789
133. Diaz, N., Sordo, T.L., Suarez, D., Mendez, R. and Martin-Villacorta, J. (2004). *New J. Chem.* **28**, 15–25
134. Suarez, D., Diaz, N. and Merz, K.M. (2002). *J. Comput. Chem.* **23**, 1587–1600
135. Krauss, M., Gresh, N. and Antony, J. (2003). *J. Phys. Chem. B* **107**, 1215–1229
136. Antony, J., Gresh, N., Olsen, L., Hemmingsen, L., Schofield, C.J. and Bauer, R. (2002). *J. Comput. Chem.* **23**, 1281–1296
137. Suarez, D., Brothers, E.N. and Merz, K.M. (2002). *Biochemistry* **41**, 6615–6630
138. Dal Peraro, M., Vila, A.J. and Carloni, P. (2003). *Inorg. Chem.* **42**, 4245–4247
139. Krauss, M., Gilson, H.S.R. and Gresh, N. (2001). *J. Phys. Chem. B* **105**, 8040–8049
140. Kaminskaia, N.V., He, C. and Lippard, S.J. (2000). *Inorg. Chem.* **39**, 3365–3373
141. He, C. and Lippard, S.J. (2000). *J. Am. Chem. Soc.* **122**, 184–185
142. Woon, T.C., Wickramasinghe, W.A. and Fairlie, D.P. (1993). *Inorg. Chem.* **32**, 2190–2194
143. Zevaco, T.A., Gorls, H. and Dinjus, E. (1998). *Polyhedron* **17**, 2199–2206
144. Kupka, T. (1997). *Spectrochim. Acta A* **53**, 2649–2658
145. Ferrer, E.G. and Williams, P.A.M. (1997). *Polyhedron* **16**, 3323–3325
146. Page, M.I. (1984). *Acc. Chem. Res.* **17**, 144–151
147. Hay, R.W., Basak, A.K., Pujari, M.P. and Perotti, A. (1989). *J. Chem. Soc. Dalton Trans*. 197–201
148. Kaminskaia, N.V., Spingler, B. and Lippard, S.J. (2000). *J. Am. Chem. Soc.* **122**, 6411–6422
149. Jencks, W.P. (1987). *Catalysis in Chemistry and Enzymology*. Dover Publications, Inc., New York
150. Kaminskaia, N.V., Spingler, B. and Lippard, S.J. (2001). *J. Am. Chem. Soc.* **123**, 6555–6563
151. Bauer-Siebenlist, B., Dechert, S. and Meyer, F. (2005). *Chem. Eur. J.* **11**, 5343–5352
152. Meyer, F. and Rutsch, P. (1998). *Chem. Commun*. 1037–1038
153. Bauer-Siebenlist, B., Meyer, F., Farkas, E., Vidovic, D., Cuesta-Seijo, J.A., Herbst-Irmer, R. and Pritzkow, H. (2004). *Inorg. Chem.* **43**, 4189–4202
154. Bauer-Siebenlist, B., Meyer, F., Farkas, E., Vidovic, D. and Dechert, S. (2005). *Chem. Eur. J.* **11**, 4349–4360
155. Meyer, F., Heinze, K., Nuber, B. and Zsolnai, L. (1998). *J. Chem. Soc. Dalton Trans*. 207–214
156. Kleywegt, G.J., Wiesmeijer, W.G.R., Van Driel, G.J., Driessen, W.L., Reedijk, J. and Noordik, J.H. (1985). *J. Chem. Soc. Dalton Trans*. 2177–2184
157. Addison, A.W., Rao, T.N., Reedijk, J. van Rijn, J. and Verschoor, G.C. (1984). *J. Chem. Soc. Dalton Trans*. 1349–1356
158. Ackermann, J., Meyer, F., Kaifer, E. and Pritzkow, H. (2002). *Chem. Eur. J.* **8**, 247–258
159. Meyer, F., Jacobi, A., Nuber, B., Rutsch, R. and Zsolnai, L. (1998). *Inorg. Chem.* **37**, 1213–1218
160. Meyer, F. and Pritzkow, H. (2005). *Eur. J. Inorg. Chem*. 2346–2351
161. Lowther, W.T. and Matthews, B.W. (2002). *Chem. Rev.* **102**, 4581–4608
162. Holz, R.C. (2002). *Coord. Chem. Rev.* **232**, 5–26
163. Chen, G., Edwards, T., D'souza, V.M. and Holz, R.C. (1997). *Biochemistry* **36**, 4278–4286

164. Luiz, M.T.B., Szpoganicz, B., Rizzoto, M., Basallote, M.G. and Martell, A.E. (1999). *A.E. Martell Inorg. Chim. Acta* **287**, 134–141
165. Sakiyama, H., Mochizuki, R., Sugawara, A., Sakamoto, M., Nishida, Y. and Yamasaki, M. (1999). *Dalton Trans*. 997–1000
166. Sakiyama, H., Igarashi, Y., Nakayama, Y., Hossain, M.J., Unoura, K. and Nishida, Y. (2003). *Inorg. Chim. Acta* **351**, 256–260
167. Bazzicalupi, C., Bencini, A., Berni, E., Bianchi, A., Fornasari, P., Giorgi, C. and Valtancoli, B. (2003). *Eur. J. Inorg. Chem*. 1974–1983
168. Mareque-Rivas, J.C., Salvagni, E. and Parsons, S. (2004). *Chem. Commun*. 460–461
169. Iturrioz, X., Rozenfeld, R., Michaud, A., Corvol, P. and Llorens-Cortes, C. (2001). *Biochemistry* **40**, 14440–14448
170. Stamper, C., Bennett, B., Edwards, T., Holz, R.C., Ringe, D. and Petsko, G. (2001). *Biochemistry* **40**, 7035–7046
171. Sakiyama, H., Ono, K., Suzuki, T., Tone, K., Ueno, T. and Nishida, Y. (2005). *Inorg. Chem. Commun.* **8**, 372–374
172. Cacciapaglia, R., Casnati, A., Mandolini, L., Reinhoudt, D.N., Salvio, R., Sartori, A. and Ungaro, R. (2005). *J. Org. Chem.* **70**, 624–630
173. Neverov, A.A., Montoya-Pelaez, P.J. and Brown, R.S. (2001). *J. Am. Chem. Soc.* **123**, 210–217
174. Montoya-Pelaez, P.J. and Brown, R.S. (2002). *Inorg. Chem.* **41**, 309–316
175. Szajna, E., Makowska-Grzyska, M.M., Wasden, C.W., Arif, A.M. and Berreau, L.M. (2005). *Inorg. Chem.* **44**, 7595–7605
176. Mareque-Rivas, J.C., de Rosales, R.T.M. and Parsons, S. (2003). *Dalton Trans*. 2156–2163
177. Mareque-Rivas, J.C., Salvagni, E., Prabaharan, R., de Rosales, R.T.M. and Parsons, S. (2004). *Dalton Trans*. 172–177
178. Coleman, J.E. (1992). *Annu. Rev. Biophys. Biomol. Struct.* **21**, 441–483
179. Strater, N., Lipscomb, W.N., Klabunde, T. and Krebs, B. (1996). *Angew. Chem. Int. Edit.* **35**, 2024–2055
180. Wilcox, D.E. (1996). *Chem. Rev.* **96**, 2435–2458
181. Coleman, J.E. (1998). *Curr. Opin. Chem. Biol.* **2**, 222–234
182. Holtz, K.M. and Kantrowitz, E.R. (1999). *FEBS Lett* **462**, 7–11
183. Holtz, K.M., Stec, B. and Kantrowitz, E.R. (1999). *J. Biol. Chem.* **274**, 8351–8354
184. Stec, B., Holtz, K.M. and Kantrowitz, E.R. (2000). *J. Mol. Biol.* **299**, 1303–1311
185. Jedrzejas, M.J. and Setlow, P. (2001). *Chem. Rev.* **101**, 607–618
186. O'Brien, P.J. and Herschlag, D. (2002). *Biochemistry* **41**, 3207–3225
187. Hengge, A.C. (2005). In *Advances in Physical Organic Chemistry*, Richard, J. (ed.), Vol. 40, pp. 49–107. Academic Press, New York, NY
188. Harrowfield, J.M., Jones, D.R., Lindoy, L.F. and Sargeson, A.M. (1980). *J. Am. Chem. Soc.* **102**, 7733–7741
189. Jones, D.R., Lindoy, L.F. and Sargeson, A.M. (1983). *J. Am. Chem. Soc.* **105**, 7327–7336
190. Chin, J. and Banaszczyk, M. (1989). *J. Am. Chem. Soc.* **111**, 4103–4105
191. Connolly, J.A., Banaszczyk, M., Hynes, R.C. and Chin, J. (1994). *Inorg. Chem.* **33**, 665–669
192. Rawji, G., Hediger, M. and Milburn, R.M. (1983). *Inorg. Chim. Acta* **79**, 247–248
193. Rawlings, J., Hengge, A.C. and Cleland, W.W. (1997). *J. Am. Chem. Soc.* **119**, 542–549
194. Hendry, P. and Sargeson, A.M. (1990). *Inorg. Chem.* **29**, 92–97
195. Williams, N.H., Lebuis, A.-M. and Chin, J. (1999). *J. Am. Chem. Soc.* **121**, 3341–3348
196. Williams, N.H. (2004). *Biochem. Biophys. Acta* **1697**, 279–287
197. Humphry, T., Forconi, M., Williams, N.H. and Hengge, A.C. (2004). *J. Am. Chem. Soc.* **126**, 11864–11869
198. Hettich, R. and Schneider, H. (1997). *J. Am. Chem. Soc.* **119**, 5638–5647

199. Seo, J.S., Sung, N.D., Hynes, R.C. and Chin, J. (1996). *Inorg. Chem.* **35**, 7472–7473
200. Kenley, R.A., Fleming, R.H., Laine, R.M., Tse, D.S. and Winterle, J.S. (1984). *Inorg. Chem.* **23**, 1870–1876
201. Norman, P.R. and Cornelius, R.D. (1982). *J. Am. Chem. Soc.* **104**, 2356–2361
202. Hendry, P. and Sargeson, A.M. (1990). *Prog. Inorg. Chem.* **38**, 201–258
203. Koike, T., Inoue, M., Kimura, E. and Shiro, M. (1996). *J. Am. Chem. Soc.* **118**, 3091–3099
204. Chapman, W.H. and Breslow, R. (1995). *J. Am. Chem. Soc.* **117**, 5462–5469
205. Hikichi, S., Tanaka, M., Moro-Oka, Y. and Kitajima, N. (1992). *J. Chem. Soc. Chem. Commun*. 814–815
206. Dumas, D.P., Caldwell, S.R., Wild, J.R. and Raushel, F.M. (1989). *J. Biol. Chem.* **264**, 19659–19665
207. Mulbry, W.W., Karns, J.S., Kearney, P.C., Nelson, J.O., McDaniel, C.S. and Wild, J.R. (1986). *Appl. Environ. Microbiol.* **51**, 926–930
208. Benning, M.M., Shim, H., Raushel, F.M. and Holden, H.M. (2001). *Biochemistry* **40**, 2712–2722
209. Vanhooke, J.L., Benning, M.M., Raushel, F.M. and Holden, H.M. (1996). *Biochemistry* **35**, 6020–6025
210. Aubert, S.D., Li, Y. and Raushel, F.M. (2004). *Biochemistry* **43**, 5707–5715
211. Chin, J., Banaszczyk, M., Jubian, V. and Zou, X. (1989). *J. Am. Chem. Soc.* **111**, 186–190
212 Williams, N.H., Cheung, W. and Chin, J. (1998). *J. Am. Chem. Soc.* **120**, 8079–8087
213. Williams, N.H., Takasaki, B., Wall, M. and Chin, J. (1999). *Acc. Chem. Res.* **32**, 485–493
214. Kim, J.H. and Chin, J. (1992). *J. Am. Chem. Soc.* **114**, 9792–9795
215. Chung, Y.S., Akkaya, E.U., Venkatachalam, T.K. and Czarnik, A.W. (1990). *Tetrahedron Lett.* **31**, 5413–5416
216. Chin, J. and Zou, X. (1988). *J. Am. Chem. Soc.* **110**, 223–225
217. Wahnon, D., Lebuis, A.-M. and Chin, J. (1995). *Angew. Chem. Int. Edit.* **34**, 2412–2414
218. Humphry, T., Forconi, M., Williams, N.H. and Hengge, A.C. (2002). *J. Am. Chem. Soc.* **124**, 14860–14861
219. Tafesse, F. and Milburn, R.M. (1987). *Inorg. Chim. Acta* **135**, 119–122
220. Jones, D.R., Lindoy, L.F. and Sargeson, A.M. (1984). *J. Am. Chem. Soc.* **106**, 7807–7819
221. Gellman, S.H., Petter, R. and Breslow, R. (1986). *J. Am. Chem. Soc.* **108**, 2388–2394
222. Breslow, R., Berger, D. and Huang, D.-L. (1990). *J. Am. Chem. Soc.* **112**, 3686–3687
223. Norman, P.R. (1987). *Inorg. Chim. Acta* **130**, 1–4
224. Norman, P.R., Tate, A. and Rich, P. (1988). *Inorg. Chim. Acta* **145**, 211–217
225. Koike, T. and Kimura, E. (1991). *J. Am. Chem. Soc.* **113**, 8935–8941
226. Kimura, E., Kodama, Y., Koike, T. and Shiro, M. (1995). *J. Am. Chem. Soc.* **117**, 8304–8311
227. Kady, I.O., Tan, B., Ho, Z. and Scarborough, T. (1995). *J. Chem. Soc. Chem. Commun*. 1137–1138
228. Goldberg, D.P., diTargiani, R.C., Namuswe, F., Minnihan, E.C., Chang, S., Zakharov, L.N. and Rheingold, A.L. (2005). *Inorg. Chem.* **44**, 7559–7569
229. Fujii, Y., Itoh, T., Onodera, K. and Tada, T. (1995). *Chem. Lett.* **24**, 305–306
230. Itoh, T., Fujii, Y., Tada, T., Yoshikawa, Y. and Hisada, H. (1996). *Bull. Chem. Soc. Jpn.* **69**, 1265–1274
231. Bonfa, L., Gatos, M., Mancin, F., Tecilla, P. and Tonellato, U. (2003). *Inorg. Chem.* **42**, 3943–3949
232. Ibrahim, M.M., Shimomura, N., Ichikawa, K. and Shiro, M. (2001). *Inorg. Chim. Acta* **313**, 125–136
233. Ibrahim, M.M., Ichikawa, K. and Shiro, M. (2003). *Inorg. Chim. Acta* **353**, 187–196

234. Adams, H., Bailey, N.A., Fenton, D.E. and He, Q.-Y. (1996). *J. Chem. Soc. Dalton Trans*. 2857–2865
235. Feng, G., Mareque-Rivas, J.C., de Rosales, R.T.M. and Williams, N.H. (2005). *J. Am. Chem. Soc.* **127**, 13470–13471
236. Clewley, R.G., Slebocka-Tilk, H. and Brown, R.S. (1989). *Inorg. Chim. Acta* **157**, 233–238
237. Jurek, P. and Martell, A.E. (1999). *Inorg. Chim. Acta* **287**, 47–51
238. Aguilar, J., Bencini, A., Berni, E., Bianchi, A., Garcia-Espana, E., Gil, L., Mendoza, A., Ruiz-Ramirez, L. and Soriano. C. (2004). *Eur. J. Inorg. Chem*. 4061–4071
239. Bazzicalupi, C., Bencini, A., Berni, E., Bianchi, A., Fedi, V., Fusi, V., Giorgi, C., Paoletti, P. and Valtancoli, B. (1999). *Inorg. Chem.* **38**, 4115–4122
240. Bazzicalupi, C., Bencini, A., Berni, E., Bianchi, A., Fornasari, P., Giorgi, C. and Valtancoli, B. (2004). *Inorg. Chem.* **43**, 6255–6265
241. Kong, D., Martell, A.E. and Reibenspies, J. (2002). *Inorg. Chim. Acta* **333**, 7–14
242. Kong, D. and Martell, A.E. (2002). *J. Reibenspies Inorg. Chim. Acta* **333**, 7–14
243. Abe, K.-J., Izumi, J., Ohba, M., Yohoyama, T. and Okawa, H. (2001). *Bull. Chem. Soc. Jpn.* **74**, 85–95
244. Mancin, F., Rampazzo, E., Tecilla, P. and Tonellato, U. (2004). *Eur. J. Org. Chem*. 281–288
245. Carlsson, H., Haukka, M. and Nordlander, E. (2004). *Inorg. Chem.* **43**, 5681–5687
246. Chen, J., Wang, X., Zhu, Y., Lin, J., Yang, X., Li, Y., Lu, Y. and Guo, Z. (2005). *Inorg. Chem.* **44**, 3422–3430
247. Arca, M., Bencini, A., Berni, E., Caltagirone, C., Devillanova, F.A., Isaia, F., Garau, A., Giorgi, C., Lippolis, V., Perra, A., Tei, L. and Valtancoli, B. (2003). *Inorg. Chem.* **42**, 6929–6939
248. Molenveld, P., Kapsabelis, S., Engbersen, J.F.J. and Reinhoudt, D.N. (1997). *J. Am. Chem. Soc.* **119**, 2948–2949
249. Molenveld, P., Stikvoort, W.M.G., Kooijman, H., Spek, A.L., Engbersen, J.F.J. and Reinhoudt, D.N. (1999). *J. Org. Chem.* **64**, 3896–3906
250. Molenveld, P., Engbersen, J.F.J. and Reinhoudt, D.N. (1999). *Eur. J. Org. Chem*. 3269–3275
251. Molenveld, P., Engbersen, J.F.J. and Reinhoudt, D.N. (2000). *Chem. Soc. Rev.* **29**, 75–86
252. Albedyhl, S., Schnieders, D., Jancso, A., Gajda, T. and Krebs, B. (2002). *Eur. J. Inorg. Chem*., 1400–1409
253. Gajda, T., Kramer, R. and Jancso, A. (2000). *Eur. J. Inorg. Chem*. 1635–1644
254. Worm, K., Chu, F., Matsumoto, K., Best, M.D., Lynch, V. and Anslyn, E.V. (2003). *Chem. Eur. J.* **9**, 741–747
255. Iranzo, O., Kovalevsky, A.Y., Morrow, J.R. and Richard, J.P. (2003). *J. Am. Chem. Soc.* **125**, 1988–1993
256. Iranzo, O., Elmer, T., Richard, J.P. and Morrow, J.R. (2003). *Inorg. Chem.* **42**, 7737–7746
257. Iranzo, O., Richard, J.P. and Morrow, J.R. (2004). *Inorg. Chem.* **43**, 1743–1750
258. Yang, M.Y., Iranzo, O., Richard, J.P. and Morrow, J.R. (2005). *J. Am. Chem. Soc.* **127**, 1064–1065
259. Bazzicalupi, C., Bencini, A., Berni, E., Giorgi, C., Maoggi, S. and Valtancoli, B. (2003). *Dalton Trans.* 3574–3580
260. Scarso, A., Scheffer, U., Gobel, M., Broxterman, Q.B., Kaptein, B., Formaggio, F., Toniolo, C. and Scrimin, P. (2002). *Proc. Natl. Acad. Sci.* **99**, 5144–5149
261. Ichikawa, K., Tarani, M., Uddin, M.K., Nakata, K. and Sato, S. (2002). *J. Inorg. Biochem.* **91**, 437–450
262. Yamada, K., Takahashi, Y., Yamamura, H., Araki, S., Saito, K. and Kawai, M. (2000). *Chem. Commun.* 1315–1316

263. Shelton, V.M. and Morrow, J.R. (1991). *Inorg. Chem.* **30**, 4295–4299
264. Morrow, J.R. (1996). *Met Ions Biol Syst* **33**, 561–592
265. Kovari, E. and Kramer, R. (1994). *Chem. Ber.* **127**, 2151–2157
266. Yashiro, M., Ishikubo, A. and Komiyama, M. (1995). *J. Chem. Soc. Chem. Commun.* 1793–1794
267. Yashiro, M., Ishikubo, A. and Komiyama, M. (1997). *Chem. Commun.* 83–84
268. Matsuda, S., Ishikubo, A., Kuzuya, A., Yashiro, M. and Komiyama, M. (1998). *Angew. Chem. Int. Edit.* **37**, 3284–3286
269. Kawahara, S. and Uchimaru, T. (2001). *Eur. J. Inorg. Chem.* 2437–2442
270. Ait-Haddou, H., Sumaoka, J., Wiskur, S.L., Folmer-Andersen, J.F. and Anslyn, E.V. (2002). *Angew. Chem. Int. Edit.* **41**, 4013–4016
271. Yashiro, M. and Kawahara, R. (2004). *J. Biol. Inorg. Chem.* **9**, 914–921
272. Yashiro, M., Kaneiwa, H., Onaka, K. and Komiyama, M. (2004). *Dalton Trans.* 605–610
273. Basile, L.A., Raphael, A.L. and Barton, J.K. (1987). *J. Am. Chem. Soc.* **109**, 7550–7551
274. Fitzsimons, M.P. and Barton, J.K. (1997). *J. Am. Chem. Soc.* **119**, 3379–3380
275. Sissi, C., Mancin, F., Palumbo, M., Scrimin, P., Tecilla, P. and Tonellato, U. (2000). *Nucleos. Nucleot. Nucl.* **19**, 1265–1271
276. Sissi, C., Rossi, P., Felluga, F., Formaggio, F., Palumbo, M., Tecilla, P., Toniolo, C. and Scrimin, P. (2001). *J. Am. Chem. Soc.* **123**, 3169–3170
277. Aka, F.N., Akkaya, M.S. and Akkaya, E.U. (2001). *J. Mol. Catal. A* **165**, 291–294
278. Copeland, K.D., Fitzsimons, M.P., Houser, R.P. and Barton, J.K. (2002). *Biochemistry* **41**, 343–356
279. Boseggia, E., Gatos, M., Lucatello, L., Mancin, F., Moro, S., Palumbo, M., Sissi, C., Tecilla, P., Tonellato, U. and Zagotto, G. (2004). *J. Am. Chem. Soc.* **126**, 4543–4549
280. Nomura, A. and Sugiura, Y. (2004). *J. Am. Chem. Soc.* **126**, 15374–15375
281. Morrow, J.R. and Iranzo, O. (2004). *Curr. Opin. Chem. Biol.* **8**, 192–200
282. Liu, C., Wang, M., Zhang, T. and Sun, H. (2004). *Coord. Chem. Rev.* **248**, 147–168
283. Mancin, F., Scrimin, P., Tecilla, P. and Tonellato, U. (2005). *Chem. Commun.* 2540–2548
284. Reddy, P.R., Mohan, S.K. and Rao, K.S. (2005). *Chem. Biodivers.* **2**, 672–683
285. Xiang, Q., Zhang, J., Liu, P., Xia, C., Zhou, Z., Xie, R. and Yu, X. (2005). *J. Inorg. Biochem.* **99**, 1661–1669
286. Peng, W., Liu, P., Jiang, N., Lin, H., Zhang, G., Liu, Y. and Yu, X. (2005). *Bioorg. Chem.* **33**, 374–385
287. Molenveld, P., Engbersen, J.F.J. and Reinhoudt, D.N. (1999). *Angew. Chem. Int. Ed.* **38**, 3189–3192
288. Chu, F., Smith, J., Lynch, V.M. and Anslyn, E.V. (1995). *Inorg. Chem.* **34**, 5689–5690